

# Aging of NAPLs interfaces in porous media and their effects on mass transfer of organic contaminants

Dissertation

zur Erlangung des Grades eines Doktors der Naturwissenschaften

der Geowissenschaftlichen Fakultät  
der Eberhard Karls Universität Tübingen

vorgelegt von  
Lihua Liu  
aus Beijing, V.R.China

2008

Tag der mündlichen Prüfung: 21th April 2008

Dekan: Prof. Dr. Peter Grathwohl

1. Berichterstatter: Prof. Dr. Stefan Haderlein

2. Berichterstatter: Prof. Dr. Torsten Schmidt



Herausgeber: Institut für Geowissenschaften der Universität  
Tübingen  
Sigwartstraße 10, D-72076 Tübingen

Schriftleitung der Reihe C: Zentrum für Angewandte Geowissenschaften (ZAG)  
Lehrstuhl für Angewandte Geologie  
Prof. Dr. Thomas Aigner  
Prof. Dr. Erwin Appel  
Prof. Dr. Peter Grathwohl  
Prof. Dr. Stefan Haderlein  
Prof. Dr.-Ing. Olaf Kolditz  
Prof. Dr. Georg Teutsch

Redaktion: Dipl.-Geol. Björn Sack-Kühner

ISSN 0935-4948 (Print)  
ISSN 1610-4706 (Internet)

## Acknowledgements

I would like first to thank Prof. Dr. Torsten C. Schmidt and Prof. Dr. Stefan Haderlein for their offering this chance to do research work, thanks for their support, discussions and suggestion. Thanks Prof. Dr. Peter Grathwohl for his unvarying support and encouragement throughout my study.

Thanks to those who have aided me in the lab, Dr. Thomas Wendel for his endless patience and assistance, Bernic Nish for preparing all of the internal standards, Renate Seeling for GC-MS knowledge and data.

Thanks Christina Eberhardt for her nice discussion and lab technique. Thanks Dr. Ulrich Maier for the formatting of the numerical model, thanks Fei Wu, Prakash Srinivasan for their lab assistance, Dr. Philip Larese-Casanova and Dr. Rajapaksha Arachchilage Maithreepala for their grammatical corrections.

Thanks for all of my friends and colleagues Jing Li, Dr. Guohui Wang, Dr. Yannian Lee, Satoshi Endo, Michaela Blessing, Anke Schmidt, Dr. Sayonara Brederode Ferreira Reckhorn.

Thank the Deutsche Forschungsgemeinschaft (DFG) for providing financial support for this work.

## Abstract

Groundwater and soil contaminated by organic compounds is a world wide environmental problem. Coal tar, crude oil and other complex multicomponent mixtures introduced into the subsurface by accident, uncontrolled discharging and unsuitable treatment of the products and byproducts, were persistent and act as continuous sources of contaminants. These complex mixtures are liquid, immiscible with water and known as non-aqueous phase liquids (NAPLs).

The compounds inside the bulk NAPLs phase may move into gas, water and solid phase in the subsurface environment. This transferring process includes evaporation, volatilization, dissolution, diffusion, sorption and chemical and biochemical reaction. The NAPLs interfacial phase may be subject to a visible phase change during this process, that is the bulk liquid phase may change to a viscous or solid phase. This process of phase change is referred to as “aging”, and the newly formed visible interfacial phase is named as “aged film” or “skin film”. This aging process may change the mechanical, physical and chemical properties of the interfacial phase. Subsequently, affect the mass transfer, spreading, recovery and bioavailability of NAPL and solutes in NAPL. The aging phenomenon of NAPLs was studied in this work by pendant drop test and batch experiment, and the compositions of fresh and aged NAPLs were analyzed by GC-MS. All of the NAPLs tested in the lab showed visible aged films within shorter or longer time periods. The compositions of fresh and aged coal tars were dramatically different, especially for BTEX, polar compounds and light molecular weight PAHs, which were much lower in the aged coal tars than fresh ones. The effects of environmental conditions on aging process were investigated using batch and continuously flow through experiments. The results indicated that, (i) depletion of water soluble compounds is important to the aging process of crude oil, (ii) evaporation and volatilization contribute more to the aging of coal tar, (iii) oxidation by  $H_2O_2$  or  $O_2$  is not a decisive condition in the aging process of coal tar, and (iv) pH of the solution is key to the leaching properties of certain compounds, however, it has no detectable effect on the formation of interfacial film.

The mass transfer of organic compounds from NAPLs to other phases determines the extent of contamination and persistence of the residual phase. Therefore, the understanding of this process is important for the risk assessment and remediation

effectiveness to the sites contaminated by NAPLs. This process is known involving multiple processes and no single process alone is responsible for it. A lumped parameter – mass transfer coefficient ( $k$ , cm/s) was therefore introduced to describe the combined processes. The mass transfer process can be described by different model depending on the boundary conditions, and  $k$  can be obtained as a fitting datum. The batch model was used to describe the experimental data of simple model NAPLs and aged coal tar-water systems. The simulated concentration profiles matched well the experimental data, and  $k$  values were obtained for individual compounds and compared well with published experimental data. Remarkably, the  $k$  of most compounds are about two orders of magnitude lower in aged coal tars than those in model and fresh NAPLs, which indicated the resistance of mass transfer increased with aging process of NAPLs.

However, the batch model used here can only describe the kinetic mass transfer process for batch system. A model that could simulate dynamic mass transfer process is needed, especially for the mass transfer process accompanied by aging of NAPLs. Therefore, a small-scale experiment was performed, which was conducted by a continuously stirring flow through reaction system (CSFTRS). A continuously flow model coupling mass transfer through interface and advective flow was used to analyze the experimental data. The analytical solution of this flow model can be used to simulate the mass transfer process in simple model NAPL-water system. A numerical model considering the general form of Raoult's law was established to simulate the complex NAPL-water system. The simulated concentration profiles agreed with the experimental results. The functions of activity coefficient to mole fraction and  $k$  were also obtained from this numerical model. All of these data matched with the published in the literatures.

The physicochemical parameters obtained from NAPL-water systems enhanced our understanding of the properties of the interfacial phase, especially when it underwent aging process. Further experiment should be performed with real NAPL-water system by CSFTRS, and the numerical model could be modified by more experimental data. Thus, an improved understanding of dynamic mass transfer process along with NAPLs aging process may be obtained.

## Zusammenfassung

Grundwasser- und Bodenverunreinigungen durch organische Schadstoffe stellen weltweit ein Problem für die Umwelt dar. Steinkohlenteer, Rohöl und andere komplexe Schadstoffmischungen, die durch Unfälle, unkontrollierte Entsorgung und den unsachgemäßen Umgang mit diesen Stoffen in den Untergrund gelangen, bilden persistente und langanhaltende Schadstoffquellen. Diese komplexen Mischungen sind flüssig, mit Wasser nicht mischbar und daher als nichtwässrige flüssige Schadstoffphasen (NAPLs) bekannt.

Die einzelnen Schadstoffverbindungen können aus dem NAPL-Phasenkörper in die ungesättigte und die gesättigte Bodenzone austreten. Dieser Übergang beinhaltet Evaporations-, Verflüchtigungs-, Lösungs-, Diffusions-, und Sorptionsprozesse sowie chemische und biochemische Reaktionen. Die Grenzfläche zwischen NAPL-Phase und Luft, bzw. Wasser kann dabei einer sichtbaren Veränderung unterliegen, die sich in einem viskosen bzw. festen Film auf der Oberfläche der Flüssigkeit äußert. Diese Veränderung wird auch als "Alterungsprozess" bezeichnet und die neu gebildete Oberfläche ist als "Alterungsfilm oder -haut" bekannt. Der Alterungsprozess der NAPLs wurde mithilfe eines "Tropfentests" und in Batchreaktoren untersucht und die Zusammensetzung der frischen, sowie der gealterten NAPL-Phase mittels GC-MS-Analyse bestimmt. Alle der im Labor untersuchten NAPL-Phasen bildeten früher oder später diesen sichtbaren Alterungsfilm an der Oberfläche. Die Zusammensetzung der frischen und der gealterten Steinkohlenteere zeigte große Unterschiede, vor allem für BTEX, polare Verbindungen und PAKs mit geringen Molekulargewichten, die im gealterten Produkt weitaus niedriger waren als im frischen Steinkohlenteer. Der Einfluss von verschiedenen Umweltbedingungen auf diesen Alterungsprozess wurde mithilfe von Batch- und Durchflussreaktoren untersucht. Die Ergebnisse zeigen, dass (i) die Abnahme von wasserlöslichen Verbindungen einen wichtigen Effekt auf den Alterungsprozess von Rohölen hat, (ii) Evaporation und Verflüchtigung bei der Alterung von Steinkohlenteer eine größere Rolle spielen, (iii) Oxidationsprozesse dagegen kaum einen Einfluss auf den Alterungsvorgang von Steinkohlenteer haben und (iv) der pH-Wert der Lösung zwar entscheidend für die Auslaugungseigenschaften der einzelnen Verbindungen ist, aber keinen nachweisbaren Einfluss auf die Bildung des Grenzflächenfilms hat.



Der Massentransfer organischer Verbindungen aus der NAPL-Phase in andere Phasen bestimmt den Verbleib der Schadstoffe und die Persistenz der Schadstoffquelle. Daher ist das Verständnis dieser Prozesse wichtig bei der Risikoabschätzung und dem Sanierungserfolg kontaminierter Standorte. Nicht nur ein einzelner Prozess ist dafür verantwortlich, sondern viele unterschiedliche Prozesse finden gleichzeitig statt. Um das Gesamtsystem zu beschreiben, wurde ein Summenparameter, der Massentransferkoeffizient ( $k$ , cm/s) eingeführt. Der Massentransferprozess kann abhängig von den Rahmenbedingungen durch unterschiedliche Modelle beschrieben werden und  $k$  kann dabei als Fittingparameter ermittelt werden. Der Batchversuch wurde als Modell benutzt, um Lösungsprofile einfacher Modell-NAPLs und gealterter Steinkohlenteer-Wasser-Systeme zu beschreiben. Die simulierten Konzentrationsprofile stimmen dabei sehr gut mit den experimentellen Daten überein, und die Werte für  $k$ , die dabei ermittelt wurden, sind gut mit bereits veröffentlichten Daten vergleichbar. Zudem zeigte sich, dass die Massentransferkoeffizienten der meisten Verbindungen um etwa zwei Größenordnungen niedriger in den gealterten Steinkohlenteeren als in den Modell- und frischen NAPLs waren, was einen Hinweis auf die Resistenz des Massentransfers mit zunehmendem Alterungsprozess der NAPLs liefert.

Allerdings kann das Batchmodell lediglich den kinetischen Stoffübergang innerhalb von Batchsystemen beschreiben. Notwendig ist ein Modell, das den dynamischen Massentransferprozess simulieren kann, vor allem beim Alterungsprozess von NAPL-Phasen. Dazu wurde ein Experiment durchgeführt, das im kleinen Maßstab Umweltprozesse simuliert, ein sog. ständig bewegtes Durchflussreaktor-System (CSFTRS). Ein kontinuierliches Strömungsmodell, das den Massentransfer durch die Oberfläche und den advektiven Transport verbindet, wurde benutzt. Die analytische Lösung dieses Modells kann dazu eingesetzt werden, den Massentransfer in einfachen Modell-NAPL-Wasser-Systemen zu simulieren. Das numerische Modell, das die Aktivitätskoeffizienten und das Raoult'sche Gesetz beachtet, kann die Prozesse in komplexen NAPL-Wasser-Systemen abbilden. Der Aktivitätskoeffizient und Stoffmengenanteil sowie  $k$  konnten auch mithilfe des numerischen Modells erhalten werden.

Sinnvoll wäre es, zusätzliche CSFTRS-Experimente mit reellen NAPL-Wasser-Systemen durchzuführen und das numerische Modell mithilfe weiterer experimenteller Daten zusätzlich zu validieren und zu optimieren. Der dynamische Massentransfer, der mit dem Alterungsprozess von NAPL-Phasen verbunden ist, könnte mithilfe dieses Modells beschrieben werden.

## Nomenclature

$a_{nm}$	Specific interfacial area ( $\text{cm}^2/\text{cm}^3$ )
$A$	interfacial or surface area ( $\text{cm}^2$ )
$C$	concentration ( $\text{mg/L}$ or $\mu\text{g/L}$ ), it could be the concentration in water and organic solvent or organic mixture
$C_{eq}$	equilibrium aqueous phase concentration ( $\text{mg/L}$ or $\mu\text{g/L}$ )
$D_L$	longitudinal dispersion coefficient ( $\text{cm}^2/\text{s}$ )
$f/f^l$	fugacity ratio (-)
$F$	mass flux ( $\text{mg}\cdot\text{s}^{-1}\cdot\text{cm}^{-2}$ )
$k$	mass transfer coefficient ( $\text{cm/s}$ )
$v$	mass transfer rate coefficient ( $1/\text{s}$ )
$M$	mass ( $\text{g}$ or $\text{mol}$ )
$n$	empirical fitting exponent (-)
$P_{a/b}$	two-phase partition coefficient ( $\text{L/kg}$ or $\text{mL/g}$ ); a could be organic solvent or organic mixture, b could be water and other phases
$Q$	flow rate ( $\text{mL/min}$ )
$R$	mass transfer resistance ( $\text{kg/L}$ or $\text{g/mL}$ )
$S$	Water solubility ( $\text{mg/L}$ )
$S_{sub}$	Subcooled liquid solubility ( $\text{mg/L}$ )
$T, T_m, T_t$	temperature ( $\text{K}$ ), melting temperature, triple point temperature
$V$	volume ( $\text{L}$ or $\text{cm}^3$ )
$R$	universal gas constant ( $8.3145 \text{ J}\cdot\text{mol}^{-1}\cdot\text{K}^{-1}$ )
$\Delta C_p$	heat capacity difference ( $\text{J}\cdot\text{mol}^{-1}\cdot\text{K}^{-1}$ )
$\Delta H$	enthalpy change ( $\text{kJ/mol}$ )
$\Delta S$	entropy change ( $\text{kJ}\cdot\text{mol}^{-1}\cdot\text{K}^{-1}$ )
$\chi$	mole fraction (-)
$\gamma$	activity coefficient (-)

## Acronyms

BE	batch experiment
BTEX	benzene, toluene, ethylbenzene, xylene
CFTE	continuously flow through experiment
CSFTRS	continuously stirred flow through reaction system
MGPs	manufactured gas plants
NAPLs, LNAPLs, DNAPLs	non-aqueous phase liquids, light NAPLs, dense NAPLS
PAHs	polycyclic aromatic hydrocarbons
PDT	pendant drop test
RRSS	relative residual sum of squares
SCT	surface coating test

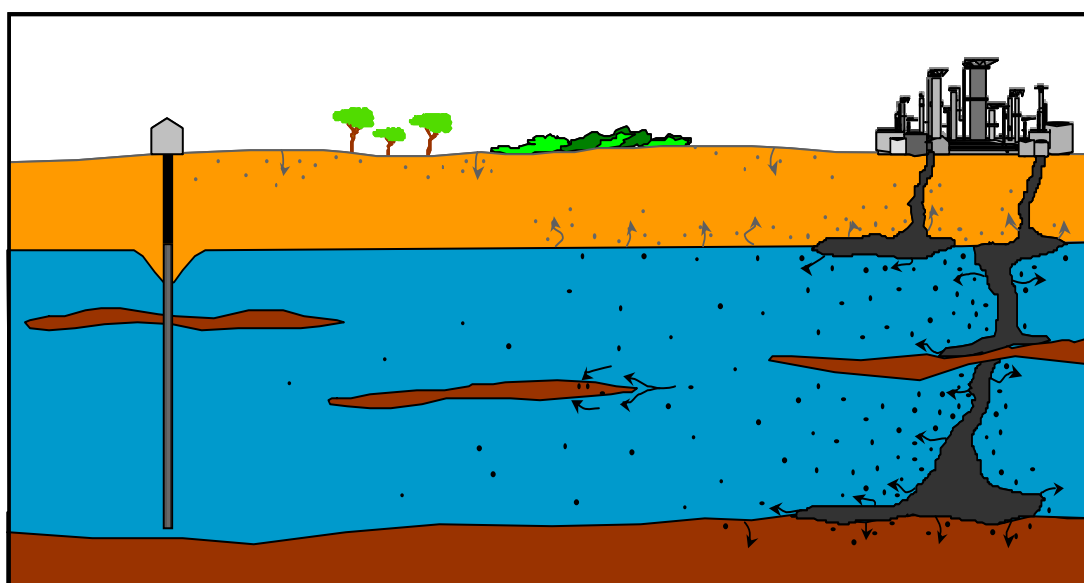
Acknowledgements.....	vii
Abstract.....	viii
Zusammenfassung.....	x
Nomenclature.....	xiii
Acronyms.....	xiv
Chapter 1 Introduction.....	1
1.1 Motivation.....	1
1.2 Aging phenomena in NAPLs boundary layer.....	2
1.2.1 Introduction.....	2
1.2.2 Knowledge about Asphaltenes.....	4
1.3 Mass transfer - theory and experimental methodology.....	5
1.3.1 Introduction.....	5
1.3.2 Theories.....	6
1.3.3 Experimental methods.....	7
1.4 Effect of aging on mass transfer.....	9
1.5 Objectives.....	10
1.6 References.....	11
Chapter 2 Determination of the subcooled liquid solubilities of PAHs in partitioning batch experiments.....	17
2.1 Motivation.....	17
2.2 Thermodynamic theory.....	17
2.2.1 Solubility and activity coefficient.....	17
2.2.2 Subcooled liquid solubility and fugacity ratio.....	18
2.3 Objectives.....	19
2.4 Materials and methods.....	20
2.4.1 Materials.....	20
2.4.2 Approach of the method design.....	20
2.4.3 Batch technique.....	20
2.4.4 Estimation of partitioning coefficient and activity coefficient.....	22
2.4.5 Analytical methods.....	23
2.5 Results and discussion.....	24
2.5.1 Mass transfer coefficient.....	24
2.5.2 Subcooled liquid solubility and enthalpy of fusion.....	25
2.5.2 Partitioning coefficient.....	28
2.6 Conclusion.....	29
2.7 References.....	30
Chapter 3 Aging phenomena of NAPLs interfacial phase.....	33
3.1 Aging phenomena.....	33
3.2 Experimental methods to study the aging phenomena.....	33
3.2.1 Pendant drop test (PDT).....	34
3.2.2 Continuously flow through experiments (CFTE).....	36
3.2.3 Batch experiment (BT).....	37
3.2.4 Surface coating test (SCT) to prepare the aged NAPLs sample.....	39

3.3 Results and discussion .....	40
3.3.1 Effect of the NAPL source on aging process .....	40
3.3.2 Effect of evaporation and dissolution on aging process .....	41
3.3.3 Effect of oxygen concentration on aging process .....	42
3.3.4 Effect of pH on aging process .....	43
3.3.5 Summary and conclusions .....	43
3.4 References .....	44
Chapter 4 Aging of coal tar and its effects on mass transfer .....	47
4.1 Introduction .....	47
4.2 Materials and experimental methods .....	48
4.2.1 Materials .....	48
4.2.2 Experiments to measure the aqueous phase concentrations .....	48
4.2.3 Analytical methods .....	49
4.3 Results and discussion .....	51
4.3.1 Concentrations of solutes in fresh and aged coal tars .....	51
4.3.2 Equilibrium concentrations of fresh coal tar-water system .....	53
4.3.3 Aqueous phase concentrations in aged coal tar-water system .....	55
4.3.4 Partitioning coefficients of compounds from different NAPLs .....	58
4.3.5 Mass transfer coefficients of compounds in different NAPLs .....	58
4.4 Conclusions .....	61
4.5 References .....	63
Chapter 5 Mass Transfer Process from NAPLs to water studied in a Continuously Stirring Flow Through Reactor .....	65
5.1 Introduction .....	65
5.2 Research Objectives .....	65
5.3 Materials and methods .....	66
5.3.1 Materials - Model NAPL .....	66
5.3.2 Continuously Stirred Flow Through Reaction System (CSFTRS) .....	67
5.3.3 Chemical analyses .....	68
5.3.4 Modeling approach .....	68
5.4 Results and discussion .....	71
5.4.1 Simple model NAPL .....	71
5.4 Results and discussion .....	72
5.4.1 Simple model NAPL .....	72
5.4.1 Complex model NAPL .....	72
5.5 Conclusions .....	76
5.6 References .....	76
Chapter 6 Conclusions and Outlook .....	78
6.1 Research of aging phenomena .....	78
6.2 Study of mass transfer process .....	80
6.3 Model research .....	80
Appendixes .....	i

# Chapter 1 Introduction

## 1.1 Motivation

With the industrial development, more and more chemicals were produced and introduced into the environment. Some of these chemicals may enter the subsurface as a liquid that is immiscible with water and is known as non-aqueous phase liquid (NAPL). NAPL is less dense than water is termed light non-aqueous phase liquid (LNAPL, e.g., gasoline, diesel fuel, heating oil) and commonly collect and pool at, or above, the water table. The other type of NAPL is denser than water (DNAPL, e.g., coal tars, creosotes, chlorinated solvent mixtures, PCBs, hydraulic oils containing PCBs). The DNAPL migrates through the unsaturated zone, continues on a downward migration through the water table to the saturated zone below, and forms trapped pools or immobilized ganglia as illustrated in Figure 1.1.



**Figure 1.1 Release of NAPLs into porous media, source and plume**  
From Center for applied geoscience (ZAG), University of Tuebingen

The groundwater, soils and sediments therefore may be polluted by these contaminants as a form of NAPL by accident, uncontrolled discharging, unsuitable treatment of the products and byproducts. Particularly in former manufactured gas plants (MGPs) sites (coal tar), wood treatment facilities (creosotes), dry cleaning shop and metal degreasing plants (TCE), oil exploration and production sites, oil refineries or storage facilities (crude oil, or other petrochemicals). The release of NAPL into natural porous media is an extensive problem at contaminated sites around the world. The transfer of pollutants across the NAPL interfacial phase (or boundary layer)

determines both the extent of contamination as well as the persistence of residual NAPL phases. Thus, the knowledge of mass transfer phenomena and partitioning behavior of the NAPL interface is essential to the understanding of the fate of the contaminants and the effect to environmental system.

Previous research has shown that NAPL interfaces may be subject to "aging" phenomena when exposed to water or air. That is the gradual deformation of a interfacial phase, it changed from flowing liquid to viscous solid skin-like film [1-8]. This change of the NAPL interfacial phase in natural multiphase systems (i.e., porous medium, water, NAPL) accompanied with a change of physical and chemical properties of the NAPL interfaces, and the deformation of mechanical and compositional change of NAPL itself. These changes implicated for mass transfer, spreading, recovery and bioavailability of NAPLs and their components [9-12]. However, surprisingly little is known about the processes and factors that control the deformations of NAPL interface, neither about the effects of such films on mass transfer of organic compounds, despite some effort was made in this field by a few research groups [5, 6, 10, 13-15].

## 1.2 Aging phenomena in NAPLs boundary layer

### 1.2.1 Introduction

Aging is a universal phenomenon, and this study concerns specifically to this phenomenon of NAPLs interfacial layer. It is a dynamic process occurred where NAPLs exposure to water and/or air. The deformation of the interfacial phase can be observed visibly by some experimental methods, the commonly used are pendant drop test and batch experiment. Numerous studies on bulk phase aging of fuels date back almost to the onset of crude oil refining [1, 2]. Formation of fuel insoluble matter has been described frequently and is still of interest because of the industrial problems found during oil recovery, transport, refining and long-term storage. This phenomenon was studied by the researchers in the environmental field, and it was assumed that environmental impact would be decreased and the time span for remediation would become longer [4, 5, 7, 8, 10].



However, the consistent conclusion of the factors and mechanisms that result in the formation of interfacial layer is missing, only a few hypotheses and/or factors were reported and they are followed.

The widely accepted assumption is the film formed mainly because of the aggregation and deposition of asphaltenes, since asphaltens are of amphiphilic nature, they can adsorb at the water-NAPL interface acting like surfactants, with their polar groups residing in the aqueous phase and nonpolar groups residing in the oil phase. The high molecular weight compounds, resin and asphaltenes associated with fine particles to form at first micelle. The micelle increased from monomeric sheets to reversed, super and giant super micelle, later may form floc [13, 15]. The colloidal aggregate associated to form an interfacial film [15, 16]. This film increases from the expanded liquid film to condensed liquid film and solid-like three-dimensional network film. Meanwhile, the structure of the asphaltene film is also changed from two-dimensional to three-dimensional network [17, 18].

Another possible reason is the oxygen-induced oxidation subsequently leading to polymerisation, alternative oxidation reactions and acid catalyzed condensations [19]. While under anoxic conditions, aging processes of NAPLs in the contaminated porous media may be triggered by other factors, e.g., microbial oxidation, catalysis by metals and their oxides.

Additional processes being invoked to contribute to aging of NAPLs interface are (i) preferential depletion of polar and high water soluble organic compounds from the NAPLs [5], and (ii) microbial activity at the bulk and boundary of NAPLs phase [20, 21].

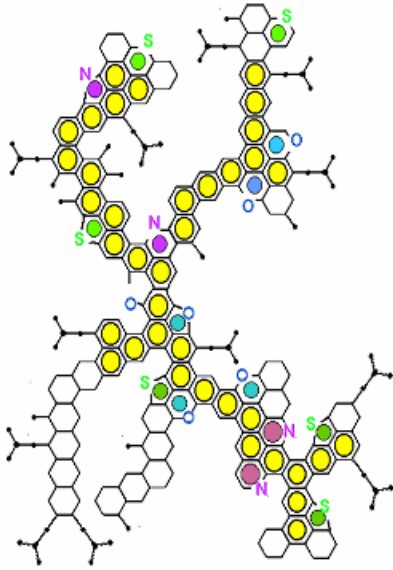
The aging process is thought to be concurred with the change of the composition. Asphaltene, resin (or malene), naturally occurring metal porphyrinse, high molecular weight carboxylic acids and aromatic carboxylic esters have been tentatively identified as interfacial film constituents [16, 22]. Totsche [11] found in a NMR study substantial differences in bulk and interface chemical composition, an increase in "chemical diversity" at the interface in particular regarding polar oxygen-containing compounds was reported. The components thought to be connected to aging effects include N-heterocyclic compounds (e.g. pyrroles, pyridines, furan, and quinolines), diolefins, phenols, styrene, organic acids, naphthenic acids, thiols, thiophenes,

organometallic compounds, copper, other metals and oxides ( $\text{TiO}_2/\text{SiO}_2$ ) as catalysts. Some of these compounds, including phenols and anilines, have been shown to react with manganese and iron oxides in aqueous systems [22-33]. However, Nelson et al found that there is no dramatic difference between the composition of the fresh and aged coal tar film except for the existence of “weakly bound” water in the aged NAPLs [5, 15, 33].

### 1.2.2 Knowledge about Asphaltenes

It is commonly believed that water droplets in crude oil or bitumen as well as other oil droplets in aqueous phase are stabilized by asphaltene macromolecules and/or aggregates. The presence of the surface-active asphaltenes is also suggested by some researchers as the main compounds of the aged interfacial films [10, 13, 17, 22, 34]. Therefore, the current knowledge on asphaltenes is summarized here, even though the information is still limited.

Asphaltenes are a solubility classified molecules, and defined by ASTM D 2007 – 03 for separation from coal tar and creosotes [35]. In brief, asphaltenes are soluble in carbon disulfide but insoluble in short-chain alkanes such as n-pentane and n-heptane. Molecular weight of asphaltens range from 1,000 to 2,000,000 [36], and it depends on the source, separating temperature, concentration of resin and maltene, separation techniques etc. [37, 38]. Coal asphaltenes have lower molecular weights, hydrogen, sulfur, but higher aromaticity and oxygen contents (mainly in phenolic OH and aromatic carbonyl forms) than petroleum asphaltenes. The definition of petroleum asphaltenes is according to ASTM D 4124, IP 143. They have been a hot topic for petroleum chemists for more than 50 years [3, 18, 39-44]. The term “asphaltene” is generally applied in the narrow sense of petroleum asphaltene for them. The postulated generic molecular structure of asphaltene is shown in Figure 1.2. Asphaltene molecules carry a core of stacked, flat sheets of condensed (fused) aromatic rings linked at their edges by chains of aliphatic and/or naphthenic-aromatic ring systems. The condensed sheets contain nitrogen, sulphur, oxygen atoms and probably vanadium and nickel complexes. The condensed aromatic rings exist in the form of a non-homogeneous flat sheet. However, the sheets have the tendency to be attracted towards each other, thus result in the formation of an agglomeration. The structure of the which is similar to that of a book [45-47].



**Figure 1.2 Illustration of the molecular structure of asphaltene (The Heavy Oil Science Centre)**  
[http://tiger.uic.edu/~mansoori/Asphaltene.Molecule\\_html](http://tiger.uic.edu/~mansoori/Asphaltene.Molecule_html)

## 1.3 Mass transfer - theory and experimental methodology

### 1.3.1 Introduction

Mass transfer is referred to as a physical process that involves molecular and convective transport of atoms and molecules within physical systems. It can be aqueous and gaseous diffusion within a phase and interphase mass transfer between phases when there is a fugacity gradient. It occurs during convection, advection, sorption, diffusion, dispersion and chemical reactions. For the mass transfer between two phases, it can be described as series of steps: (i) diffusion and advection through the bulk phase of one of the liquids toward the interface, (ii) accumulation, adsorption / desorption, advection, diffusion or chemical reaction at the interface, and (iii) diffusion and advection away from the interface into the bulk phase of the other liquid [48, 49]. The 2<sup>nd</sup> step closely related to the aging process of interfacial phase. As mass transfer involves multiple processes and no single process alone is responsible for that. A grouped or lumped parameter-mass transfer coefficient  $k$ , (cm/s) is therefore used to describe the combined processes.

**Mass transfer coefficient ( $k$ )** is a rate constant for the overall process caused by a driving force due to thermodynamic nonequilibrium and sometimes electrostatic potential difference. It can be estimated from different theoretical equations depending on the relations of the environmental and boundary conditions [49, 50]. A first-order approximation with a linear driving force is commonly used because of the

computational simplicity and the involving of  $k$ . The mass flux  $F$ , ( $\text{mg}\cdot\text{s}^{-1}\cdot\text{cm}^{-2}$ ) defined by Fick's first law as the amount of compound removed during a unit time period, depends on the  $k$  and concentration gradient and is expressed as:

$$F(x) = -k \cdot (C_{eq} - C) \quad (1.1)$$

where,  $C_{eq}$  ( $\text{mg/L}$ ) is the equilibrium concentration, and  $C$  is the concentration at a certain point.

**Mass transfer resistance ( $R$ ):** The numerical value of  $R$  is equal to the reciprocal of mass transfer coefficient ( $1/k$ ). The overall mass transfer resistance is related to the individual layer (or phases) resistances. For multi-phases system (e.g., a interfacial film is present between the NAPL and aqueous phases)(Figure 1.3), the overall mass transfer resistance can be expressed as [10, 50, 51]:

$$\frac{1}{k_t} = \frac{1}{k_n} + \frac{1}{P_{n/a} \cdot k_n} + \frac{1}{P_{a/w} \cdot k_a} + \frac{1}{k_w} \quad (1.2)$$

where,  $P$  (-) are the partitioning coefficients between different phases.

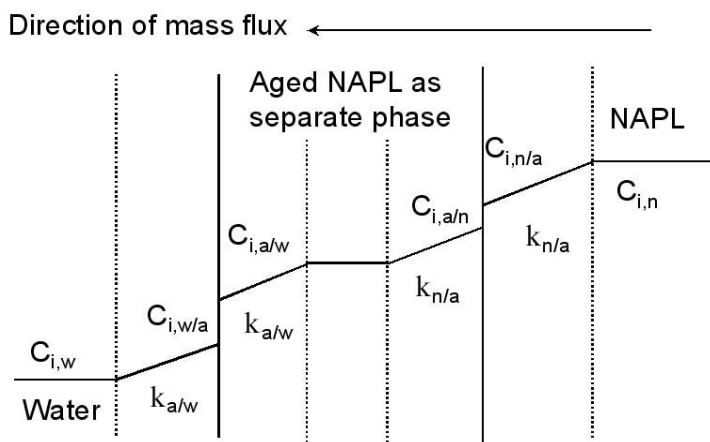


Figure 1.3 Illustration for mass transfer through multi-phase layers

### 1.3.2 Theories

Several theories describe the mechanisms controlling the mass transfer process according to different boundary conditions and are used to describe various real cases.

**Film theory** is the oldest and commonly accepted approach, first proposed by Lewis [52] and Whitman [53], which assumed a stagnant film exists near interface (Figure 1.3), a solute present at high dilution is slowly diffusing across this film.

**Penetration theory** works for the situation that there is a flux at the interface, and the film is very thick [54]. In the vertical direction ( $z$ ), diffusion is much more important than convection, and in the horizontal direction ( $x$ ), diffusion is much less important than convection.

**Surface renewal theory** consists of two regions, interfacial region and renewal region [55].

**Boundary layer theory** is another well-known and more complete description of mass transfer, based on the analogy between mass and momentum transport in the fluid boundary layer at the interface. It can be applied to the flow of fluids with high viscosity (i.e. water) at low velocity (laminar flow) through flow channels characterized by small characteristic dimensions (i.e. groundwater flow, fixed bed adsorption processes, packed-bed contactors) [56].

Many important processes in the environment occur at boundaries, this layer plays an important role controlling the transport components. This theory was accordingly well studied and utilized. Schwarzenbach et al. discusses three types of boundary models according to the shape of the generalized diffusivity profile across the boundary. They are bottleneck boundary, wall and diffusive boundary [50] (p 837). Since the concentration gradient is the driving force for the transfer of chemical compounds through NAPL-water boundary, this diffusive model was accordingly often used in many studies.

However, it is very difficult to determine the necessary parameters in all theories, e.g., film thickness for mass transfer, or velocity and concentration profiles adjacent to surfaces from which mass transfer is occurring. As a result,  $k$  is usually fit to data, and empirical coefficients are developed to define it rather than measured.

### 1.3.3 Experimental methods

Several research groups have developed various experimental methods to determine the mass transfer coefficients for different NAPL-aqueous systems. Some of which are related to NAPL-water, especially coal tar-water systems are introduced below.

**Batch experiment** is the simplest method, and performed at various laboratories for different objectives [8, 57, 58]. Mahjoub installed a batch reactor inside a water bath and evaluated the mass transfer coefficient. The dependent concentrations of phenols,

toluene and PAHs in aqueous phase at different pH, temperature and ionic strength conditions were obtained. The mass transfer coefficient was also estimated. The dissolution of pollutants can be described by:

$$V_w \frac{dC_i}{dt} = A \cdot k_i (C_{i,eq} - C_i) \quad (1.3)$$

where  $V_w$  (L or  $\text{cm}^3$ ) is the volume of the aqueous phase,  $A$  is the interfacial area ( $\text{cm}^2$ ),  $C_{i,eq}$  (mg/L) is the equilibrium concentration,  $C_i$  (mg/L) is the concentration of the solute  $i$  in the aqueous phase at time  $t$ . The numerical values of parameter  $k_i$  (cm/s) were calculated by best-fit adjustment to the experimental results to the integrating function.

**Continuously flow through reaction system (CFTRS)** has been employed by many researchers to perform their experiments and study the releasing of chemicals from NAPL to aqueous phase [7, 8, 10, 51, 59-61]. This system couples mass transfer and one dimensional advection flux. The change of concentration in aqueous phase is described by:

$$\frac{dC_i}{dt} = \frac{A}{V_w} \cdot k_i \cdot \left( \frac{C_{i,o,t}}{P_{o/w}} - C_{i,t} \right) - \frac{Q}{V_w} \cdot C_{i,t} \quad (1.4)$$

where, the first term on the right-hand side of the equation is the first order rate model (similar to the model described for the batch experiment of eq 1.3),  $C_{i,o,t}$  is the concentration of solute  $i$  in organic phase at time  $t$ , and the second part describes the advection flux ( $Q$  is the flow rate mL/min) through the reactor,  $k_i$  (cm/s) can be obtained by fitting, using least squares regression to the integrated form of eq 1.4.

Another experiment was performed by Ramaswami and Luthy [59, 60] in slurry systems. However, a modeling framework, multi-step mass transport degradation model was used. That considers equilibrium partitioning at the NAPL-water interface, and three kinetic processes occurring in the aqueous phase: micropore sorption-diffusion, bulk aqueous phase transport and first order degradation of bulk phase substrate. The lumped  $k$  was computed from the experimental data for naphthalene and phenanthrene.

**Column experiments:** Two groups performed their experiments with the glass column [62, 63]. In Cho's work, the measured results were combined together to calculate bulk mass transfer rate coefficient  $\nu$  (1/s) as follows:

$$\nu = \frac{1}{4D_L} \left[ \left( q - \frac{2D_L}{L} \ln\left(1 - \frac{C}{C_s}\right) \right)^2 - q^2 \right] \quad (1.5)$$

where  $L$  is the length of the column,  $D_L$  (cm<sup>2</sup>/s) is the longitudinal dispersion coefficient, which was estimated from the experimental data, and  $q$  (cm/s) is the pore water velocity in the flow direction. The value of  $k$  and the specific interfacial areas  $a_{nw}$  (cm<sup>2</sup>/cm<sup>3</sup>) were used to extract so called mass transfer coefficient  $k_i$  (cm/s) using the following equation [64]:

$$k = \frac{\nu}{a_{nw}} \quad (1.6)$$

**Tank experiment:** tank experiment was carried out in Ahn's work [65], and the experimental results were compared with the estimated data by modified rigid sphere model and obtained the mass transfer coefficient  $k$  (cm/s).

$$k = \frac{d}{6} \frac{1}{1 - E_d} \frac{d(1 - E_d)}{d_a} \quad (1.7)$$

where,  $E_d$  is a dimensionless datum of the system computed by a numerical solution of the measured data,  $d_a$  is the characteristic length. And the results indicate that the mass transfer resistance depends on the resistances of the dispersed and the continuous phases under different limit conditions.

Above all, the mass transfer in aqueous system depends on the water flow velocity, on the contact area between NAPLs and other phase, on the physical properties of the porous medium, and on the properties and resistance of the interfacial and NAPL phase. It can be imagined as involving a series of several steps, of which one or more may be rate limiting. [49, 62, 63, 66, 67].

## 1.4 Effect of aging on mass transfer

Petrochemists have studied the crude oil interfacial phase for long time. These studies have shown temporal changes of the developing film on viscosity, interfacial tension and surface wettability of NAPLs interface. In the environmental field most of the studies focused on coal tar, creosote and crude oil, presumably because the interface

aging develops quite rapidly in contact with oxygenated water, air and solid particles (clay minerals etc.) [15] and sometimes could be observed visually. A few studies have reported a pronounced effect of film formation on PAHs partitioning from NAPLs in aqueous phase [4, 8, 58]. Aging processes at the NAPLs-water interface also affect the migration and the distribution of residual NAPLs phases in porous media, as well as the susceptibility of NAPLs to remediation by flushing technologies [13, 68-71]. The impacts of aging on the availability of a complex mixture of PAHs were evaluated by Reeves [9] and Huesemeann [12]. The results suggested that aging causes hydrophobic organic chemicals to become with time less extractable, less bioavailable, and therefore less threatening to environmental receptors.

However, the studies so far are limited and there is no direct method available to study such film. Therefore, application of indirect methods such as a set of chemical probe compounds and model NAPLs may be a promising approach to study the properties of NAPLs-water interface. A better understanding of the properties of NAPLs interface as well as the environmental factors that control the formation of such aged film is expected to improve our ability to assess and model processes in contaminated sites.

## 1.5 Objectives

The objectives of this research were therefore to study, (i) the effect of environmental conditions on formation of a viscous boundary layer, (ii) the compositional and properties' difference of the interfacial layers forming under different environmental conditions and (iii) the effect of boundary layer formation on mass transfer process of organic contaminants (e.g., phenols, heteroaromatics, PAHs) from NAPL to water phase. Accordingly, a simple batch experiment will be performed in a series of single solute NAPL-water systems to obtain the subcooled liquid solubilities, partitioning coefficient and mass transfer coefficients for some solutes. From that experiment activity coefficient can also be estimated. These experimental data can be used as references to compare with the data obtained in the complex and real NAPL-water systems. Further, pendant drop test, batch experiment, surface coating test and continuously flow through experiments will be performed to study the aging phenomena and prepare aged NAPLs. These experiments will be carried out under different environmental conditions, different pH value, appearance of oxidant or not



in aqueous solution which were assumed to be important factors affecting the properties of NAPL interface. The results from these tests can be used to evaluate the effects of these factors on aging process and concentration change of solutes in NAPL. Later, a continuously stirring flow through reaction system will be set up to perform the mass transfer experiment with model NAPL-water system. The experimental concentrations of different solutes will be used to modify and validate a numerical model, which needs to be established according to the mass balance equation. The simulated results can therefore be further compared with that in simple and real NAPL-water systems.

## 1.6 References

1. Strassner, J.E., Effect of pH on interfacial films and stability of crude oil-water emulsions. *Journal of Petroleum Technology*, 1968. 20(3): p. 303-12.
2. Batts, B.D. and A.Z. Fathoni, A literature review on fuel stability studies with particular emphasis on diesel oil. *Energy & Fuels*, 1991. 5(1): p. 2-21.
3. Spiecker, P.M. and P.K. Kilpatrick, Interfacial Rheology of Petroleum Asphaltenes at the Oil-Water Interface. *Langmuir*, 2004. 20(10): p. 4022-4032.
4. Luthy, R.G., et al., Interfacial films in coal tar nonaqueous-phase liquid-water systems. *Environmental Science and Technology*, 1993. 27(13): p. 2914-18.
5. Nelson, E.C., et al., Chemical Characterization of Coal Tar-Water Interfacial Films. *Environmental Science and Technology*, 1996. 30(3): p. 1014-22.
6. Barranco, F.T. and H.E. Dawson, Influence of aqueous pH on the interfacial properties of coal tar. *Environmental Science & Technology*, 1999. 33(10): p. 1598-1603.
7. Alshafie, M. and S. Ghoshal, The role of interfacial films in the mass transfer of naphthalene from creosotes to water. *Journal of Contaminant Hydrology*, 2004. 74(1-4): p. 283-298.
8. Ortiz, E., M. Kraatz, and R.G. Luthy, Organic phase resistance to dissolution of polycyclic aromatic hydrocarbon compounds. *Environmental Science & Technology*, 1999. 33(2): p. 235-242.
9. Reeves, W.R., et al., Impacts of Aging on In Vivo and In Vitro Measurements of Soil-Bound Polycyclic Aromatic Hydrocarbon Availability. *Environmental Science and Technology*, 2001. 35(8): p. 1637-1643.
10. Ghoshal, S., C. Pasion, and M. Alshafie, Reduction of benzene and naphthalene mass transfer from crude oils by aging-induced interfacial films. *Environmental Science & Technology*, 2004. 38(7): p. 2102-2110.
11. Totsche, K.U., Preferential flow and aging of NAPL in the unsaturated soil zone of a hazardous waste site: implicatins for contaminant transport. *J. Plant Nutr. Soil Sci* 2003. 166: p. 102-110.

12. Huesemann, M.H., T.S. Hausmann, and T.J. Fortman, Assessment of bioavailability limitations during slurry biodegradation of petroleum hydrocarbons in aged soils. *Environmental Toxicology and Chemistry*, 2003. 22(12): p. 2853-2860.
13. Zheng, J., J. Shao, and S.E. Powers, Asphaltenes from Coal Tar and Creosote: Their Role in Reversing the Wettability of Aquifer Systems. *Journal of Colloid and Interface Science*, 2001. 244(2): p. 365-371.
14. Poteau, S., et al., Influence of pH on Stability and Dynamic Properties of Asphaltenes and Other Amphiphilic Molecules at the Oil-Water Interface. *Energy & Fuels*, 2005. 19(4): p. 1337-1341.
15. Sullivan, A.P. and P.K. Kilpatrick, The Effects of Inorganic Solid Particles on Water and Crude Oil Emulsion Stability. *Industrial & Engineering Chemistry Research*, 2002. 41(14): p. 3389-3404.
16. Acevedo, S., et al., Isolation and Characterization of Low and High Molecular Weight Acidic Compounds from Cerro Negro Extraheavy Crude Oil. Role of These Acids in the Interfacial Properties of the Crude Oil Emulsions. *Energy & Fuels*, 1999. 13(2): p. 333-335.
17. Li, M., et al., Interfacial film properties of asphaltenes and resins. *Fuel*, 2002. 81(14): p. 1847-1853.
18. Acevedo, S., et al., Asphaltenes and Other Natural Surfactants from Cerro Negro Crude Oil. Stepwise Adsorption at the Water/Toluene Interface: Film Formation and Hydrophobic Effects. *Energy & Fuels*, 2005: p. ACS ASAP.
19. Anonymous, Petroleum products - Determination of oxidation stability of gasoline - Induction period method, IOS, Editor. 1994, International Organisation for Standardization.
20. Fathoni, A.Z. and B.D. Batts, A literature review of fuel stability studies with a particular emphasis on shale oil. *Energy & Fuels*, 1992. 6(6): p. 681-93.
21. Holden, P.A., et al., Assessing the role of *Pseudomonas aeruginosa* surface-active gene expression in hexadecane biodegradation in sand. *Applied and Environmental Microbiology*, 2002. 68(5): p. 2509-2518.
22. Viamajala, S., et al., Solubilization, solution equilibria, and biodegradation of PAH's under thermophilic conditions. *Chemosphere*, 2007. 66(6): p. 1094-1106.
23. Li, H., et al., Role of Soil Manganese in the Oxidation of Aromatic Amines. *Environmental Science and Technology*, 2003. 37(12): p. 2686-2693.
24. McBride, M.B., Adsorption and oxidation of phenolic compounds by iron and manganese oxides. *Soil Science Society of America Journal*, 1987. 51(6): p. 1466-72.
25. Petrie, R.A., P.R. Grossl, and R.C. Sims, Oxidation of Pentachlorophenol in Manganese Oxide Suspensions under Controlled Eh and pH Environments. *Environmental Science and Technology*, 2002. 36(17): p. 3744-3748.
26. Pizzigallo, M.D.R., et al., Manganese and iron oxides as reactants for oxidation of chlorophenols. *Soil Science Society of America Journal*, 1995. 59(2): p. 444-52.

27. Stone, A.T. and J.J. Morgan, Reduction and dissolution of manganese(III) and manganese(IV) oxides by organics: 2. Survey of the reactivity of organics. *Environmental Science and Technology*, 1984. 18(8): p. 617-24.
28. Altarawneh, M., et al., Quantum Chemical Study of Low Temperature Oxidation Mechanism of Dibenzofuran. *Journal of Physical Chemistry A*, 2006. 110(50): p. 13560-13567.
29. Baik, J.S. and N.H. Lee, Mechanistic studies on the O<sub>2</sub>-mediated oxidation of olefins in the presence of (Schiff-base)Mn(III) catalyst and NaBH<sub>4</sub>. *Bulletin of the Korean Chemical Society*, 2006. 27(5): p. 765-768.
30. Tursi, F., et al., Styrene oxidation to styrene oxide in human erythrocytes is catalyzed by oxyhemoglobin. *Experientia* FIELD Full Journal Title:Experientia, 1983. 39(6): p. 593-4.
31. Nie, L., et al., Benzaldehyde synthesis via styrene oxidation by O<sub>2</sub> over TiO<sub>2</sub> and TiO<sub>2</sub>/SiO<sub>2</sub>. *Catalysis Communications*, 2007. 8(3): p. 488-492.
32. Mijangos, F., F. Varona, and N. Villota, Changes in Solution Color During Phenol Oxidation by Fenton Reagent. *Environmental Science & Technology*, 2006. 40(17): p. 5538-5543.
33. Haderlein, S.S., Torsten, Aging of NAPLs interfacial phase and its effects on mass transfer. 2006. *DFG proposal*
34. Jeribi, M., et al., Adsorption kinetics of asphaltenes at liquid interfaces. *Journal of Colloid and Interface Science*, 2002. 256(2): p. 268-272.
35. ASTM, Standard Test Method for Characteristic Groups in Rubber Extender and Processing Oils and Other Petroleum -Derived Oils by the Clay-Gel nAbsorption Chromatographic Method, in *Annual Book of ASTM Standards*. 2003.
36. Mansoori, G.A., Principles of Nanotechnology: Molecular-Based Study Of Condensed Matter In Small Systems. 2005: World Scientific Publishing Company 341.
37. Espinat, D., et al., Effects of Temperature and Pressure on Asphaltenes Agglomeration in Toluene. A Light, X-ray, and Neutron Scattering Investigation. *Energy & Fuels*, 2004. 18(5): p. 1243-1249.
38. Alboudwarej, H., et al., Sensitivity of Asphaltene Properties to Separation Techniques. *Energy & Fuels*, 2002. 16(2): p. 462-469.
39. Acevedo, S., et al., Adsorption of Asphaltenes at the Toluene-Silica Interface: A Kinetic Study. *Energy & Fuels*, 2003. 17(2): p. 257-261.
40. Rahmani, N.H.G., T. Dabros, and J.H. Masliyah, Online Optical Monitoring of Asphaltene Aggregation. *Industrial & Engineering Chemistry Research*, 2005. 44(1): p. 75-84.
41. Strausz, O.P., et al., Additional Structural Details on Athabasca Asphaltene and Their Ramifications. *Energy & Fuels*, 1999. 13(2): p. 207-227.
42. Gray, M.R., et al., Melting and Fluid Behavior of Asphaltene Films at 200-500 DegC. *Energy & Fuels*, 2004. 18(5): p. 1419-1423.

43. Alboudwarej, H., et al., Adsorption of Asphaltenes on Metals. *Industrial & Engineering Chemistry Research*, 2005. 44(15): p. 5585-5592.
44. Branco, V.A.M., et al., Asphaltene flocculation and collapse from petroleum fluids. *Journal of Petroleum Science & Engineering*, 2001. 32(2-4): p. 217-230.
45. Harvey W. Yarranton, H.A., Rajesh Jakher, Investigation of asphaltene association with vapor pressure osmometry and interfacial tension measurements. *Ind. Eng. Chem. Res.*, 2000. 39(8): p. 2916-2924.
46. Artok, L., et al., Structure and Reactivity of Petroleum-Derived Asphaltene. *Energy & Fuels*, 1999. 13(2): p. 287-296.
47. Peng, P.a., et al., Chemical Structure and Biomarker Content of Jinghan Asphaltenes and Kerogens. *Energy & Fuels*, 1999. 13(2): p. 248-265.
48. Giavedoni, M.D. and J.A. Deiber, A model of mass transfer through a fluid-fluid interface. *Chemical Engineering Science*, 1986. 41(7): p. 1921-5.
49. Heyse, E., et al., Nonaqueous phase liquid dissolution and soil organic matter sorption in porous media: review of system similarities. *Critical Reviews in Environmental Science and Technology*, 2002. 32(4): p. 337-397.
50. Schwarzenbach, R.P., *Environmental Organic Chemistry*. 2003, New Jersey: John Wiley & Sons. 1313.
51. Schlupe, M., et al., Mechanisms affecting the dissolution of nonaqueous phase liquids into the aqueous phase in slow-stirring batch systems. *Environmental Toxicology and Chemistry*, 2001. 20(3): p. 459-466.
52. Lewis, W.K., *The principles of countercurrent extraction*. *Journal of Industrial and Engineering Chemistry (Washington, D. C.)*, 1916. 8: p. 825-33.
53. Whitman, W.G., Preliminary experimental confirmation of the two-film theory of gas absorption. *Chemical and Metallurgical Engineering*, 1923. 29: p. 146-8.
54. Higbie, R., The rate of absorption of a pure gas into a still liquid during short periods of exposure. *Transactions of American Institute of Chemical Engineers*, 1935. 31: p. 365-89.
55. Danckwerts, P.V., Significance of liquid-film coefficients in gas absorption. *Journal of Industrial and Engineering Chemistry (Washington, D. C.)*, 1951. 43: p. 1460-7.
56. Bennett, C.O. and J.E. Myers, *Momentum, Heat and Mass Transfer*. 3rd Ed. 1981. 864 pp.
57. Ghoshal, S., A. Ramaswami, and R.G. Luthy, Biodegradation of Naphthalene from Coal Tar and Heptamethylnonane in Mixed Batch Systems. *Environmental Science and Technology*, 1996. 30(4): p. 1282-91.
58. Mahjoub, B., et al., Phase partition of organic pollutants between coal tar and water under variable experimental conditions. *Water Research*, 2000. 34(14): p. 3551-3560.
59. Ramaswami, A. and R.G. Luthy, Mass Transfer and Bioavailability of PAH Compounds in Coal Tar NAPL-Slurry Systems. 1. Model Development. *Environmental Science and Technology*, 1997. 31(8): p. 2260-2267.

60. Ramaswami, A., S. Ghoshal, and R.G. Luthy, Mass Transfer and Bioavailability of PAH Compounds in Coal Tar NAPL-Slurry Systems. 2. Experimental Evaluations. *Environmental Science and Technology*, 1997. 31(8): p. 2268-2276.
61. Mukherji, S., C.A. Peters, and W.J. Weber, Jr., Mass Transfer of Polynuclear Aromatic Hydrocarbons from Complex DNAPL Mixtures. *Environmental Science and Technology*, 1997. 31(2): p. 416-423.
62. Cho, J., M.D. Annable, and P.S.C. Rao, Measured Mass Transfer Coefficients in Porous Media Using Specific Interfacial Area. *Environmental Science and Technology*, 2005. 39(20): p. 7883-7888.
63. Benhabib, K., M.-O. Simonnot, and M. Sardin, PAHs and Organic Matter Partitioning and Mass Transfer from Coal Tar Particles to Water. *Environmental Science & Technology*, 2006. 40(19): p. 6038-6043.
64. Faisal Anwar, A.H.M., et al., Mass Transfer Correlation for Nonaqueous Phase Liquid Volatilization in Porous Media. *Environmental Science and Technology*, 2003. 37(7): p. 1277-1283.
65. Ahn, B.S. and W.K. Lee, Simulation and experimental analysis of mass transfer in a liquid-liquid stirred tank extractor. *Industrial & Engineering Chemistry Research*, 1990. 29(9): p. 1927-35.
66. Weber, W.J., Jr., P.M. McGinley, and L.E. Katz, Sorption phenomena in subsurface systems: concepts, models and effects on contaminant fate and transport. *Water Research*, 1991. 25(5): p. 499-528.
67. Brusseau, M.L., Q. Hu, and R. Srivastava, Using flow interruption to identify factors causing nonideal contaminant transport. *Journal of Contaminant Hydrology*, 1997. 24(3-4): p. 205-219.
68. Dwarakanath, V., R.E. Jackson, and G.A. Pope, Influence of Wettability on the Recovery of NAPLs from Alluvium. *Environmental Science and Technology*, 2002. 36(2): p. 227-231.
69. Hugaboom, D.A. and S.E. Powers, Recovery of coal tar and creosote from porous media: the influence of wettability. *Ground Water Monitoring and Remediation*, 2002. 22(4): p. 83-90.
70. Giese, S.W. and S.E. Powers, Using polymer solutions to enhance recovery of mobile coal tar and creosote DNAPLs. *Journal of Contaminant Hydrology*, 2002. 58(1-2): p. 147-167.
71. Zhao, W. and M.A. Ioannidis, Effect of NAPL film stability on the dissolution of residual wetting NAPL in porous media: A pore-scale modeling study. *Advances in Water Resources*, 2007. 30(2): p. 171-181.



## Chapter 2 Determination of the subcooled liquid solubilities of PAHs in partitioning batch experiments

### 2.1 Motivation

Many organic contaminants occur as components of complex multicomponent mixtures that are present in the environment as separate organic liquid phases, commonly referred to as nonaqueous phase liquids (NAPLs). Multicomponent NAPLs containing polycyclic aromatic hydrocarbons (PAHs) and other contaminants exist as liquids even though many of their individual components are solids in their pure form at ambient temperature. For those compounds, a suitable reference state is the pure subcooled liquid (a hypothetical state of the liquid), and their water solubility ( $S_i$ ) in equilibrium with the NAPL is determined by the solubility of the compounds in a (subcooled) liquid state ( $S_{i,sub}$ ) rather than by the solid's solubility.

In the literature subcooled liquid solubility was estimated and predicted from the solid water solubility and fugacity ratio of the solid and subcooled liquid phase ( $f^s/f^l$ ), but rarely derived from experiment. Fugacity is a measure of chemical potential of the compound from its environment, and the fugacity ratio describes how close the substance behaves like its reference state. Unfortunately, reliable water solubility data are lacking for many environmental interest compounds as well as the fugacity ratio (or enthalpy of fusion)[1, 2]. There are numerous conflicting water solubility values having been reported in the literature for many PAHs, and published data of fugacity ratios are however missing for most of the PAHs [2-5].

### 2.2 Thermodynamic theory

The partitioning of organic pollutants in the environment is determined by their thermodynamic properties in the gas, liquid, and solid phases. Some of these properties are introduced briefly as following.

#### 2.2.1 Solubility and activity coefficient

Solubility refers to the ability for a given substance (the solute) to dissolve in a solvent. Water solubility,  $S_i$ , or the aqueous solubility of the compound, tells us the maximum concentration of a given chemical that can be dissolved in pure water at a given temperature. It is one of the most important physicochemical parameters that

affects the fate and transport of organic chemicals in the environment, especially in the subsurface.

The activity coefficient,  $\gamma_i$ , accounts for the potential nonideal behavior resulting from intermolecular interactions. The value of the activity coefficient expresses the escaping tendency of a given compound from the respective solution relative to the compound's escaping tendency from its own pure liquid (or other reference states) [6](p 80). Its values close to 1 are found in those cases in which molecular interactions in the solution are nearly the same as in the pure liquid compound, and it can be positive ( $>1$ ) or negative ( $<1$ ) in the nonideal solution [6, 7]. The activity coefficient at infinite dilution in water and in liquid mixture of organic compounds is an important thermodynamic property. Different techniques and models have been used for the measurement of activity coefficients of pure compounds at infinite aqueous dilution [7-14]. However, there are a few reports about the measurement of activity coefficients in liquid organic mixtures [15-17].

### 2.2.2 Subcooled liquid solubility and fugacity ratio

A subcooled liquid is an imaginary liquid that is cooled below its melting point without allowing it to solidify [6, 18]. The aqueous solubility,  $S_{i,sub}$ , of this hypothetical liquid tells us something about the molecular interactions of the compound in its pure liquid state at a temperature where the compound is actually a solid.

The concept of fugacity  $f$ , was introduced by Lewis [19]. It is a measure of chemical potential in the form of adjusted pressure. It directly relates to the tendency of a substance to prefer one phase (liquid, solid, gas) to another and it is a state function of matter at fixed temperature. It was defined as a function of their vapor pressures of pure liquids and solids.

For compounds that are solids, a suitable reference state for the solubilities in complex NAPLs is the pure liquid (subcooled liquid) at 1 atm and the temperature of interest. When the  $S_{i,sub}$  of a solid is the “energy cost” of a solid to its subcooled liquid state is given by the ratio of the fugacity of the pure solid ( $f^s$ ) to the fugacity of the subcooled liquid (the reference state,  $f^l$ ) [20], and  $S_{i,sub}$  is given:

$$S_{i,sub} = \frac{S_i}{f^s / f^l} \quad (2.1)$$



The fugacity ratio ( $f^s/f^l$ ) can be evaluated for the pure solute from its thermodynamic properties as discussed in many texts [21, 22],

$$\ln\left(\frac{f^s}{f^l}\right) = -\frac{\Delta H_f}{RT_t}\left(1 - \frac{T_t}{T}\right) + \frac{\Delta C_p}{R}\left(\left(1 - \frac{T_t}{T}\right) + \ln\left(\frac{T_t}{T}\right)\right) \quad (2.2)$$

where  $\Delta H_f$  (kJ/mol) is the enthalpy of fusion at the triple point temperature  $T_t$  (K),  $T$  is the system temperature,  $R$  (kJ.mol<sup>-1</sup>K<sup>-1</sup>) is the universal gas constant, and  $\Delta C_p$  (kJ.mol<sup>-1</sup>K<sup>-1</sup>) is the difference in the heat capacities of the liquid and solid. This equation allows computation of the reference fugacity ratio for a particular compound at the system temperature given known values of the thermodynamic properties  $\Delta H_f$ ,  $T_t$  and  $\Delta C_p$ . With an assumption that the compound's melting temperature  $T_m$  is approximately equal to its triple point ( $T_t$ ) and the heat capacities of solid and liquid  $i$  are roughly equal, a simplified version of the equation can be obtained:

$$\ln\left(\frac{f^s}{f^l}\right) = \frac{\Delta H_f}{RT_m}\left(\frac{T_m}{T} - 1\right) \quad (2.3)$$

$T_m$  values are fairly easy to measure, and numerous observations have been reported in the literature for PAHs.  $\Delta H_f$  is difficult to measure, and fewer values have been reported for them. Where data are unavailable,  $\Delta H_f$  can be approximated from  $\Delta H_f = T_m \cdot \Delta S_f$ , where  $\Delta S_f$  (kJ.mol<sup>-1</sup>K<sup>-1</sup>) is the entropy of fusion, and Yalkowsky has shown the entropy of fusion to be roughly constant as 13.5 cal.mol<sup>-1</sup>.K<sup>-1</sup> (56.5 J.mol<sup>-1</sup>.K<sup>-1</sup>) for rigid organic molecules such as PAHs [23]. This approximation method is commonly used for data compilations [22, 24-26].

However, significant errors for  $S_{i,sub}$  and  $f^s/f^l$  result if inaccurate values are used for  $\Delta H_f$ ,  $T_m$  and the incorrect assumption for heat capacities and triple point temperature. In reality,  $T_m$  is a little higher than  $T_t$  for some compounds and a little lower for others [6] (p101).

## 2.3 Objectives

Objectives of this study are therefore to (i) develop an experimental method for the determination of subcooled liquid solubilities of PAHs presenting in a model NAPL-aqueous phase systems, (ii) extrapolate  $S_{i,sub}$  from the experimental data for PAHs, and (iii) estimate the  $\gamma_i$  and  $f^s/f^l$  of solute in one component model NAPL.

## 2.4 Materials and methods

### 2.4.1 Materials

In this study, toluene was used as solvent for the model NAPL due to its high dissolution capability and the chemical similarity to the tested PAHs.

The PAHs studied with their associated purities were: naphthalene (98%), 1-Methylnaphthalene (99%), 2-Methylnaphthalene (99%), phenanthrene (98%), anthracene (99%). They were obtained from Aldrich except for phenanthrene, which was from Alfa Aesar, and were used without further purification. Acetonitrile (HPLC-grade) was obtained from Mallinckrodt Baker.

### 2.4.2 Approach of the method design

If the compound behaves ideal in the model NAPL, which means the intermolecular interactions from the solvent-solvent and solute-solute in the pure state to the solvent-solute in the solution state are similar, then activity coefficient,  $\gamma_i$  is unity, and the equilibrium aqueous phase concentration  $C_{i,eq}$  (mg/L) can be described by a simplified version of Raoult's law (eq.2.4a),

$$C_{i,eq} = \chi_i \cdot \gamma_i \cdot S_{i,sub} \quad (\text{Raoult's law}) \quad (2.4)$$

$$C_{i,eq} = \chi_i \cdot S_{i,sub} \quad \text{while } \gamma_i=1 \quad (2.4a)$$

where  $\chi_i$  (-) is the mole fraction for compound  $i$ . Furthermore, in this special case  $C_{i,eq}$  can be linearly extrapolated to  $S_{i,sub}$  where  $\chi_i$  is unity as the relationship between  $C_{i,eq}$  and  $\chi_i$  is linear. If the relationship is non-linear, which implies that the molecular interactions of a constituent in the organic liquid solution are different from that compound in a liquid of pure material, and  $\gamma_i$  being far away from unity. Then a general form of Raoult's law including the function of  $\gamma_i$  ( $\gamma_i = f(\chi_i)$ ) can be used to express the dependency of the  $\gamma_i$  in the system composition [15, 17] as:

$$C_{i,eq} = f(\chi_i) \cdot \chi_i \cdot S_{i,sub} \quad (2.5)$$

$S_{i,sub}$  can then be obtained by a non-linear extrapolation from this modified form of Raoult's law to the region where  $\gamma_i$  is one.

### 2.4.3 Batch technique

#### **Batch experiment to determine the equilibrium aqueous phase concentration**

The batch experiment was performed in this study is shown in Figure 2.1. All of the samples were prepared in triplicate, and the operation process is as follows.



**Figure 2.1** Setting up of the batch experiment conducted in this work

The same volume of model NAPL (i.e., a toluene solution of a certain compound with known  $\chi$ ) and millipore water were added to the 5-mL crimp cap vial and sealed with a Teflon lined septum. The vials were inverted allowing water phase contacting with the caps, and put in the ultrasonic bath for 15 min followed by centrifugation (Heraeus Spatech) at 1500 rpm for 3-5 min to get rid of the fine NAPL droplets. Finally, the vials were stored in a 20 °C room until the equilibrium concentration was obtained. The equilibrium time period was determined by a separated experiment.

For most of the compounds, the experiments were performed at ambient temperature ( $22 \pm 2$  °C). However, the solubility of anthracene in toluene is too low, the water bath was used and the experiments were carried out at a higher temperature ( $40 \pm 2$  °C). For a certain compound, a series of batch experiments were conducted with various mole fractions of target compounds in NAPL as illustrated in Figure 2.1 and listed in Table 2.1.  $C_{i,t}$  is the prepared initial solute's concentration in toluene, and  $\chi_i$  is the initial mole fraction.

**Table 2.1** Initial molar fractions and concentrations of solutes employed in the batch experiment

Compound	Abbreviation	$X_i (-) / C_{i,t}(\text{g/L})$				
Naphthalene	Nap	0.001/1.50	0.01/12.22*	0.05/64.12	0.1/134.1	0.2/293.7
2-Methylnaphthalene	2-Mnap	0.01/13.73*	0.05/70.84	0.1/147.8	0.2/334.2	
1-Methylnaphthalene	1-Mnap	0.05/70.11*	0.1/147.9	0.2/335.2	0.4/895.4	0.6/2007
Acenaphthene	Ace	0.001/1.22	0.005/7.79	0.01/14.18*	0.05/76.44	
Phenanthrene	Phe	0.001/1.32	0.01/17.15*	0.05/86.63	0.1/183.9	0.15/293.2
Anthracene**	Ant	0.0007/1.63	0.004/6.91*	0.0075/12.23		

\* experiment to check the time to reach the equilibrium

\*\*the experiments performed at higher temperature of  $40 \pm 2$  °C

### Batch experiment to determine the aqueous phase concentration

It is assumed that the equilibrium time periods for a certain compound are similar even at different  $\chi_i$  with same experimental setting up, and the aqueous phase samples were taken after a longer time than the tested equilibrium time. With this test, the equilibrium time and the solute concentrations at different time period can be obtained, the mass transfer process can also be observed. In brief (detailed description of the operation process see above), seven or more identical samples were prepared and the aqueous samples were taken at different time periods from different vials. The aqueous phase concentrations were obtained. The equilibrium time period was taken when the aqueous phase concentration increased less than 5% during 3 continual sampling time periods. The tested  $\chi_i$  for different compounds are marked in Table 2.1.

The time dependent dissolution of the PAHs in aqueous phase can be given as eq 1.3, and the integration function of eq 1.3 is:

$$C_i = C_{i,eq} \left(1 - \exp\left(-k_i \frac{A}{V_w} t\right)\right) \quad (2.6)$$

where  $V$  (L, or  $\text{cm}^3$ ) is the volume of the aqueous phase,  $A$  ( $\text{cm}^2$ ) is the interfacial area,  $C_{i,eq}$  (mg/L) is the equilibrium concentration,  $C_i$  is the concentration of the solutes  $i$  in the aqueous phase at different time.  $k_i$  (cm/s) is the mass transfer coefficient, and is assumed a constant for one compound at a given environmental condition during a short time period. The values of  $k$  were calculated by best-fit adjustment to the experimental results with the minimum relative residual sum of squares (RRSS).

$$RRSS = \sum_{k=n}^n \left(\frac{C_i - C'_i}{C_i}\right)^2 \quad (2.7)$$

where  $C_i$  is the effluent concentration data point, and  $C'_i$  is the corresponding model prediction.

#### 2.4.4 Estimation of partitioning coefficient and activity coefficient

The toluene-water partitioning coefficients ( $P_{t/w}$ ) expresses as:

$$P_{i,t/w} = \frac{C_{i,t}}{C_{i,eq}} = \frac{V_w}{V_t} \cdot \frac{\gamma_{iw}}{\gamma_{it}} \quad (2.8)$$

$C_{i,t}$  (mg/L) is the equilibrium concentration of the compounds  $i$  in toluene, and it was assumed equal to that of the initial organic phase concentration (list in Table 1) since the depletion of mass is relatively small.

As introduced in the previous part, if there is a linear relationship between  $C_{i,eq}$  and  $\chi_i$ , which suggest an ideal behavior of the compound in the NAPLs solution, then  $\gamma$  is close to 1. Otherwise, a modified Raoult's law (eq. 2.5) could be used to estimate the equilibrium aqueous concentration. In this case,  $\gamma_i$  is a function of  $\chi_i$  as ( $\gamma_i = f(\chi)$ ) rather than unity.

#### 2.4.5 Analytical methods

Aqueous sample of the solutions was drawn out by a 5-mL glass syringe from the vials in the batch experiment. In this step, care should be taken to avoid that the needle of the syringe contacts the NAPL phase. The aqueous phase concentrations were measured with HPLC and/or GC-MS.

##### **HPLC**

A standard high performance liquid chromatography (HPLC) system (Bischoff Analysentechnik und Geräte GmbH, Germany) equipped with an analytical column (Reversed phase, 125×4.6 mm, Enviro Sep PP. 5.0  $\mu$ m, UV, Bischoff) was utilized in the measurements. The analytes were eluted by an isocratic acetonitrile (HPLC grade) / water (Millipore water) mixture (70:30 v:v). The eluent was degassed by an online degasser (Degasys, DG-120, Germany) before entering the HPLC system with a flow rate of 0.88 ml/min and pressure of 5.6 MPa. The sample was introduced to the column by a fixed volume injection-loop-valve (20  $\mu$ l) at ambient temperature. The inner diameter of steel capillaries was 0.13mm, and its length between injector, column, and UV detector was kept as short as possible. An UV detector with a wavelength setting of 254 nm was used during the analysis. The data interface was LC-CaDI 2214. MCADI system was used to detect the peaks and the peak area was integrated manually.

##### **GC-MS**

Acenaphthene and Anthracene were measured by GC-MS, since their  $C_{i,eq}$  were too low to be quantified by HPLC. The aqueous samples (1-1.5 mL) were spiked with internal standards (acenaphthene-d<sub>10</sub> and phenanthrene-d<sub>10</sub> toluene solution) and

extracted by 0.5 ml to 1 ml cyclohexane according to the estimated concentrations. These extracts were measured by GC-MS, a gas chromatography (HP 5890/ II ) connected to a mass selective detector (HP 5972 MSD). Analytes were separated using a 30 m × 0.25 mm DB-5 MS column (J&W Scientific) with 0.25 μm film thickness. The injector temperature was 270 °C and injection volume was 1 μl in splitless mode. Helium (99.999%) was the carrier gas at a constant flow of 0.6 mL/min. The oven temperature was held for 2 min at 50 °C, then increased at a rate of 8 °C/min to 90 °C, increased at 18 °C/min to 270 °C. held for 10 min and finally raised to 310 °C (held for 6.5 min), the total time period for a run was 48 min.

## 2.5 Results and discussion

### 2.5.1 Mass transfer coefficient

With the batch experiments,  $C_i$  at different time periods can be measured. The equilibrium time period was obtained and the mass transfer coefficient ( $k$ ) can be calculated according to eq 2.6. Figure 2.2 shows the calculated concentrations match with experimental  $C_i$  with a best fitting  $k$ . The equilibrium time periods and fitted  $k$  are listed in Table 2.2, the values of  $k$  are comparable with the published data in the literatures (Table 2.3). The data show a clear trend of decreasing  $k$  with increasing of the equilibrium time periods.

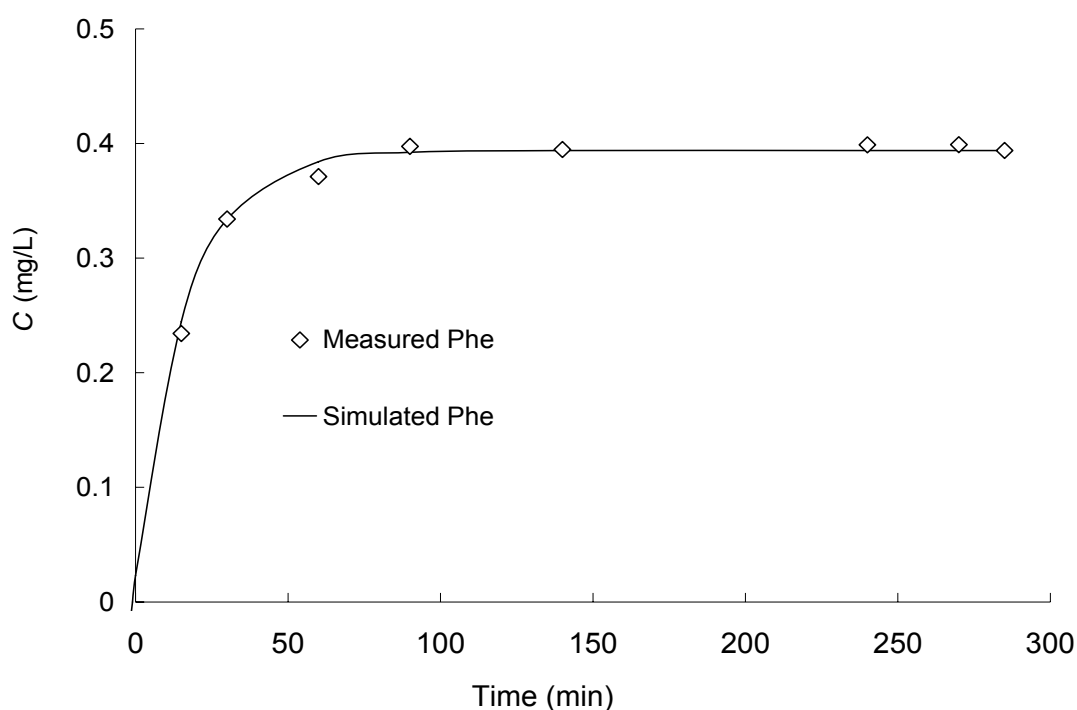


Figure 2.2 Comparison of the simulated and measured aqueous phase concentrations

**Table 2.2 Equilibrium time periods and mass transfer coefficients of PAHs**

Compound	Equilibrium time (min)	Mass transfer coefficient $k$ (cm/s10E-4)	RRSS
Naphthalene	80	11.0	0.001
2-Methylnaphthalene	170	4.08	0.011
1-Methylnaphthalene	374	0.98	0.016
Acenaphthene	250	5.77	0.016
Phenanthrene	140	10.1	0.0004
Anthracene	240	2.77	0.014

**Table 2.3 Published data for mass transfer coefficients (10e-4 cm/s)**

NAPLs		Phenanthrene	Naphthalene	Pyrene	Benzene	m/p-Xylene
Diesel	Schluep ETC 2001	3.2	3.4		3.9	3.2
Creosote	Alshafie & Ghoshal J. Contam. Hydrol. 2004		4-6			
Crude oil	Ghoshal EST 2004		7-12		6-11	
Gasoline	Ghoshal EST 2004		11.7		6.7	
Coal tar	Ghoshal EST 1996)		2.44-3.05			
Model NAPL*	Mukherji EST 1997		8.5-14.2			
Petrolatum	Ortiz et al. EST 1999	7	6	9		

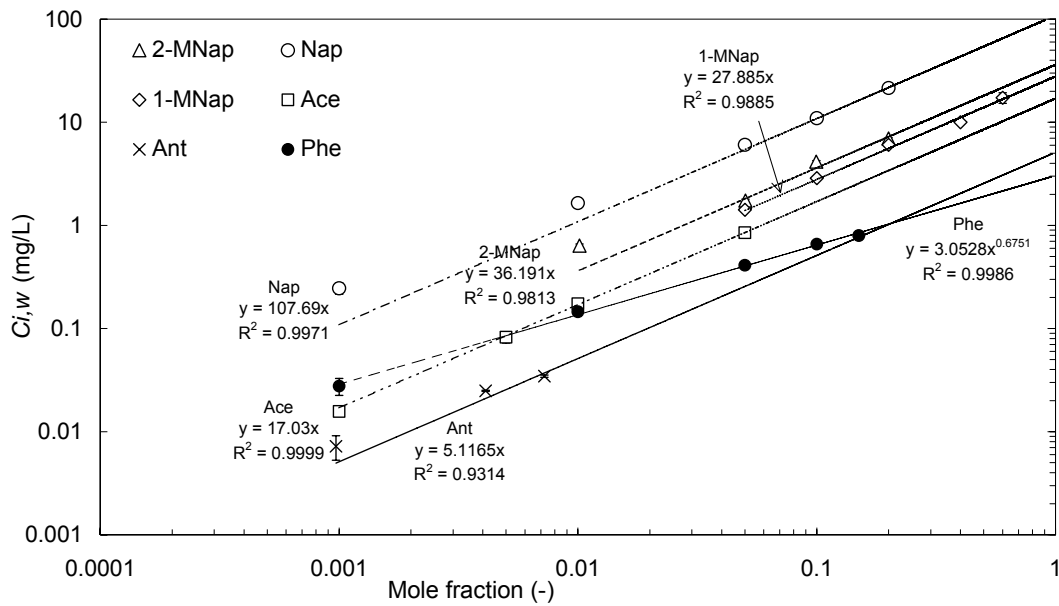
[15, 24, 29-31]

\* toluene solution of Naphthalene, 1-methylnaphthalene, 2-ethylnaphthalene, acenaphthene, fluorene, phenanthrene, fluoranthene and pyrene.

## 2.5.2 Subcooled liquid solubility and enthalpy of fusion

The subcooled liquid solubility was obtained by extrapolating the measured  $C_{i,eq}$  to a mole fraction of one. It is shown in Figure 2.3,  $C_{i,eq}$  has a linear relationship to  $\chi_i$  for Nap, 2-MNap, 1-MNap, Ace and Ant, which indicates the ideal behavior of these compounds in toluene. Their trendlines lines in log-log scale figure being parallel indicated that their slopes and  $\gamma_i$  should be similar, and  $\gamma_i$  were approximate to one for these compounds. Therefore,  $S_{i,sub}$  can be predicted by linearly while extrapolating  $\chi_i$  to unity for the solid compounds of Nap, 2-MNap, Ace and Ant. For 1-MNap, which is liquid at ambient temperature, the experimental result was used to validate this

method. The extrapolated concentration of 1-MNap, is  $S_i$ , and being 27.9 mg/L for this study which is comparable to the literature value of 28.0 mg/L [25, 27] and 26-28

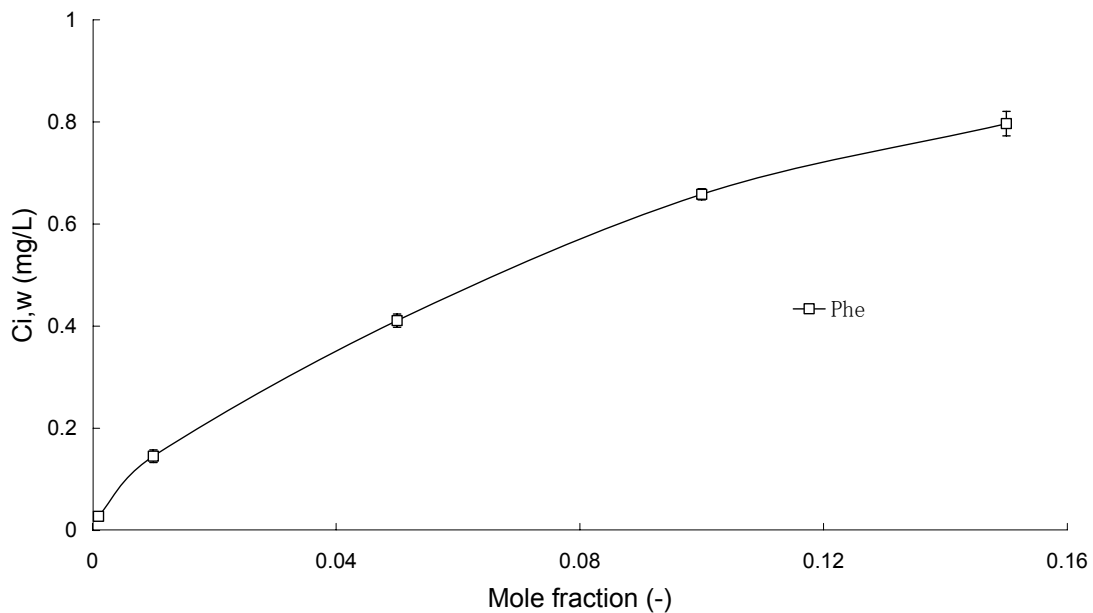


**Figure 2.3 Concentrations vs. mole fractions for compounds tested in batch experiments. It is also an illustration of extrapolation process from the  $C_{i,eq}$  to  $S_{i,sub}$  where the  $\chi_i$  is unity**

mg/L [28]. However, for Phenanthrene, the relationship between  $C_{i,eq}$  and  $\chi_i$  appears to be slightly non-linear as shown in Figure 2.4, which can be described best by.

$$C_{i,eq} = 3.1 \cdot \chi_i^{0.675} \quad R^2=0.999 \quad n=5 \quad (2.9)$$

The nonlinear relationship indicates deviation from ideality, and  $\gamma_i$  being variable in



**Figure 2.4 Concentrations vs. mole fractions for Phenanthrene**



toluene solution. In this case,  $\gamma_i$  should be positive ( $>1$ ), and decreasing with increasing  $\chi_i$  of Phe till 1 where  $\chi_i$  also being 1. This maybe attributed to the weak of attractive interactions between Phe and the water molecules and/or the very high free energy costs for cavity formation in the toluene solutions at a low mole fraction. In this case, the modified Raoult's law (eq. 2.5) can be used to describe this system, and the function of  $\gamma$  can be deduced as:

$$\gamma = f(\chi) = \chi^{-0.325} \quad (2.10)$$

which indicates that  $\gamma$  of Phe in toluene solution is a power function of the  $\chi$  in this liquid organic mixture.

With  $S_i$  and the extrapolated data of  $S_{i,sub}$ , the fugacity ratio ( $f^s/f^l$ ) can be calculated according to transforming form of eq. 2.1, as well as  $\Delta H_f$  according to eq. 2.3 with a given  $T_m$ . All of these results are listed in Table 2.4. The extrapolated  $S_{i,sub}$  and  $\Delta H_f$  are comparable with the published data, especially for Nap, Ant and 1-MNap, which proved that a sequence of batch experiments can be conducted to determine these important physicochemical parameters. However, for 2-Mnap, Ace and Phe a slight deviation exists from the predicted values comparing to that in the published literature data. This may indicate the error of the measurement for the low concentration samples, nonidealities of NAPL phase or may simply reflect the uncertainty in the parameters (e.g.,  $T_m$ ,  $S_i$ ) used in prediction of the published data.

**Table 2.4 Extrapolated Subcooled liquid solubility and enthalpy of fusion**

Compound	$S_i$ (mg/L) <sup>a</sup>	$S_{i,sub}$ by calculation (mg/L) <sup>a</sup>	Melting Point °C <sup>b</sup>	$S_{i,sub}$ from batch experiment (BE) (mg/L)	$f^s/f^l$ calculated from BE	$\Delta H$ calculated from BE (kJ/mol)	$\Delta H$ published (kJ/mol) <sup>c</sup>
Nap	31.7	105.67	80.6	107.7±1.3	0.294	-17.35	18.99
2-Mnap	25.4	29.53	34.58	36.1±1.4	0.704	-17.89	
1-MNap	28	28	-22	27.9±1.9	1.004	-0.05	
Ace	3.93	19.65	93.4	17.2±0.01	0.228	-17.92	21.46
Phe	1.18	4.21	99.5	3.05±0.06	0.387	-10.82	16.46
Ant	0.05	5	215	5.1±0.08	0.010	-28.11	29.39

a. from Peters 1997 and 1999 [25, 32]

b. from the physical properties database (PHYSPROP) <http://www.syrres.com/esc/physprop.htm>

c. from Allen [33]

However, the limitation of this method is also obvious. That is the solubility limit of the solid solute in toluene, which can be expressed thermodynamically as [25]:

$$\chi_i \leq \frac{1}{\gamma_i} \left( \frac{f^s}{f^l} \right) \quad (2.11)$$

The maximum experimental  $\chi_i$  was about 0.2 (for Nap, and 2-MNap) at ambient temperature, and it was even lower for other compounds, e.g., Ant stays below 0.01 even in the higher temperature as 40 °C ( $\pm 2$  °C). To solve this problem, another solvent 1-MNap was also used in this study to check the maximum  $\chi$  of Ant due to its too low toluene solubility, since its molecular structure is more similar to Ant. However, there was no evident increase of the solubility using another solvent or conducting at higher temper. Therefore, the error exists and also maybe amplified when extrapolating the measured data to a high  $\chi_i$  of unity. This may be contributes to the error of extrapolated  $S_{i,sub}$  of 2-MNap, Ace and Phe. Therefore, even Ant shows the linear relation, but the linearity is not so good as others, and the error is obvious.

### 2.5.2 Partitioning coefficient

The toluene-water partitioning coefficient ( $P_{t/w}$ ) was calculated according to eq. 2.7, and all of the data are shown in Figure 2.5, and listed in Table 2.5. The figure shows clearly that for different compounds, the average value of  $P_{t/w}$  and the value for an identified  $\chi_i$  increased with the decrease of water solubility. This is consistent to the essential point of view of Schwarzenbach [6] (p 215). However, all of the  $P_{t/w}$  for one

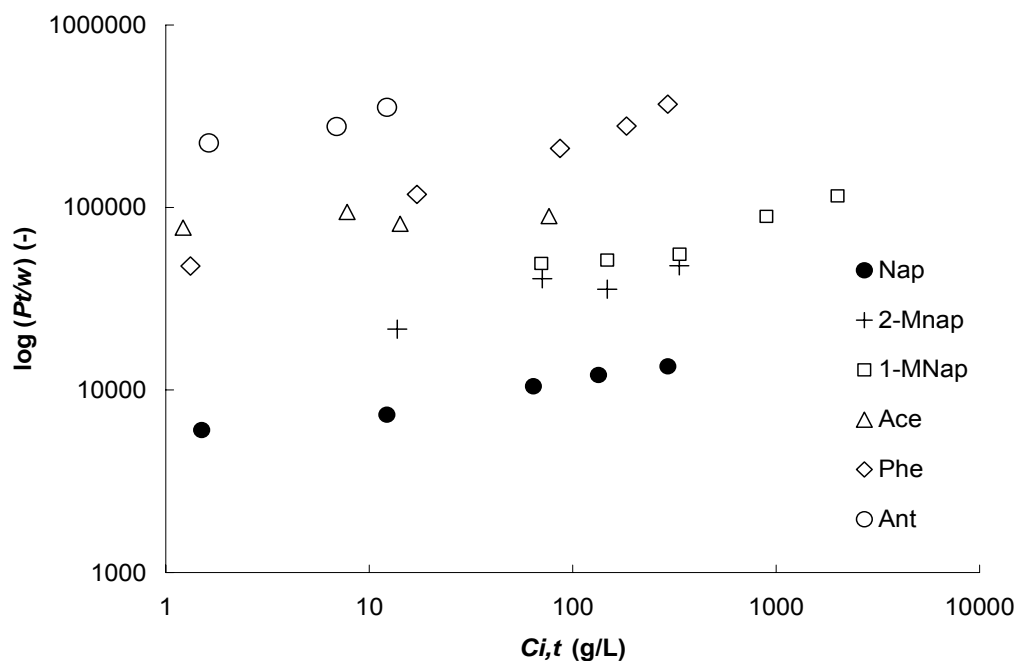


Figure 2.5 Partitioning coefficients vs. solute concentrations in model NAPL

**Table 2.5 Partitioning coefficients (log P) for of PAHs at different mole fractions**

Mole fraction	0.001	0.005	0.01	0.05	0.1	0.2	0.4	0.5	0.6	Average $\pm$ S.D.	Calculated <sup>a</sup>
Nap	3.78		3.85	4.02	4.10	4.13			4.28 <sup>b</sup>	4.03 $\pm$ 0.18	4.16
2-Mnap			4.33	4.61	4.55	4.68				4.54 $\pm$ 0.15	4.8
1-MNap				4.69	4.70	4.74	4.95		5.06	4.83 $\pm$ 0.12	4.81
Ace	4.89	4.98	4.91	4.95						4.93 $\pm$ 0.039	4.89
Phe	4.68		5.07	5.32	5.45	5.57				5.22 $\pm$ 0.35	5.65
Ant	5.35	5.44	5.55							5.45 $\pm$ 0.098	5.74

**a, calculated from a the polyparameter linear free energy relationship of Satoshi Endo [34]**

**b, this experiment was done in a high temperature about 42-43°C**

certain compound, except for Ace, increased with the increase of  $\chi_i$ , which is different to the forgone understanding of the partitioning coefficient. Since  $P_{t/w}$  can be also expressed as the ratio of activity coefficients (eq. 2.7), this probably suggests that the  $\gamma_{iw}$  increase and/or  $\gamma_{in}$  decrease with the increasing of the  $\chi_i$  in a large range of  $C_{i,t}$ . The decrease of  $\gamma_{in}$  had been described above by phenanthrene. Since no other experimental data are available, the estimated data by a polyparameter linear free energy relationship [34] were listed on the Table 2.5 to compare with these results. All of the calculated data are close to and higher than the measured data.

## 2.6 Conclusion

Simple batch experiments with toluene as solvent can be conducted to determine the  $S_{i,sub}$  for some PAHs. With the aqueous phase concentrations obtained from the experiment, the partitioning coefficient and mass transfer coefficient can also be obtained. Further, the thermodynamic parameters,  $\Delta H_f$  and  $f^s/f^l$  can be estimated with given  $S_i$  and  $T_m$ . All these measured and estimated data agreed with the published data in the literatures. In addition, value or function of  $\gamma_i$  of the solute in toluene solution can be evaluated according to the relationships of equilibrium aqueous phase concentrations and mole fractions in single solute model NAPL-water system. Most of the tested compounds behaved ideally in toluene solution ( $\gamma_i$  were unity) except for Phe, where  $\gamma$  was given best as a power function of mole fraction. However, the limitation of this method is obvious, which is the saturated concentration of solute in solvent and was low for some solutes. The mole fractions were accordingly very small for rigid compounds, which was less than 0.01 for Ant even the experiments were performed at a high temperature. The error of operation and measurement may be

subsequently amplified while extrapolating the equilibrium aqueous phase concentration to  $S_{i,sub}$ , where the  $x_i$  increase to unity. Therefore, next step work could be based on how to reach the high mole fraction and work with other solutes.

## 2.7 References

1. Shiu, W.-Y. and K.-C. Ma, Temperature Dependence of Physical-Chemical Properties of Selected Chemicals of Environmental Interest. I. Mononuclear and Polynuclear Aromatic Hydrocarbons. *Journal of Physical and Chemical Reference Data*, 2000. 29(1): p. 41-130.
2. Wauchope, R.D. and F.W. Getzen, Temperature dependence of solubilities in water and heats of fusion of solid aromatic hydrocarbons. *Journal of Chemical and Engineering Data*, 1972. 17(1): p. 38-41.
3. Whitehouse, B.G., The effects of temperature and salinity on the aqueous solubility of polynuclear aromatic hydrocarbons. *Marine Chemistry*, 1984. 14(4): p. 319-32.
4. Reza, J., A. Trejo, and L. Elena Vera-Avila, Determination of the temperature dependence of water solubilities of polycyclic aromatic hydrocarbons by a generator column-on-line solid-phase extraction-liquid chromatographic method. *Chemosphere*, 2002. 47(9): p. 933-945.
5. Van Noort, P.C.M., Fugacity ratio estimations for high-melting rigid aromatic compounds. *Chemosphere*, 2004. 56(1): p. 7-12.
6. Schwarzenbach, R.P., *Environmental Organic Chemistry*. 2003, New Jersey: John Wiley & Sons. 1313.
7. Olsson, T., Activity coefficients at infinite dilution, in department of chemical engineering. 1989, Lund University: Lund. p. 105.
8. Thomas, E.R., et al., Limiting activity coefficients of nonpolar and polar solutes in both volatile and nonvolatile solvents by gas chromatography. *Journal of Chemical and Engineering Data*, 1982. 27(4): p. 399-405.
9. Atik, Z., et al., Measurement of Activity Coefficients at Infinite Dilution of Benzene, Toluene, Ethanol, Esters, Ketones, and Ethers at Various Temperatures in Water Using the Dilutor Technique. *Journal of Chemical and Engineering Data*, 2004. 49(5): p. 1429-1432.
10. Krummen, M., D. Gruber, and J. Gmehling, Measurement of Activity Coefficients at Infinite Dilution in Solvent Mixtures Using the Dilutor Technique. *Industrial & Engineering Chemistry Research*, 2000. 39(6): p. 2114-2123.
11. Viamajala, S., et al., Solubilization, solution equilibria, and biodegradation of PAH's under thermophilic conditions. *Chemosphere*, 2007. 66(6): p. 1094-1106.
12. Gmehling, J., J. Li, and M. Schiller, A modified UNIFAC model. 2. Present parameter matrix and results for different thermodynamic properties. *Industrial & Engineering Chemistry Research*, 1993. 32(1): p. 178-93.

13. Gmehling, J., et al., A Modified UNIFAC (Dortmund) Model. 4. Revision and Extension. *Industrial & Engineering Chemistry Research*, 2002. 41(6): p. 1678-1688.
14. Poellmann, P. and M. Loebbecke, UNIFAC activity coefficient derivatives. *Gas Separation & Purification*, 1996. 10(3): p. 177-180.
15. Ghoshal, S., A. Ramaswami, and R.G. Luthy, Biodegradation of Naphthalene from Coal Tar and Heptamethylnonane in Mixed Batch Systems. *Environmental Science and Technology*, 1996. 30(4): p. 1282-91.
16. Peters, C.A.M.S., Weber WJ, UNIFAC modeling of multicomponent nonaqueous phase liquids containing polycyclic aromatic hydrocarbons. *Environmental Toxicology and Chemistry*, 1999. 18(3): p. 426-429.
17. Lee, K.Y. and C.V. Chrysikopoulos, Dissolution of a multicomponent DNAPL pool in an experimental aquifer. *Journal of Hazardous Materials*, 2006. 128(2-3): p. 218-226.
18. Schwarzenbach, R.P., *Environmental Organic Chemistry*. 1993, New Jersey: John Wiley & Sons.
19. Lewis, G.N., *The Osmotic Pressure of Concentrated Solutions, and the Laws of the Perfect Solution*. *Journal of the American Chemical Society*, 1908. 30: p. 668-83.
20. Kan, A.T. and M.B. Tomson, UNIFAC Prediction of Aqueous and Nonaqueous Solubilities of Chemicals with Environmental Interest. *Environmental Science and Technology*, 1996. 30(4): p. 1369-76.
21. Prausnitz, J.M., R.N. Lichtenthaler, and E. Gomez de Azevedo, *Molecular Thermodynamics of Fluid-Phase Equilibria*. 2nd Ed. 1986. 600 pp.
22. Peters, C.A., K.H. Wammer, and C.D. Knightes, Multicomponent NAPL solidification thermodynamics. *Transport in Porous Media*, 2000. 38(1-2): p. 57-77.
23. Yalkowsky, S.H., Estimation of entropies of fusion of organic compounds. *Industrial & Engineering Chemistry Fundamentals*, 1979. 18(2): p. 108-11.
24. Mukherji, S., C.A. Peters, and W.J. Weber, Jr., Mass Transfer of Polynuclear Aromatic Hydrocarbons from Complex DNAPL Mixtures. *Environmental Science and Technology*, 1997. 31(2): p. 416-423.
25. Peters, C.A., et al., Phase Stability of Multicomponent NAPLs Containing PAHs. *Environmental Science and Technology*, 1997. 31(9): p. 2540-2546.
26. Eberhardt, C.G., P., Time scales of organic contaminant dissolution from complex source zones: coal tar pools vs. blobs. *Journal of Contaminant Hydrology*, 2002. 59(1-2): p. 45-66.
27. Donald Mackay, W.Y.S., Kuo Ching Ma, *Illustrated handbook of physical-chemical properties and environmental fate for organic chemicals*. 1992: Lewis Publishers.
28. Verschveren, K., *Handbook of Environmental Data on Organic Chemical*, 3rd Edition. 1996.

29. Schluep, M., et al., Mechanisms affecting the dissolution of nonaqueous phase liquids into the aqueous phase in slow-stirring batch systems. *Environmental Toxicology and Chemistry*, 2001. 20(3): p. 459-466.
30. Alshafie, M. and S. Ghoshal, The role of interfacial films in the mass transfer of naphthalene from creosotes to water. *Journal of Contaminant Hydrology*, 2004. 74(1-4): p. 283-298.
31. Ortiz, E., M. Kraatz, and R.G. Luthy, Organic phase resistance to dissolution of polycyclic aromatic hydrocarbon compounds. *Environmental Science & Technology*, 1999. 33(2): p. 235-242.
32. Peters, C.A., C.D. Knightes, and D.G. Brown, Long-Term Composition Dynamics of PAH-Containing NAPLs and Implications for Risk Assessment. *Environmental Science and Technology*, 1999. 33(24): p. 4499-4507.
33. Allen, J.O., A.F. Sarofim, and K.A. Smith, Thermodynamic properties of polycyclic aromatic hydrocarbons in the subcooled liquid state. *Polycyclic Aromatic Compounds*, 1999. 13(3): p. 261-283.
34. Endo, S. and T.C. Schmidt, Prediction of Partitioning between Complex Organic Mixtures and Water: Application of Polyparameter Linear Free Energy Relationships. *Environmental Science and Technology*, 2006. 40(2): p. 536-545.

## Chapter 3 Aging phenomena of NAPLs interfacial phase

### 3.1 Aging phenomena

The interface between NAPLs of complex mixture and aqueous, gas and/or solid phases may be subject to aging phenomena. Although little is known about the mechanisms that result in aged film formation, much effort has been made and several factors and hypothetical theories have been found and developed. A widely accepted one is as following. The NAPLs undergo prolonged contact with water and/or gas, which leads to modification of the properties of the organic and interfacial phase. As a consequence, the low molecular weight, the well water soluble and/or volatile compounds are depleted from the interfacial phase. This causes an increase of the mole fractions of the sparingly soluble high molecular weight compounds and the viscosity of the NAPLs. With the enrichment of surface active compounds (e.g., asphaltene, resin) in the interfacial region, other solutes might precipitate eventually when their mole fractions reach their solubility limits in the NAPL phase, which is equal to  $\frac{1}{\gamma} \cdot \frac{f^s}{f^l}$  according to Peters 1997 [1], and form sometimes visible solid or semirigid skin-like interfacial films, accompanied by the decrease of the interfacial tension [2-8].

The objective of this chapter is therefore to study the aging phenomena of NAPLs interfacial phase under different environmental conditions. The research includes (i) performing different experiments to observe the formation of aging film, (ii) studying the effects of environmental conditions (pH, hydrogen peroxide concentration and etc.) on aging process, and (iii) producing aged NAPLs samples for further study.

### 3.2 Experimental methods to study the aging phenomena

Pendant drop test (PDT), batch experiments (BE), continuously flow through experiments (CFTE) and surface coating test (SCT) were performed to study the aging phenomena under different environmental conditions. Four kinds of NAPLs, commercial fresh coal tar, coal tar from former gas manufacture plants (GMPs), anthracene oil and crude oils were used to perform the experiments. Detailed information is given in the following sections and listed in Table 3.1.

**Table 3.1 Summary of experiments to study the formation of aged interfacial films**

Tests	NAPLs	Code / Class	Provider	In air or aqueous		Time for visible interfacial film formation
				PH	H <sub>2</sub> O <sub>2</sub> con. % (v/v) or mg/L	
PDT	Coal tar	97159	Ruetgers Chem. AG	3,6,12		No over 12 weeks
		98142	Ruetgers Chem. AG	3,6,12		No over 12 weeks
		98142	Ruetgers Chem. AG	Neutral	1%, 2%, 10%	No over 12 weeks
		05117	Ruetgers Chem. AG	3,6,12		No over 12 weeks
		GMP Reutlingen	Stadtwerke Reutlingen	Neutral		4 weeks
	Anthracene oil		Stadtwerke Reutlingen	3,6,12		in basic solution after 1 week No in others
Crude oil	Brent Blend	Dr. Ghoshal, Montreal		Neutral		4 days
		Dr. Andersson, Münster		Neutral		1 week
		Dr. Andersson, Münster		Neutral		1 week
		Dr. Andersson, Münster		Neutral		1 week
		Dr. Andersson, Münster		Neutral		1 week
		Dr. Andersson, Münster		Neutral		1 week
CFTE	Coal tar	98142	Ruetgers Chem. AG	Neutral	Degassed Millipore water (7.8 mg/L O <sub>2</sub> )	17 weeks
	Coal tar	98142	Ruetgers Chem. AG	Neutral	Millipore water (8.8 mg/L O <sub>2</sub> )	17 weeks
	Coal tar	98142	Ruetgers Chem. AG	Neutral	2% H <sub>2</sub> O <sub>2</sub> (11.1 mg/L O <sub>2</sub> )	10 weeks
BE	Coal tar	98142	Ruetgers Chem. AG	3		No after 100 weeks
	Coal tar	98142	Ruetgers Chem. AG	Neutral		No after 120 weeks
	Coal tar	98142	Ruetgers Chem. AG	12		No after 100 weeks
	Coal tar	98142	Ruetgers Chem. AG			Air 14 weeks
	Coal tar	97159	Ruetgers Chem. AG			Air 14 weeks
	Crude oil	Brent Blend	Dr. Ghoshal, Montreal		Air	
	Bachaquero	Dr. Andersson, Münster		Air		No after 64 weeks
SCT	Coal tar	98142	Ruetgers Chem. AG	Air		2 days
	Crude oil	Bachaquero	Dr. Andersson, Münster		Air	

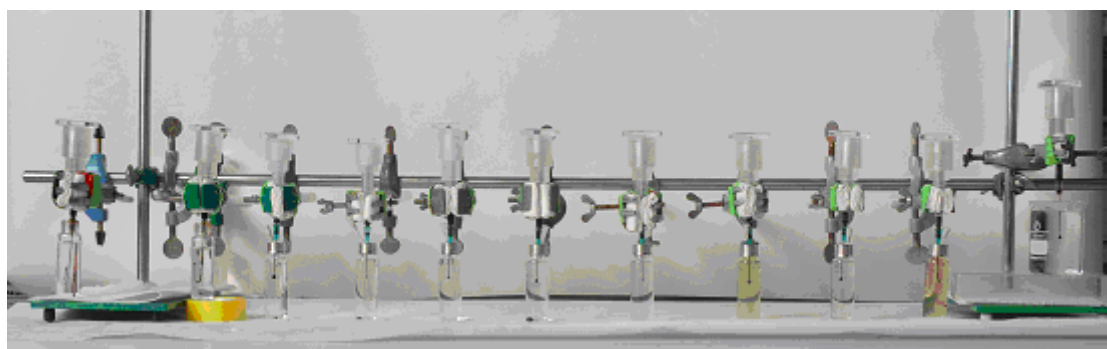
**PDT: pendant drop test, CFTE: continuously flow through experiment, BE: batch experiment, SCT: surface coating test.**  
**pH 3 and 12 were HCl and NaOH solution, respectively, pH 6 and neutral were milipore water.**

### 3.2.1 Pendant drop test (PDT)

Pendant drop is a classical rheological method to measure the surface/interfacial tension [9]. It has been used in several research groups to observe the potential



formation of aging film at the NAPLs interfacial phase [9-12]. The set-up of pendant drop test is shown in Figure 3.1. In brief, tiny amount (approximately 0.2 ml) of NAPLs was sucked into the syringe held by a sheath equipped with microscrew threads, and a drop of NAPLs was formed at the end of a syringe tip and suspended in the aqueous phase. The freshly formed drop is spherical in shape, and a semirigid or skin-like interfacial film should be detectable if present after drop exposure by subsequent partial withdraw of the bulk NAPLs into the syringe needle. This visible solid or semi-solid viscous film is referred to as aged film.



**Figure 3.1 Set-up of pendant drop test**

The results of the pendant drop tests were as follows. For coal tar, the typical freshly formed drop is shown in Figure 3.2a. The whole drop can be sucked back into the syringe for fresh coal tars (and other fresh NAPLs), and generally 3 to 7 days were enough to observe the coal tar-water interfacial films [10, 13]. However, in this work, none of the commercial coal tars, 97159, 98142 or 05117 showed any noticeable wrinkles even after 10 days. As illustrated in Figure 3.2b, the drop coal tar can be retracted totally into the syringe after 10 days, which indicated clearly that there was



**Figure 3.2a Typical pendant drop of NAPL**

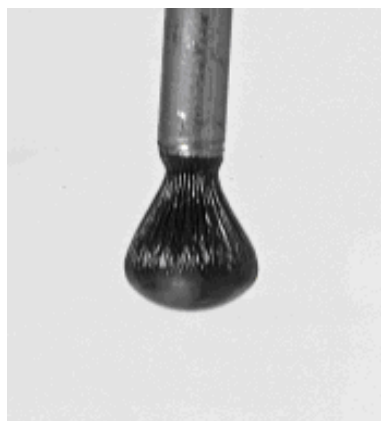


**Figure 3.2b Retraction of coal tar without apparent aging (9 days)**

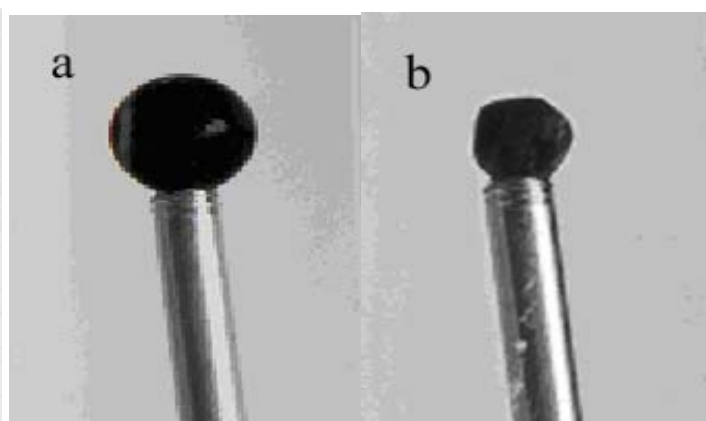
no visible film formed at that time. All of the drops kept the original shapes even after two months' experiment. Only the coal tar from a former gas manufacture plant

(MGP) in Reutlingen behaved differently, the “wrinkle” appeared after 2 months exposure in water as shown in Figure 3.3.

Six crude oils including Arabian heavy, Bachaquero, two kinds of Brent Blend from different providers, Kirkuk and Soviet Blend were investigated in this study. All of them are LNAPLs and showed visible changes in pendant drop tests after 4 to 7 days (Figure 3.4).



**Figure 3.3 Aged coal tar drop from a former GMP aged**



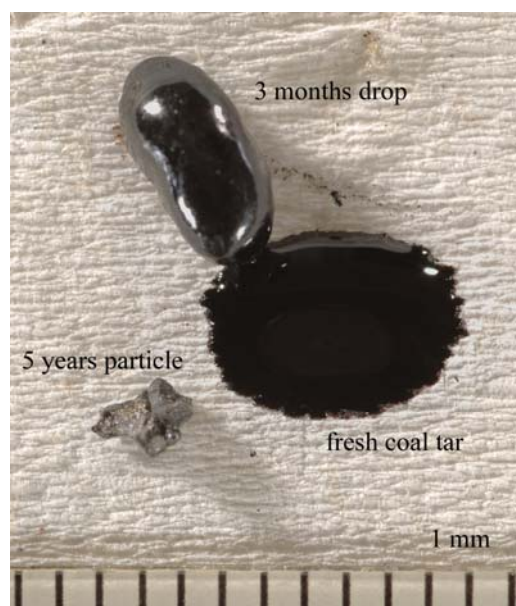
**Figure 3.4 Crude oil (Brent Blend) drops after 4 days experiment, a: before, b: after partial withdrawal**

However, it seems that the widely used pendant drop test with visual observation is not always sensitive towards changes of the interfacial phase. This becomes obvious in the comparison of the same commercial coal tar exposed to water for different time periods. This coal tar drop did not show any apparent aging information in the pendant drop test after 3 months, although its behavior had changed clearly as shown in Figure 3.5. Whereas fresh coal tar was immediately sucked into cellulose, the 3 months' coal tar drop kept its shape, which indicated the formation of a hard shell. A coal tar exposed in an artificial aquifer for 5 years had completely changed its appearance and became solid [14]. Therefore, other experimental set-ups should be performed in order to study the aging phenomena, especially to validate the environmental conditions' effect on this process.

### 3.2.2 Continuously flow through experiments (CFTE)

Oxidation is thought to be a factor to the aging process [15-22]. However, there was no visible film formation for commercial coal tar from the pendant drop tests, where the coal tar were immersed in aqueous hydrogen peroxide solutions (1, 2 and 10 % (v/v)) for 3 months. Therefore, another set-up, continuously flow through experiment (CFTE) was carried out subsequently to study the effect of oxidation on aging process (Figure

3.6) and create aged coal tars. Hydrogen peroxide solution (2%) was also used as oxidant, which kept flowing along the surface of the coal tar. Approximately 3g of



**Figure 3.5 Comparison of fresh coal tar and coal tar aged for 3 months and 5 years, respectively in contacting with water (all for coal tar 98142)**



**Figure 3.6 Setting up of the CFTE**

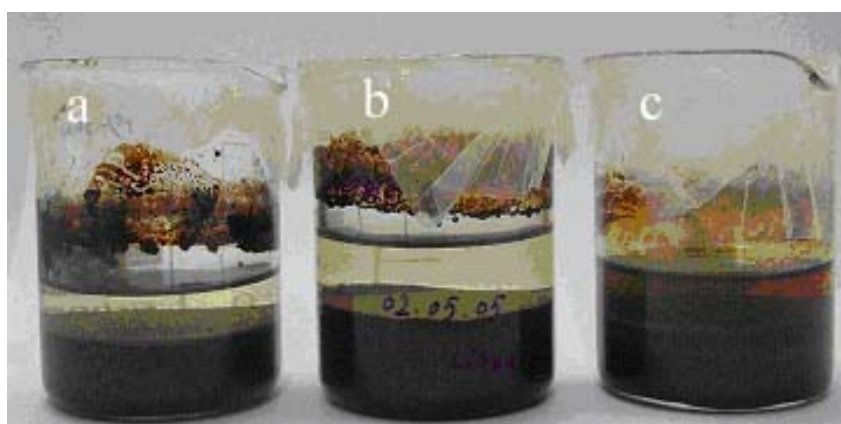
commercial coal tar were spiked into the bottom of a 50 mL glass vial, which was filled with aqueous solution of degassed millipore water (7.8 mg/L O<sub>2</sub>), millipore water (8.8 mg/L O<sub>2</sub>) and 2% H<sub>2</sub>O<sub>2</sub> solution (11.1 mg/L O<sub>2</sub>), respectively. The vials were sealed with viton septa. All of the vials were fed from reservoirs by a peristaltic pump (ISMATEC, Switzerland) through stainless steel (1/16", Klaus Ziemer GmbH, Germany) with a flow rate of 0.5 mL/min. The reservoirs were also degassed millipore water, millipore water and 2% hydrogen peroxide solution, respectively. The source bottles stayed in the lab for 3 days before refilling. There should be gas exchange during this time period, accordingly the oxygen concentrations could change during the experimental time period. The oxygen concentrations were measured on the 2<sup>nd</sup> day after the refilling at 21 °C by a single channel oxygen meters (Precision Sensing GmbH, Germany).

### 3.2.3 Batch experiment (BT)

#### **Study the pH effect on aging process**

There are some reasons that support the hypothesis the pH of the aqueous solution could be an important factor to the aging process. First, some functional groups inside

NAPLs and wetting properties of NAPLs interfacial phase are sensitive to pH of the aqueous solution [23-26]. Second, Barranco et al. observed the different behaviors of coal tar-water interfacial film formation at different pH conditions. Last, pendant drop test of anthracene oil, a coal tar fraction that distills between 245 °C and 390 °C showed aged film formation in one week only in basic solution (pH=12, NaOH solution). Therefore, a batch experiment was performed with commercial coal tar to study further the pH effect on aging process and to prepare aged coal tar samples under different pH conditions. The set-up was simple and similar to Nelson [13] and shown in Figure 3.7. Similar amount of coal tars (35g) and aqueous solution (40g) were filled in the 100 mL beaker. The aqueous phases were acid (pH=3, HCl solution), neutral (millipore water) and basic (pH=12, NaOH solution), respectively.



**Figure 3.7 Coal tar (98142) contacted with acid (a), neutral (b) and basic (c) aqueous solutions in batch experiments**

### **Study the effect of dissolution and volatilization/evaporation on aging process**

Depletion of well soluble and volatile compounds is assumed to be a factor contributing to the aging process [11], although Nelson et al. found the chemical composition of interfacial films was very similar to that of the bulk phase [13]. Since pendant drop test could not study the effect of volatilization. The batch experiments with a similar set-up to CFTE were performed. As shown in Figure 3.8 (Batch H<sub>2</sub>O and Batch Air), approximately 3 g of coal tar were put inside a 50 mL vial, then the vial was filled with water and sealed with teflon septum (Figure 3.8 left), or exposure to the air without septum (Figure 3.8 right). Same batch experiments of air exposure were also performed by heavy and light crude oils and illustrated in Figure 3.9.



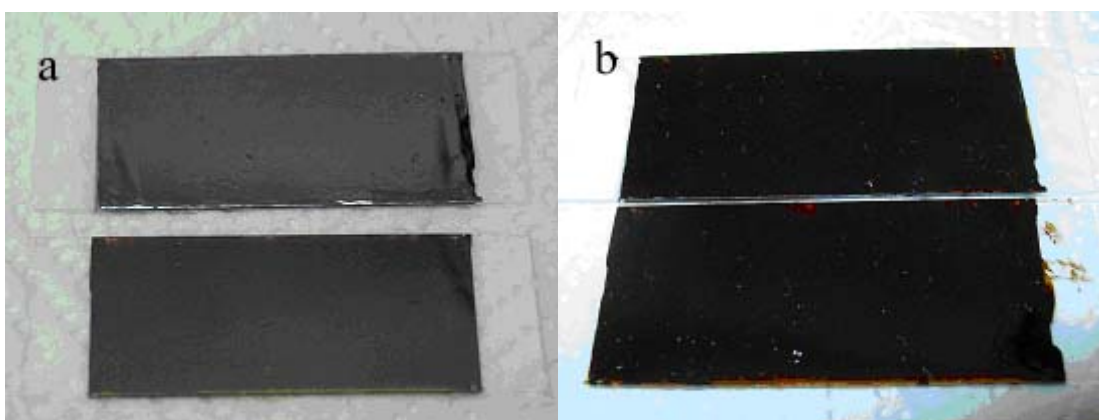
**Figure 3.8** Setting up of the batch experiments coal tar open to water and air



**Figure 3.9** Setting up of batch experiments heavy and light crude oil open to air

### 3.2.4 Surface coating test (SCT) to prepare the aged NAPLs sample

Pendant drop test, continuously flow through experiment and batch experiments were conducted to study the aging phenomena of the tested NAPLs. However, it is hard to separate aged NAPLs from the bulk phase, and the aged film is too little to be utilized further from pendant drop test. Continuously flow through experiment and batch experiment need too long time to obtain aged NAPLs (see next section). Therefore, a new experimental set up is needed to prepare enough aged NAPLs for next step study. Accordingly, the surface coating test was performed. A tiny amount (approximately 0.1 to 0.2 g) of NAPLs was coated evenly on the surface of glass plates (2.5cm X 6.6cm), and the glass plate was kept inside of fume hood or glove bag under nitrogen atmosphere (Figure 3.10). The treated coal tars were collected after 2 and 7 days, and the composition and leaching/partitioning properties were investigated. The oxygen concentration inside the glove bag was about 0.6 mg/L (1.4% O<sub>2</sub>), which was measured by an oxygen meter (Precision Sensing GmbH, Germany).



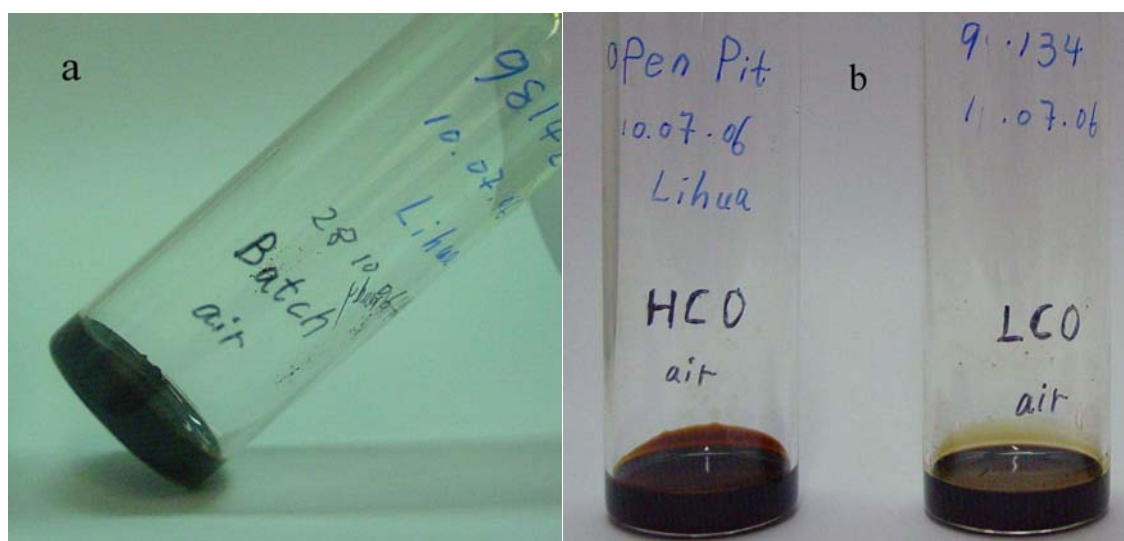
**Figure 3.10** Coating of coal tar on the surface of glass plates. a, fresh coal tar; b, 2 days later.



### 3.3 Results and discussion

#### 3.3.1 Effect of the NAPL source on aging process

In pendant drop test, the commercial coal tars did not show any aging indication in 10 days (Figure 3.2) and crude oil demonstrated clear “wrinkle” in 4 to 7 days. Meanwhile, in the air exposure batch experiments (Figure 3.8, 3.9), the commercial coal tars 97159 and 98142 became solid or semi-solid after 14 weeks (Figure 3.11a). However, the crude oil showed no sign of solidification even after 64 weeks (Figure 3.11b) conducted in the same experiment. This indicates that crude oil and coal tar



**Figure 3.11 Results of opening to air batch experiments a. aged coal tar with solid interface, b. free-flowing heavy and light crude oils**

underwent different aging process even under the same environmental conditions. This may be due to the chemical differences between crude oils and coal tars, even if both of them contain thousands of species and most of them can not be identified. Crude oils contain a broad spectrum of n-alkane ( $n\text{-C}_{10}$  to  $n\text{-C}_{30+}$ ) and volatile compositions whereas coal tars contain significant amounts of aromatic components.

In addition, different coal tars behaved also dramatically different. Luthy and Nelson performed pendant drop tests and observed “wrinkles” in about 3 days [10, 13] for coal tars obtained from former MGP sites. It took 4 weeks to show the clear aging film for the coal tar obtained from a former GMP in this study. However, no similar film was observed for all of the commercial coal tars in pendant drop test. This might be because of the compositional difference of the coal tars. The composition of coal tar depends on the source and industrial process such as feedstock and operation conditions of the coal tar. For coal tar obtained from former GMP, which has kept

contacting with water and porous medium at least for 50 years and most of the highly water soluble compounds were depleted. The fractions of the other compounds should be relatively higher than fresh coal tars, which are probably the major constituents in the interfacial films. This result strongly indicates that the source and the composition of the NAPLs are the most important factors for the formation of visible aging film.

### 3.3.2 Effect of evaporation and dissolution on aging process

Batch experiments (Figure 3.8) were performed to study the effect of volatilization / evaporation and dissolution on aging processes of coal tar. The results are as following.

For coal tar (Figure 3.12), there was no detectable formation of aging film after 16 months exposure of coal tar in water, and air exposure batch experiment (Figure 3.11a) showed clear interfacial film in 14 weeks. The formation of aging film in air exposure experiment was even faster than in CFTR system with 2%  $H_2O_2$  solution flowing along the coal tar surface. Therefore, evaporation/volatilization was a more effective factor to aging of coal tar than the dissolution of high water soluble compounds. Meanwhile, as indicated in CFTE the solid interfacial phase was observed after 17 weeks in millipore water flowing through system (Figure 3.13).



**Figure 3.12 Batch experiment of coal tar, free-flowing NAPL inside a full of water vial**

Compare this result to the exposure in water batch experiment (Figure 3.12), which did not show any indication of aging even after 16 months. It demonstrates that the depletion of the well soluble compounds was also an important factor to the aging process of coal tar.



**Figure 3.13 Results of CWFTE, all of them showed solid or semi-solid interfacial phase**

For crude oils, same set-up to coal tar was carried out (Figure 3.9). However, none of the three samples (Brent Blend, Bachaqueoro and oils from an old oil exaction field near Hannover, Germany) showed any visible phase change even after 1 year. Figure 3.11b shows clearly heavy and light crude oils were flowable at the endpoint of the test. Therefore, evaporation/volatilization was only a second order important factor to aging of crude oils. The result of pendant drop test shows that the formation of a visible aging film only needed 4 to 7 days (Figure 3.2). This indicated that the depletion of high water soluble compounds contributed more to the aging of crude oils.

### 3.3.3 Effect of oxygen concentration on aging process

During the CFTE (Figure 3.6), the aged interfacial film formed in about 10 weeks in 2% hydrogen peroxide solution flowing system, and 17 weeks were needed for the coal tar-millipore water and degassed millipore water systems to show similar phenomena (Figure 3.12). Thus, the appearance of hydrogen peroxide accelerated the aging process. The degassed and millipore water showed this formation within similar time period. It is because of their similar oxygen concentration, and also because the precision of the observation by naked eye is too low to find the little information of semi-solid film. These experiments demonstrated that the presence of oxidant did affect the aging, however, it was a small important factor for the aging process of the coal tar interface. This result agree with the observations of many researches, where the oxidation only occurred at relative high temperature (the lowest one is 80 °C) or with the presence of catalyst [15-17, 27]. However, some previous



studies showed the oxidation by Fenton's reaction and hydrogen peroxide were capable of oxidative degradation of numerous important hydrocarbon and aromatic hydrocarbons [18-21, 28]. Therefore, the tiny amount of catalysts inside NAPLs may be also important and need to be investigated in the next step work.

### 3.3.4 Effect of pH on aging process

The commercial coal tar samples and anthracene oil had contacted with acid, neutral and basic solution for more than three months in the pendant drop tests (Table 3.1, Figure 3.1). The color of all acidic and basic solutions changed to yellow. However, only anthracene oil in basic solution showed wrinkled interfacial film. Similar observations were obtained from the batch experiments performed with different pH solutions (Figure 3.7). There was no visible interfacial film formed even after two and a half years, except for the colour change to light yellow, yellow and brown for neutral, acid and basic solutions, respectively. These results indicated pH of the aqueous solution had no detectable effects on the formation of interfacial film, and basic solution's leaching capability was high for some compounds. This conclusion is contrary to that of previous studies for coal tars and crude oils [23, 24, 29-31]. The previous studies showed that pH variation influenced significantly the film formation and the interfacial properties. The different result in this study is probably due to the difference of the chemical composition of the coal tar used in this study, the amount of the acidic and basic organic compounds (e.g., asphaltenes) might be too low, or the organic acids or bases are weak functional groups.. Another reason should be the mass of the NAPL used in the experiments especially in the batch experiments (Figure 3.7) was too much, the depletion due to leaching was too small. To get more information, further experimental work could study the concentrations of more solutes in NAPLs.

### 3.3.5 Summary and conclusions

All of the tested NAPL underwent aging process under different environmental conditions, and aging is a ubiquitous phenomenon in the NAPLs interface. Different kinds of physical processes, e.g., evaporation, volatilization and dissolution working together contributed to the aging process. Different NAPLs experienced different aging processes under the same environmental conditions, evaporation/volatilization contributed more to the aging of commercial coal tar, and depletion of well soluble compounds was a significant factor to the aging process of crude oils. Same NAPL

demonstrated different aging behavior under different environmental conditions. The commercial coal tar tested in this work needed different time periods to illustrate aging film formation for different experimental methods, and the time periods increased in this order: CFTE with 2% hydrogen peroxide (10 weeks) < batch experiment in air (14 weeks) < CFTE with millipore water (17 weeks) ~ CFTE with degassed millipore water (17 weeks) < batch experiment in water (no “wrinkle” after 100 weeks). The appearance of oxidant in the aqueous phase accelerated the aging process of interface, however, it was only a second important factor. The pH value of the solution was critical to the leaching behavior of some compounds from NAPLs phase.

### 3.4 References

1. Peters, C.A., et al., Phase Stability of Multicomponent NAPLs Containing PAHs. *Environmental Science and Technology*, 1997. 31(9): p. 2540-2546.
2. Harvey W. Yarranton, H.A., Rajesh Jakher, Investigation of asphaltene association with vapor pressure osmometry and interfacial tension measurements. *Ind. Eng. Chem. Res.*, 2000. 39(8): p. 2916-2924.
3. Branco, V.A.M., et al., Asphaltene flocculation and collapse from petroleum fluids. *Journal of Petroleum Science & Engineering*, 2001. 32(2-4): p. 217-230.
4. Mahjoub, B., et al., Phase partition of organic pollutants between coal tar and water under variable experimental conditions. *Water Research*, 2000. 34(14): p. 3551-3560.
5. Lee, K.Y. and C.A. Peters, UNIFAC Modeling of Cosolvent Phase Partitioning in Nonaqueous Phase Liquid-Water Systems. *Journal of Environmental Engineering* (Reston, VA, United States), 2004. 130(4): p. 478-483.
6. Peters, C.A., K.H. Wammer, and C.D. Knightes, Multicomponent NAPL solidification thermodynamics. *Transport in Porous Media*, 2000. 38(1-2): p. 57-77.
7. Sullivan, A.P. and P.K. Kilpatrick, The Effects of Inorganic Solid Particles on Water and Crude Oil Emulsion Stability. *Industrial & Engineering Chemistry Research*, 2002. 41(14): p. 3389-3404.
8. Acevedo, S., et al., Asphaltenes and Other Natural Surfactants from Cerro Negro Crude Oil. Stepwise Adsorption at the Water/Toluene Interface: Film Formation and Hydrophobic Effects. *Energy & Fuels*, 2005: p. ACS ASAP.
9. Jeribi, M., et al., Adsorption kinetics of asphaltenes at liquid interfaces. *Journal of Colloid and Interface Science*, 2002. 256(2): p. 268-272.
10. Luthy, R.G., et al., Interfacial films in coal tar nonaqueous-phase liquid-water systems. *Environmental Science and Technology*, 1993. 27(13): p. 2914-18.

11. Alshafie, M. and S. Ghoshal, The role of interfacial films in the mass transfer of naphthalene from creosotes to water. *Journal of Contaminant Hydrology*, 2004. 74(1-4): p. 283-298.
12. Ghoshal, S., C. Pasion, and M. Alshafie, Reduction of benzene and naphthalene mass transfer from crude oils by aging-induced interfacial films. *Environmental Science & Technology*, 2004. 38(7): p. 2102-2110.
13. Nelson, E.C., et al., Chemical Characterization of Coal Tar-Water Interfacial Films. *Environmental Science and Technology*, 1996. 30(3): p. 1014-22.
14. Liu, L.E., Satoshi; Eberhardt, Christina; Grathwohl, Peterl; Schmidt C, Torsten, Partition behavior of polycyclic aromatic hydrocarbons between aged coal tar and water. *Environmental Toxicology & Chemistry*, 2008. *submitted*
15. Terzian, R. and N. Serpone, Heterogeneous photocatalyzed oxidation of creosote components: mineralization of xylenols by illuminated TiO<sub>2</sub> in oxygenated aqueous media. *Journal of Photochemistry and Photobiology, A: Chemistry*, 1995. 89(2): p. 163-75.
16. Bermejo, J., et al., Monitoring the synthesis of new pitches from coal tar and its fractions by chromatography and related techniques. *Journal of Chromatography, A*, 1999. 849(2): p. 507-519.
17. Nie, L., et al., Benzaldehyde synthesis via styrene oxidation by O<sub>2</sub> over TiO<sub>2</sub> and TiO<sub>2</sub>/SiO<sub>2</sub>. *Catalysis Communications*, 2007. 8(3): p. 488-492.
18. Bogan, B.W. and V. Trbovic, Effect of sequestration on PAH degradability with Fenton's reagent: roles of total organic carbon, humin, and soil porosity. *Journal of Hazardous Materials*, 2003. 100(1-3): p. 285-300.
19. Watts, R.J. and P.C. Stanton, Mineralization of sorbed and NAPL-phase hexadecane by catalyzed hydrogen peroxide. *Water Research*, 1999. 33(6): p. 1405-1414.
20. Bissey, L.L., J.L. Smith, and R.J. Watts, Soil organic matter-hydrogen peroxide dynamics in the treatment of contaminated soils and groundwater using catalyzed H<sub>2</sub>O<sub>2</sub> propagations (modified Fenton's reagent). *Water Research*, 2006. 40(13): p. 2477-2484.
21. Esumi, K., et al., Carbonaceous gel obtained by oxidation of coal-tar pitch with hydrogen peroxide. *Carbon*, 1993. 31(8): p. 1357-8.
22. Rodgers, R.P., T.M. Schaub, and A.G. Marshall, *Petroleomics: MS returns to its roots*. *Analytical Chemistry*, 2005. 77(1): p. 20A-27A.
23. Zheng, J. and S.E. Powers, Organic bases in NAPLs and their impact on wettability. *Journal of Contaminant Hydrology*, 1999. 39(1-2): p. 161-181.
24. Barranco, F.T. and H.E. Dawson, Influence of aqueous pH on the interfacial properties of coal tar. *Environmental Science & Technology*, 1999. 33(10): p. 1598-1603.
25. Dong, J., B. Chowdhry, and S. Leharne, Investigation of the Wetting Behavior of Coal Tar in Three Phase Systems and its Modification by Poloxamine Block Copolymeric Surfactants. *Environmental Science and Technology*, 2004. 38(2): p. 594-602.

26. Liu, J., et al., Colloidal interactions between asphaltene surfaces in aqueous solutions. *Langmuir : the ACS journal of surfaces and colloids* FIELD Publication Date:2006, 2006. 22(4): p. 1485-92. FIELD Reference Number: FIELD Journal Code:9882736 FIELD Call Number:.
27. Lu, C.-x., et al., An investigation of the preparation of coal tar- and petroleum pitch spheres and their oxidation stabilization. *Xinxing Tan Cailiao*, 2004. 19(3): p. 186-191.
28. Watts, R.J., et al., Fenton-like soil remediation catalyzed by naturally occurring iron minerals. *Environmental Engineering Science*, 1999. 16(1): p. 93-103.
29. Zheng, J., J. Shao, and S.E. Powers, Asphaltenes from Coal Tar and Creosote: Their Role in Reversing the Wettability of Aquifer Systems. *Journal of Colloid and Interface Science*, 2001. 244(2): p. 365-371.
30. Zheng, J., et al., Predicting the Wettability of Quartz Surfaces Exposed to Dense Nonaqueous Phase Liquids. *Environmental Science and Technology*, 2001. 35(11): p. 2207-2213.
31. Zheng, J.Z. and S.E. Powers, Identifying the effect of polar constituents in coal-derived NAPLs on interfacial tension. *Environmental Science & Technology*, 2003. 37(14): p. 3090-3094.

## Chapter 4 Aging of coal tar and its effects on mass transfer

### 4.1 Introduction

Coal tar was a major by-product of carbonization of coal by former manufactured gas plants (MGPs), and it is the by-product of modern cokemaking facilities. It is a viscous, dark-colored, dense non-aqueous phase liquid (DNAPL), containing a wide variety of organic constituents, including heterocyclic, monocyclic and polycyclic aromatic hydrocarbons (PAHs), volatile aromatic compounds, phenols, organic and inorganic sulfur compounds, metals and asphaltenes. In many cases, coal tar wastes were left on-site in pits or containers, or by accidental spillage, resulting in a persistent source of contamination of soils and groundwater at many former MGP sites.

Transfer of pollutants across the NAPL-water interface determines both the extent of groundwater contamination as well as the persistence of residual NAPLs phases in porous media.

Recent experiments have demonstrated that the coal tar interface phase may undergo a visible change of phase after a certain time period of exposure to water and air [1-4]. This visible change of state is commonly referred to as aging. The aging process may be important to the risk assessment and the technique of remediation of the contaminated sites, since it is hypothesized that surface aging may influence both the fluid mechanics and the mass transfer properties of the compounds inside the coal tar in porous media. Luthy and Ghoshal observed a decrease of the mass transfer of PAHs after 3 or 16 experimental days from coal tar and crude oil, respectively [1, 5]. However, Eberhardt found a constant mass transfer rate during one year's test in an artificial aquifer [6].

The objective of this study is therefore to examine the effects of interfacial aging on the change of the chemical composition of NAPLs and on the mass transfer properties of selected contaminants (e.g., PAHs, BTEX, Phenols). The research includes (i) comparison of the concentrations of solutes in fresh and aged coal tars, and evaluation of the effect of environmental conditions on the change of composition, and (ii) measurement of the aqueous phase concentrations of compounds leaching from

NAPLs as a function of time, and estimation of the mass transfer process from NAPL to water in batch experiments.

## 4.2 Materials and experimental methods

### 4.2.1 Materials

#### **Fresh coal tar**

Commercial coal tar was taken from Ruetgers Chem. AG (Germany), and stored in the lab at ambient temperature.

**Aged coal tars** were obtained from batch experiment (BE), continuously flow through experiment (CFTE) and surface coating test (SCT), the detail methods and operational processes were given in Chapter 3.

The concentrations of solutes in aged and fresh coal tar were measured by GC-MS.

### 4.2.2 Experiments to measure the aqueous phase concentrations

#### **Equilibrium aqueous phase concentrations of solutes in coal tar exposure to different pH solutions**

Batch experiments were carried out with the similar setting up to Nelson's [2]. The equilibrium aqueous phase concentrations of PAHs, phenols and 2,3-benzofuran in aqueous solution with different pH values were determined (Figure 3.7). The original objective of this test was to study the effect of pH on aging process and obtain the aged coal tars under different pH conditions. Unfortunately, all of coal tars inside the beaker could flow freely and showed no detectable formation of aging film after 27 months exposure to aqueous solutions, except for the color of the aqueous solutions changed to yellow. The pH values of these aqueous solutions were 5, 5.5 and 8, respectively at the end point of the test. This indicated both acid and basic solutions shifted toward neutral during the experimental time period, which may be due to the neutralisation during the leaching process. The millipore water shifted to acid because of the dissolution of CO<sub>2</sub>. About 5 mL aqueous phase sample was taken triplicate by glass pipette and extracted with 1 mL cyclohexane for GC-MS measurements.

#### **Steady state concentrations from CFTE and equilibrium concentrations from BE**

With continuously flow through experiment and batch experiment the steady state and equilibrium aqueous phase concentrations of compounds in aqueous phase contacted

with coal tars were measured. Similar amounts of coal tar (about 3 g) were spiked into five 50-mL vials, and the vials were filled with aqueous solutions with similar NAPL-water volume ratios of about 1:20. The fourth and fifth vials were used to perform the batch experiment at ambient temperature. The fourth was sealed with an aluminium cap with Teflon septum, and the fifth was exposed to air directly (Figure 3.8). The aqueous sample was obtained 16 months later from the fourth vial and the concentrations of tested compounds were equilibrium aqueous phase concentrations. During the experimental time period, coal tars inside the first three vials (CFTE) became solid. This indicated the coal tar experienced aging process and became aged coal tar. The concentrations of flowing aqueous were determined and kept relatively constant for a few months. Accordingly, the aqueous phase concentrations measured at the end point of the test (16 months) were steady state concentrations of compounds in aged coal tar-water system.

#### **Aqueous phase concentrations in aged coal tar-water systems**

Aged coal tar prepared by SCT was used to perform the BE. The glass plates covered with coal tar had been treated in air and nitrogen atmosphere for 2 or 7 days (Figure 3.10). Eight glass plates (each 2.5 X 6.6 cm<sup>2</sup>) with about 0.12 g of NAPLs were combined together and put inside a 100 mL bottle, the bottle was filled with millipore water (about 110 mL) (Figure 4.1). 1-5 mL aqueous phase sample was taken by glass pipettes at different periods and extracted by 0.5-1 mL cyclohexane for GC-MS measurement. The volume ratios of the aqueous phase and organic solvent were changed depending on the estimated concentration. The sampling was similar to Mukherji [7], which is day by day for first two weeks, then every two days until 24<sup>th</sup> day.

#### **4.2.3 Analytical methods**

Aged and fresh coal tars were diluted 1000 (aged) to 3000 (fresh) times. Cyclohexane was the extracting solvent for PAHs, phenols, styrene and 2,3-benzofurane analysis, and n-pentane was the solvent for BTEX. Dilutions were spiked with 5-10 µl internal standards (they are phenol-d<sub>6</sub>, styrene-d<sub>8</sub>, naphthalene-d<sub>8</sub>, acenaphthene-d<sub>10</sub>, phenanthrene-d<sub>10</sub>, chrysene-d<sub>12</sub>, and perylene-d<sub>12</sub> toluene solution for PAHs, phenols and benzofuran analysis, and fluorobenzene in methanol solution for BTEX) at

concentrations matching the expected analysed concentrations according to the preliminary experiments.



**Figure 4.1.** Batch experiment performed with the aged coal tars coating on the surface of the glass plates.

Depending on the estimated concentrations, 3-5 mL aqueous sample was spiked with internal standard (same as above) and extracted by 0.5-5 mL cyclohexane for PAHs, phenols and benzofuran analysis (or n-pentane for BTEX analysis).

Concentrations of PAHs, phenols and benzofuran were determined by a gas chromatograph (HP 5890/II) connected to a mass selective detector (HP 5972 MSD). Analytes were separated using a 30 m × 0.25 mm DB-5MS column (J&W Scientific) with 0.25 μm film thickness. The injector temperature was 270 °C, and injection volume was 1 μL. Helium (99.999%) was the carrier gas at a constant flow of 0.6 mL/min. The oven temperature was held for 2 min at 50 °C, then increased at a rate of 8 °C/min to 90 °C, increased to 270 °C at a rate of 18 °C/min, held for 10 min and finally raised to 310 °C (held for 6.5 min). The total time period was 48.5 min.

BTEX concentrations were measured by another GC-MS system, gas chromatography (HP 6890) connected to a mass selective detector (HP 5972 MSD). Separations were done using a 60 m × 0.25 mm DB-624 column (J&W Scientific) with 1.4 μm film thickness. The injector temperature was 200 °C, and injection volume was 1 μL. Helium was the carrier gas at a constant flow of 1 mL/min. The oven temperature was held for 5 min at 45 °C, then increased to 90 °C within 8 min, hold 4 min, increased to 200 °C within 6 min, held for 5 min and finally raised at a rate of 1.5 °C/min to 230 °C (held for 3 min). The total time period was 42.46 min.

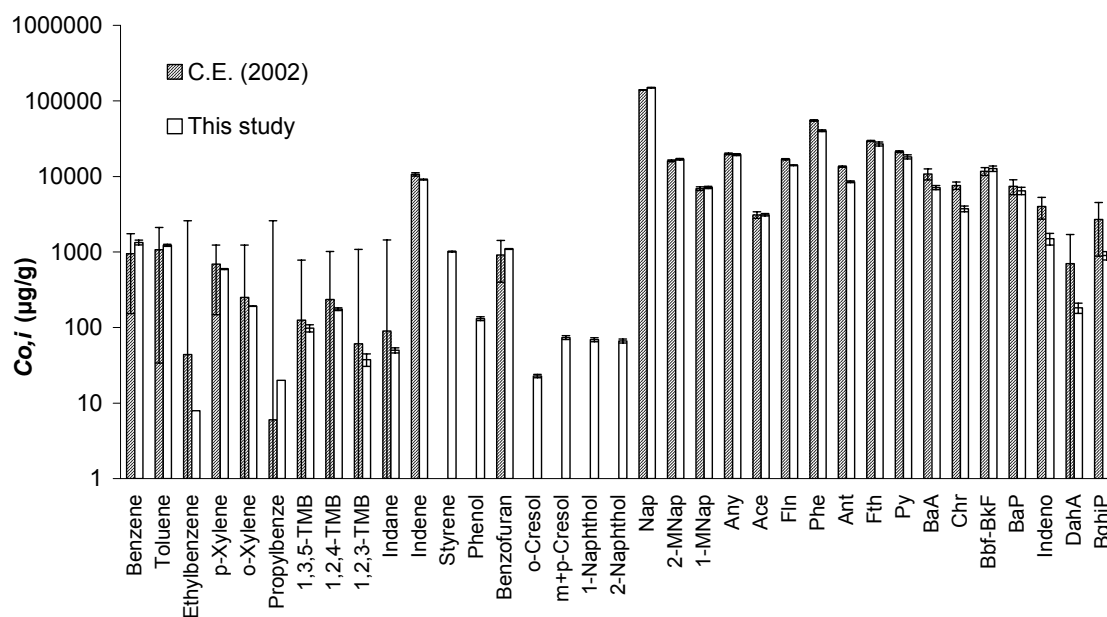


## 4.3 Results and discussion

### 4.3.1 Concentrations of solutes in fresh and aged coal tars

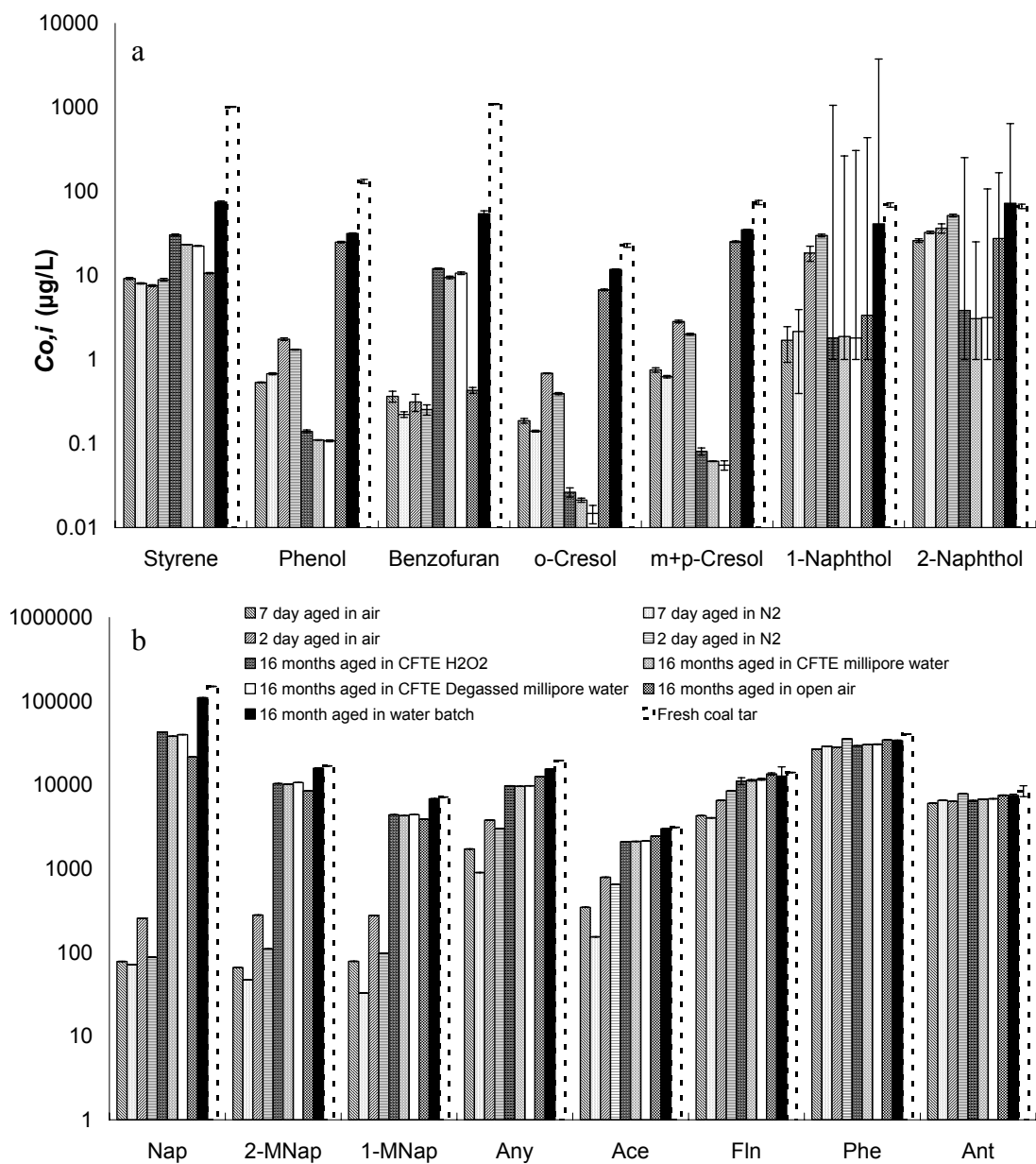
The solutes' concentrations present in fresh and aged coal tar were obtained by GC-MS measurement and converted into wt% (listed in Appendix Table 3 and 4). The mass fractions identified in aged coal tar varied (12-20%) according to different treatments and less than in fresh coal tar as 33%.

**Fresh coal tar:** The concentrations of solutes in fresh coal tar (98142) was measured in this work and compared to that in coal tar used in a previous work [6] which had been stored inside bucket for about 8 years. The data are shown in Figure 4.2 and listed in Appendix Table 3, note that styrene and phenols were only measured in this work. The figure shows that there were no obvious differences between these two coal tar samples. Therefore, the composition of the coal tar stored in a bucket was invariant without contacting to air/water even after 8 years.



**Figure 4.2 Concentrations of solutes in fresh commercial coal tar analyzed this work and 8 years ago (C.E.) [6]. Styrene and phenols were only determined in this work. Standard deviations are shown as error bars based on triplicate measurements of samples, same to below figures.**

**Aged coal tar:** The concentrations of solutes in coal tars aged under different conditions are listed in Appendix 4, and some are shown in Figure 4.3. They were obviously different to fresh coal tar.



**Figure 4.3 Concentrations of solutes in coal tars aged under different environmental conditions. The concentrations of compounds in fresh coal tar were marked here as reference. The compounds are shown in two parts to increase legibility.**

There were no detected BTEX for most of the aged coal tar except for toluene (283 µg/L) in one sample. The concentrations of 4-6 ring PAHs were similar in all of coal tars. Therefore, BTEX and high molecular weight PAHs were not marked in this figure. As shown in Figure 4.3, the concentrations of polar compounds (phenols), volatile compounds (benzofuran, naphthalene) and lighter molecular weight compounds (naphthalenes) were very low in aged coal tars, since they can escape easily during the treating processes due to evaporation and/or dissolution. The concentrations of 3 and 4 ring PAHs were similar to that in fresh coal tar. This may be due to their high concentrations in NAPL and the small amount of depletion during

treatment. However, a few 5-6 ring PAHs (Indeno, DahA and BghiP) had even higher concentrations in aged coal tars. This maybe due to the measurement errors associated with their low concentrations.

The concentrations of solutes in aged coal tars treated under different conditions were different. The concentrations of light molecular weight PAHs and polar compounds increased roughly in this order: 16 months air exposure BE < 2 days air SCT < 2 days N<sub>2</sub> SCT < 7 days air SCT < 7 day N<sub>2</sub> SCT < CFTE with 2% H<sub>2</sub>O<sub>2</sub> ~ CFTE with millipore water ~ CFTE with degassed millipore water < 16 months water BE. This indicated that the change of coal tars' compositions depending on the treatment methods, and evaporation and volatilization contributed more to the change than dissolution. The area of NAPL-air interface was important compare to the experimental time span for evaporation/volatilization process. The oxidation due to the appearance of oxygen (exposure to air) or hydrogen peroxide (CFTE) in solution did affect the aging process, however, its effect was minor important for aging under the experimental conditions.

#### 4.3.2 Equilibrium concentrations of fresh coal tar-water system

##### **Equilibrium aqueous phase concentrations of coal tar-water system**

The equilibrium aqueous phase concentrations ( $C_{i,eq}$ ) were measured in this and the previous work [6]. They can be used in determining the equilibrium partitioning coefficients ( $P_{o/w}$ ).  $C_{i,eq}$  were obtained by (i) 2 years BE performed in 100 ml beaker with about 1:1 (v:v) NAPL and water, and (ii) 16 months BE in a sealed 50 ml vial with about 1:20 of coal tar and water. The previous work was performed with dialysis membrane for 10 months [6]. All the data are shown in Figure 4.4 and listed in Appendix Table 5.

Figure 4.4 shows that most compounds'  $C_{i,eq}$  obtaining from different experiments were similar, especially for polar compounds and most PAHs. 5-6 ring PAHs' concentrations were higher in 16 months batch experimental extracts. The values of 16 months batch experiment were high for most of the compounds except for phenol and cresol. Therefore, the data of this experiment were used consequently in next step.

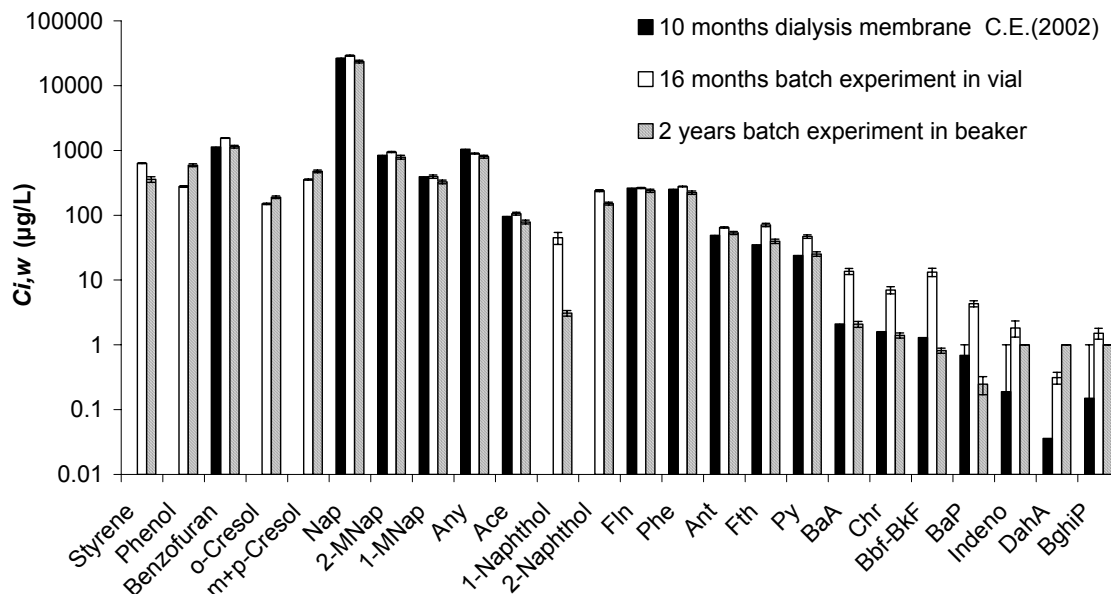
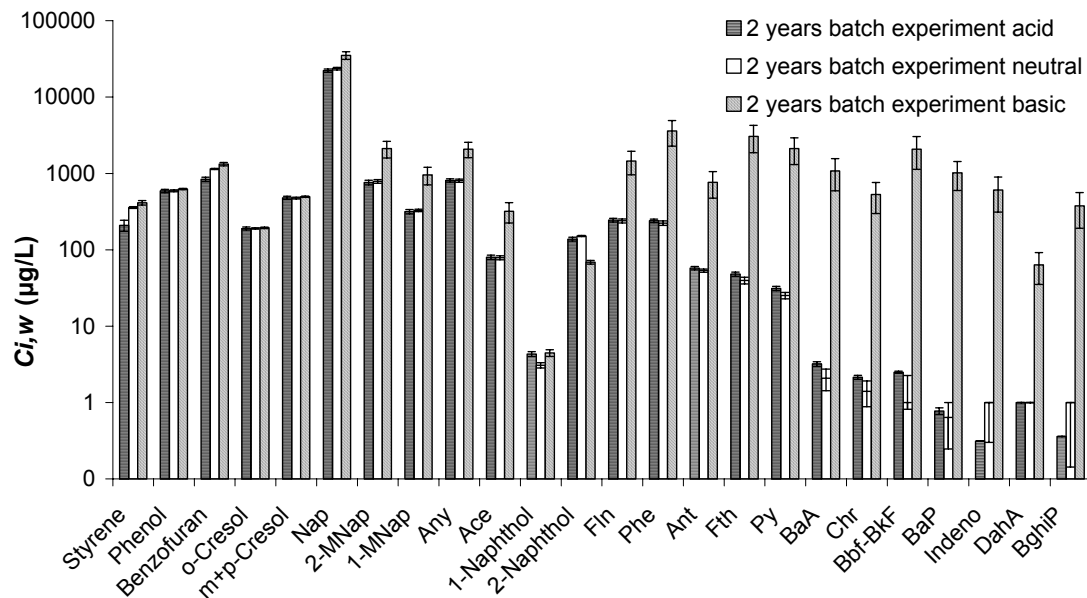


Figure 4.4 Comparison of  $C_{i,eq}$  obtained from different experiments.

### Equilibrium aqueous phase concentrations in solutions of different pH

The batch experiments were performed to see the effect of pH on the ability of aqueous phase to leach compounds from coal tar. As described above, the coal tars were still flowable after 2 more years' exposure to solutions with different pH. The pH of acid and basic solutions shifted toward neutral, and millipore water to acid. The leachates from acid (pH=5), millipore water (pH shift to 5.5) and basic solutions (pH=8) were analysed by GC-MS. Comparison of the aqueous phase concentrations (Figure 4.5, Appendix Table 5) shows clearly the basic solution extracted more organic compounds especially more 4-6 ring PAHs (20% of total PAHs concentration) than others (less than 1%), and the acid solution leached small amount more PAHs than millipore water. The total PAHs leached in aqueous phase were 24.8, 26.1 and 57.3 mg/L for acid, neutral and basic solutions, respectively. It is because the pH of the acid solution was near to that of neutral one at the endpoint of the experiment, and the aqueous phase concentrations should be similar. The higher concentrations of high molecular weight PAHs in basic solution were probably due to the most polar compounds being preferentially extracted in basic solution, and the mole fractions of PAHs in organic phase were relatively higher, which resulted in the higher PAHs' extraction in the aqueous phase. The high PAHs concentrations in basic solution is consistent with the observation of Barrance [8], where film did not form in basic solutions. The mass transfer resistance was subsequently lower in NAPL-basic solution system, and more compounds could be leached to aqueous phase. This result

demonstrates that pH condition is an important factor to the leaching of organic compounds from coal tar, and also important to the composition change of NAPL. It is corresponding to the observation of Liu [9] and Barranco [8]. They found that the pH values significantly influenced film formation and altered interfacial properties, even if Mader found that solution pH did not affect sorption of PAHs to mineral surface [10].



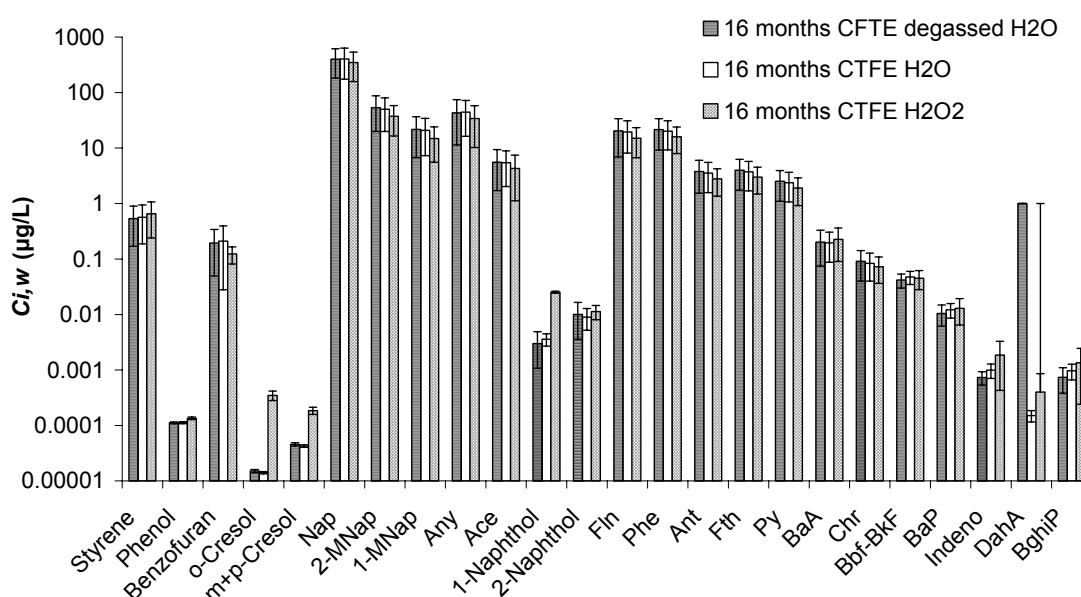
**Figure 4.5 Comparison of the aqueous equilibrium concentrations extracted by solutions of different pH**

However, pH of solution maybe also an essential condition to the aging process. Andersen [11] showed that polar functional groups including phenol enhance the adsorption of asphaltene molecules at the solvent-water interface. Other polar group such as carboxylic acid and amine definitely affect the aging process [12]. However, there is no detectable formation of aging film in performed experiments. This may be due to the aging film can only form and be observed while the depleted mass (or mass ratio) being higher than a critical level. Since batch experiments were performed with about 1:1 NAPL and aqueous, the mass leached from NAPL was limited by  $C_{i,eq}$ , the total mass in aqueous phase was therefore negligible compare to the mass of NAPL (<0.01%). This assumption can be checked by a CFTE system with different pH solutions in next step work.

#### 4.3.3 Aqueous phase concentrations in aged coal tar-water system

##### **Aqueous phase concentrations leached from solutions with different oxidant's concentrations**

The aqueous phase concentrations from the CFTE were analyzed to estimate the leaching ability of solutions under different oxidant concentrations. The CFTE had run for 16 months, and the NAPLs became solid during this time period. The endpoint aqueous phase concentrations are listed in Appendix Table 5 and shown in Figure 4.6. For a certain compound, the concentrations were similar in different samples, except for the higher values of Cresols and 1-Naphthol in H<sub>2</sub>O<sub>2</sub> solution flowing system. Consider the similar solutes' concentration in these NAPLs (Figure 4.3), this result only demonstrated that the appearance of oxidant was neither an essential factor to the leaching properties nor contributed to the aging process under the experimental condition.



**Figure 4.6 Comparison of the steady state concentrations extracted from CFTE with different oxidant concentrations.**

Compare these data to the  $C_{i,eq}$  obtained from fresh coal tar-water system, most of the compounds were 1 to 6 orders of magnitude lower. However, the concentrations of 2-4 ring PAHs were still very high in CFTE system even after long time of leaching and with an additional resistance of the aged interfacial phase.

#### **Aqueous phase concentrations at different time periods in aged coal tar-water system**

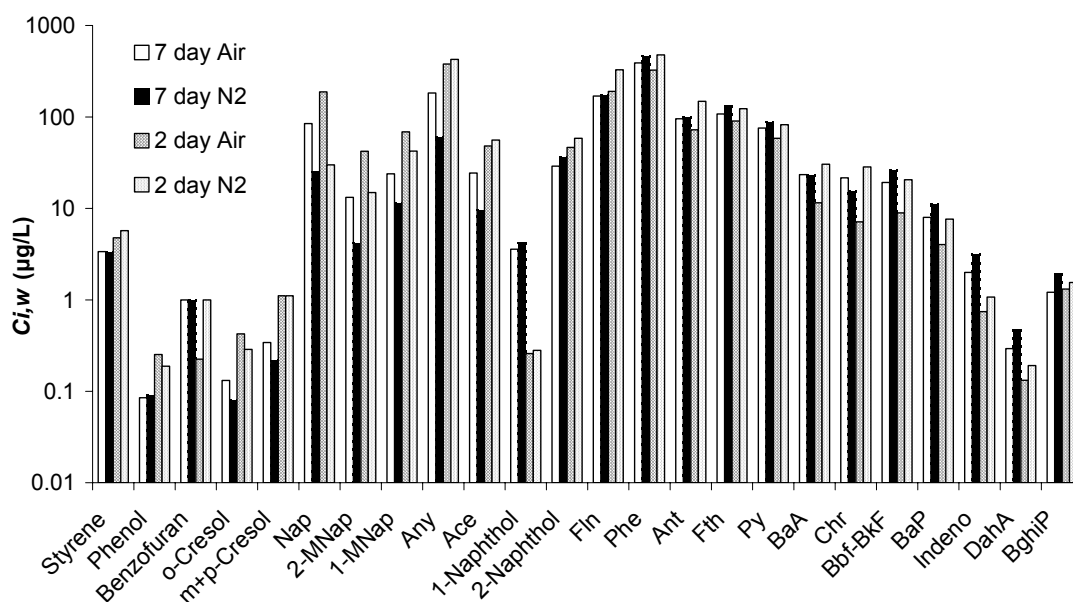
The aqueous phase concentrations contacted with aged coal tars were obtained at different time periods from the batch experiment (Figure 4.1). The concentrations of analyzed compounds are listed Appendix Table 6. There was almost no detectable 2,3- benzofuran for most of the samples. Samples of 7 day aged in air and N<sub>2</sub> showed

similar aqueous phase concentrations, and same to 2 day air and N<sub>2</sub> samples. This further demonstrated the appearance of O<sub>2</sub> was not a decisive factor to the compositional change of coal tar and aging process. The differences existed between the data of 7 and 2 day NAPL-water systems as expected. The different leaching behavior of 2 and 7 day samples indicates that 2 day aged coal tar probably had intermediate properties of aged (e.g. 7 day aged) and fresh coal tars. This is consistent with the observations of its consistency during sampling. The NAPLs formed at day 2 easily to small beads after scratched from the glass plates rather than pieces of thin film of 7 day NAPLs

In addition, different compounds needed different time periods to reach equilibrium for all of the NAPL-water systems. The equilibrium time depends on the molecular weight, naphthalenes were the fast group, and 4-5 ring compounds needed longer time.

### Equilibrium aqueous phase concentrations of aged coal tar-water systems

The data of  $C_{i,eq}$  were taken from different day's concentrations for aged coal tars-water systems, since different time periods were needed to reach the equilibrium. All data are shown in Figure 4.7, and marked in Appendix Table 6. The concentrations of



**Figure 4.7** Equilibrium concentrations contacted with aged coal tars from batch experiments

different samples were similar for most of the components except for 1-Naphthol, which were extremely low in 2 day batch experimental solutions. This is may be due to the measurement error. Two day aged coal tar in air had the highest  $C_{i,eq}$  of the light molecular weight compounds (lower than 1-MNAP).

#### 4.3.4 Partitioning coefficients of compounds from different NAPLs

With concentrations of solutes in coal tars  $C_o$ , and the equilibrium aqueous phase concentrations  $C_{i,eq}$ , the partitioning coefficients can be calculated for compounds in aged coal tars.

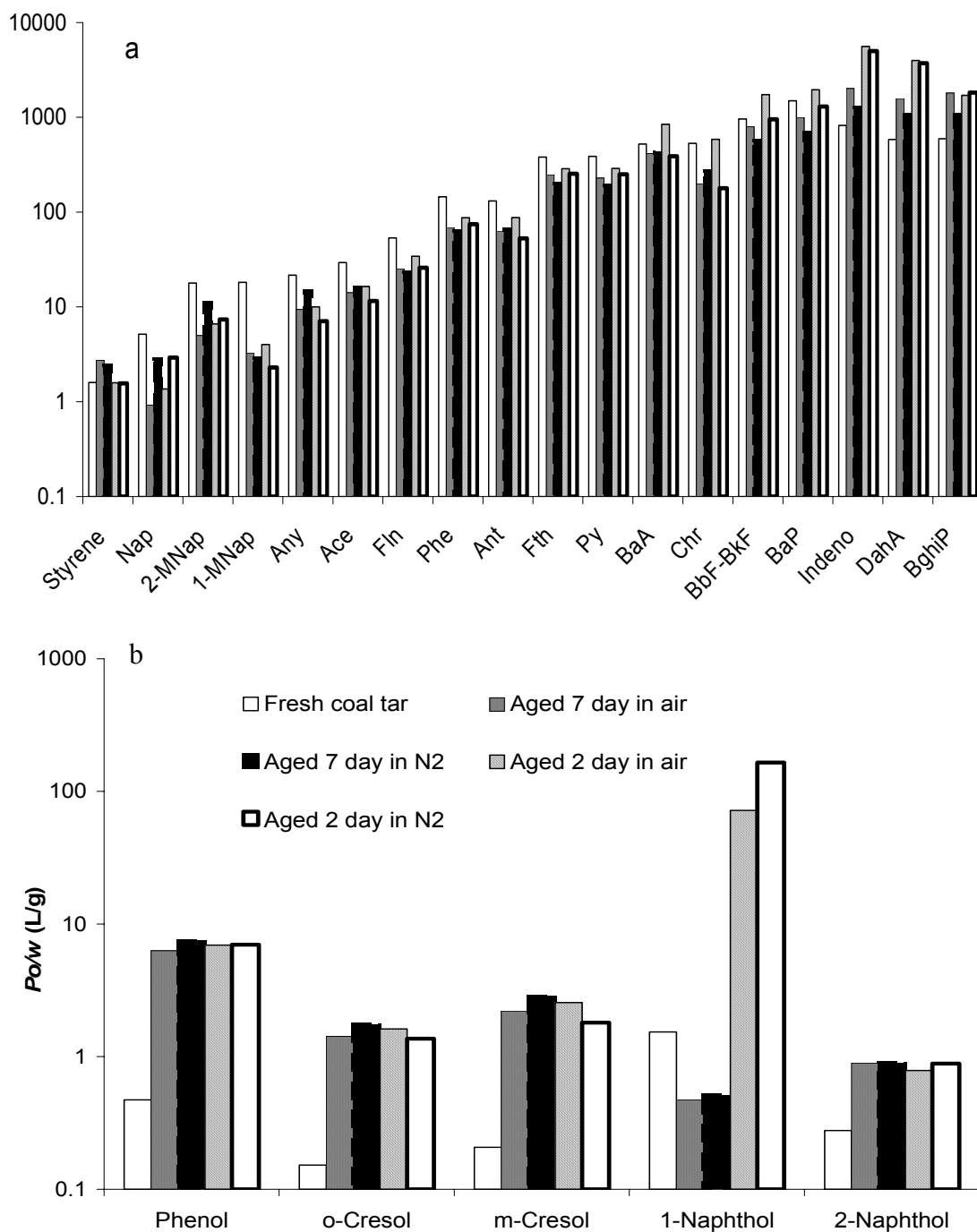
$$P_{o/w} = C_o / C_{eq} \quad (4.1)$$

All of the computed data are shown in Figure 4.8 and listed in Table 4.1. Most of these data were close to but lower than the published data [13]. The partitioning coefficients of one compound in different samples were similar. For PAHs the partitioning coefficients increased with the increase of the molecular weight and decreased with the water solubility as expected (Appendix Figure). Fresh coal tar showed the highest values for most of the PAHs, which is probably due to their lower vapor pressures, the depletion of mass due to evaporation/volatilization during treatment was almost negligible for these components. It is also due to the solidification of the interfacial phase, the newly formed solid film can hinder the transfer of PAHs from organic phase to water. For phenols, all of the components in aged coal tars had similar higher values than that of fresh coal tar except for the 1-Naphthol, which may be due to the measurement error, and the partitioning coefficients increased with the increase of the water solubility. Further, there were no obvious different between the samples aged in air and in nitrogen atmosphere. Consider the solid interfacial film can hinder compounds transfer to water. This high  $C_{i,eq}$  or low  $P_{o/w}$  can only explain by (i) these compounds are component of the interfacial film as showed by Andersen [11], and/or (ii) this solid film prevent more the transfer of PAHs than phenols. Therefore, the study of the interfacial structure is necessary.

#### 4.3.5 Mass transfer coefficients of compounds in different NAPLs

With the dynamic concentrations from batch equilibrium, a value of mass transfer coefficient for the compounds in 2 and 7 day aged coal tars were obtained as fitted parameters was obtained according to the mass balance equation (eq 1.3) [14], the analytical solution of eq 2.6, the analytical solution of eq 1.3.





**Figure 4.8 Comparison of partitioning coefficients of compounds between coal tar and water phase. a, aromatic compounds, b, phenols**

The numerical values of the overall mass transfer coefficient,  $k$  (cm/s) was obtained by fitting eq 2.6 to the measured aqueous concentrations of  $i$  over the experimental period. The objective function, which was minimized, was given by relative residual sum of square (RRSS) in eq 2.7.

**Table 4.1 Partitioning coefficients of compounds between coal tar and water (log p)**

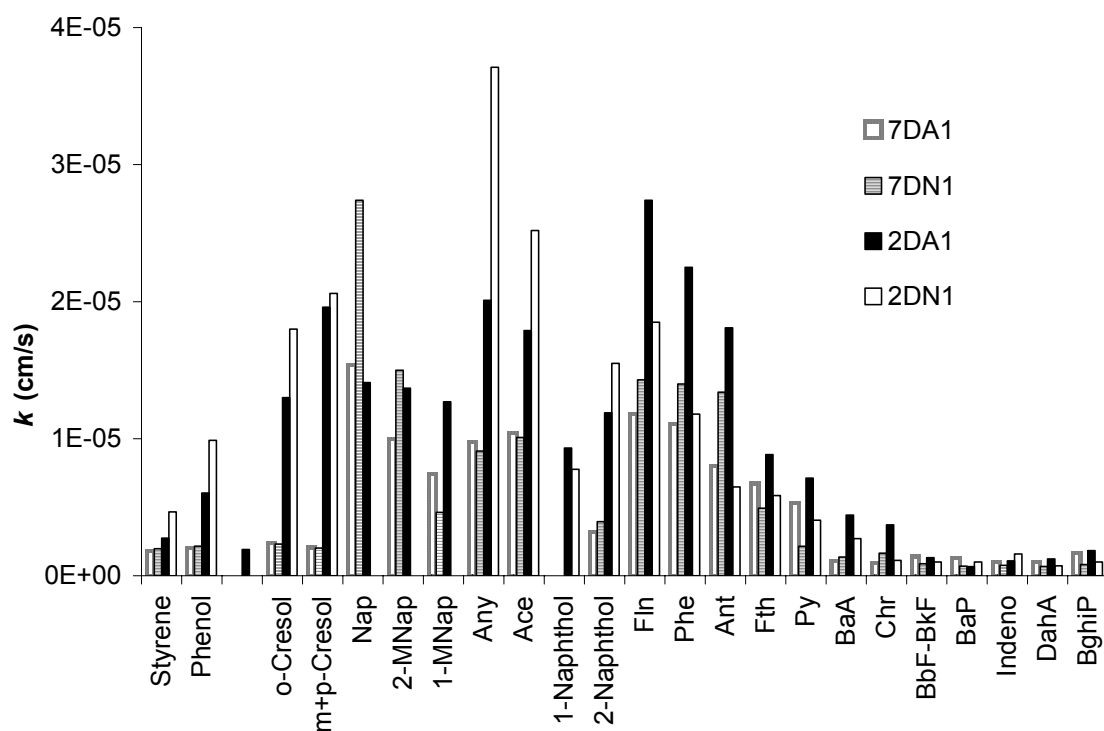
	Fresh coal tar	7 day in air	7 day in N2	2 day in air	2 day in N2	Published data <sup>a</sup>
Styrene	3.20	3.44	3.38	3.20	3.19	2.99
Phenol	2.67	3.80	3.87	3.84	3.84	1.91
o-Kesol	2.18	3.15	3.24	3.21	3.14	
m-Kresol	2.32	3.34	3.46	3.41	3.26	
Nap	3.71	2.96	3.45	3.13	3.47	3.83
2-MNap	4.25	3.70	4.05	3.82	3.87	4.40
1-MNap	4.26	3.51	3.57	3.60	3.36	4.33
Any	4.34	3.97	4.17	4.00	3.85	4.46
Ace	4.47	4.15	4.20	4.22	4.06	4.48
2-Naphthol	2.44	2.95	2.95	2.90	2.95	
Fln	4.73	4.40	4.37	4.53	4.41	4.83
Phe	5.16	4.84	4.80	4.94	4.87	5.27
Ant	5.12	4.80	4.82	4.94	4.72	5.39
Fth	5.58	5.39	5.30	5.46	5.40	6.00
Py	5.59	5.36	5.29	5.46	5.40	6.11
BaA	5.72	5.62	5.63	5.93	5.59	6.24
Chr	5.73	5.30	5.43	5.77	5.25	6.48
BbF-BkF	5.98	5.90	5.75	6.24	5.98	7.15
BaP	6.17	6.00	5.84	6.29	6.11	7.06
Indeno	5.92	6.30	6.10	6.75	6.70	7.34
DahA	5.77	6.20	6.03	6.60	6.57	7.29 <sup>b</sup>
BghiP	5.77	6.26	6.02	6.23	6.26	7.10 <sup>b</sup>

**a [13], experimental data from 1 to 17 coal tar samples; b from [6]**

The data of  $k$  are shown in Figure 4.9, and listed in Table 4.2. Figure 4.9 shows that compounds in 2 day treated coal tar had higher values than in 7 day's as expected. For 2 day treated coal tars, aged in nitrogen sample obtained higher values than aged in air for most of the light molecular weight compounds and vice versa. This is because of the flow rate inside the glove bag being lower than the fume hood, and resulting in the less depletion of volatile compounds by evaporation.

For 7 day aged coal tars, most compounds in air treated NAPL had similar to, or small amount higher values than in nitrogen, which further suggests that oxidation is not a factor on mass transfer of compounds. For PAHs the mass transfer coefficients decreased with the increase of the molecular weight, and decrease of the water solubilities. 2-3 ring PAHs obtained highest values. This may be due to the aged film did not hinder the transfer of these components. Phenols and high molecular weight

PAHs had lower coefficients of all samples. This is because of their lower concentrations of phenols in NAPL, since most of which had depleted during the treating process (about 99% phenol and 96-99% cresols) or formed part of the interfacial layer. For high molecular weight compounds, their large molecular sizes and low water solubilities should hinder their transfer to aqueous phase.



**Figure 4.9** Mass transfer coefficients of aged NAPLs obtained as a fitting parameter of eq 2.6 to experimental data

Above all, the mass transfer coefficients vary in the range of  $10E-5$  to  $10E-7$  cm/s, which is about two orders of magnitude lower than the data in the simple model NAPL-water system (Table 2.2) and various fresh NAPLs-water system published in the literatures (Appendix Table 2). This proves that the mass transfer process was delayed by aging of the interface. Further research work is necessary to check the mass transfer process of the fresh coal tar. The experiment can be performed by continuously stirring flow through reaction system, which will be introduced in next chapter.

#### 4.4 Conclusions

The concentrations of some solutes in fresh and aged coal tars were dramatically different. Aged coal tars showed no detectable BTEX, and had less concentrations of

phenols, 2,3-benzofuran, styrene and light molecular weight PAHs than fresh coal tar. However, the high molecular weight PAHs showed no obvious difference. Therefore,

**Table 4.2 Mass transfer coefficients of compounds from aged coal tars (cm/s)**

	7 day Aged in Air $\pm$ RRSS	7 day Aged in N2 $\pm$ RRSS	2 day Aged in Air $\pm$ RRSS	2 day Aged in N2 $\pm$ RRSS
Styrene	1.8E-06 $\pm$ 0.27	2.0E-06 $\pm$ 0.1	2.7E-06 $\pm$ 0.24	4.7E-06 $\pm$ 0.19
Phenol	2.0E-06 $\pm$ 0.28	2.2E-06 $\pm$ 0.25	6.0E-06 $\pm$ 0.19	9.9E-06 $\pm$ 0.24
o-Cresol	2.4E-06 $\pm$ 0.19	2.3E-06 $\pm$ 0.28	1.3E-05 $\pm$ 0.13	1.8E-05 $\pm$ 0.25
m+p-Cresol	2.1E-06 $\pm$ 0.21	2.0E-06 $\pm$ 0.28	2.0E-05 $\pm$ 0.12	2.1E-05 $\pm$ 0.26
Naphthalene	1.5E-05 $\pm$ 0.014	2.7E-05 $\pm$ 0.006	1.4E-05 $\pm$ 0.076	
2-Methylnaphthalene	1.0E-05 $\pm$ 0.04	1.5E-05 $\pm$ 0.02	1.4E-05 $\pm$ 0.028	
1-Methylnaphthalene	7.4E-06 $\pm$ 0.05	4.6E-06 $\pm$ 0.6	1.3E-05 $\pm$ 0.02	
Acenaphthylene	9.8E-06 $\pm$ 0.04	9.1E-06 $\pm$ 0.06	2.0E-05 $\pm$ 0.021	3.7E-05 $\pm$ 0.13
Acenaphthene	1.0E-05 $\pm$ 0.045	1.0E-05 $\pm$ 0.05	1.8E-05 $\pm$ 0.026	2.5E-05 $\pm$ 0.25
2-Naphthol	3.2E-06 $\pm$ 0.07	3.9E-06 $\pm$ 0.07	1.2E-05 $\pm$ 0.08	1.6E-05 $\pm$ 0.1
Fluorine	1.2E-05 $\pm$ 0.26	1.4E-05 $\pm$ 0.027	2.7E-05 $\pm$ 0.019	1.8E-05 $\pm$ 0.21
Phenanthrene	1.1E-05 $\pm$ 0.04	1.4E-05 $\pm$ 0.047	2.2E-05 $\pm$ 0.025	1.2E-05 $\pm$ 0.03
Anthracene	8.0E-06 $\pm$ 0.04	1.3E-05 $\pm$ 0.039	1.8E-05 $\pm$ 0.11	6.5E-06 $\pm$ 0.027
Fluoranthene	6.7E-06 $\pm$ 0.05	4.9E-06 $\pm$ 0.17	8.8E-06 $\pm$ 0.22	5.9E-06 $\pm$ 0.13
Pyrene	5.3E-06 $\pm$ 0.12	2.1E-06 $\pm$ 0.61	7.1E-06 $\pm$ 0.68	4.0E-06 $\pm$ 0.24
Benz(a)anthracene	1.1E-06 $\pm$ 0.58	1.4E-06 $\pm$ 0.23	4.4E-06 $\pm$ 0.44	2.7E-06 $\pm$ 0.06
Chrysene	9.6E-07 $\pm$ 0.3	1.6E-06 $\pm$ 0.28	3.7E-06 $\pm$ 0.6	1.1E-06 $\pm$ 0.047
Benzo(b)fluoranthene Benzo(k)fluoranthene	1.4E-06 $\pm$ 0.46	8.8E-07 $\pm$ 0.21	1.3E-06 $\pm$ 0.44	1.0E-06 $\pm$ 0.24
Benzo(a)pyrene	1.3E-06 $\pm$ 3.9	7.0E-07 $\pm$ 0.9	6.7E-07 $\pm$ 0.49	1.0E-06 $\pm$ 1.57
Indeno(1,2,3-cd)pyrene	1.0E-06 $\pm$ 0.48	7.6E-07 $\pm$ 0.28	1.1E-06 $\pm$ 0.66	1.6E-06 $\pm$ 0.87
Dibenzo(a,h)anthracene	1.0E-06 $\pm$ 0.51	6.8E-07 $\pm$ 1.39	1.2E-06 $\pm$ 0.84	7.2E-07 $\pm$ 0.44
Benzo(g,h,i)perylene	1.7E-06 $\pm$ 0.016	8.3E-07 $\pm$ 0.65	1.8E-06 $\pm$ 0.87	1.0E-06 $\pm$ 33

**There are a few data points for Benzofuran, naphthalenes and 1-Naphthol in some NAPLs. Mass transfer coefficient could not be obtained for these compounds.**

the risk of pollution by organic contaminants still existed for groundwater, and was still high for some compounds near the contaminated sites even though some well water soluble compounds were depleted during the leaching process. The change of solute concentration and the degree of aging depended more on the treatment process and environmental conditions than on experimental time span. The evaporation / volatilization and leaching processes had significant effects on aging process of coal tar. For the commercial coal tar, under investigation evaporation of volatile

components was a more important factor than dissolution of components for the formation of an aged interfacial film. Oxidation due to the presence of oxygen or hydrogen peroxide in solution did somewhat affect the aging process, however, it was only a second order factor under the studied experimental conditions. The pH value of the solution was significant to the extraction/leaching properties of compounds from NAPLs phase, and it might be also important to the aging process. The overall mass transfer coefficients of the experimental compounds, the best fitting parameters for the operation system increased with the water solubilities and decreased with the molecular weight for PAHs. Further, phenols behaved different to PAHs in this test. There was no obvious rule for phenols, except for the mass transfer coefficients in 2 day aged samples were higher than 7 days sample. All of analyzed compounds' mass transfer coefficients in 7 and 2 day treated coal tars were about two orders of magnitude lower than that in fresh and model NAPLs. This indicated the mass transfer resistance increased during aging process. The increase of the mass transfer resistance is due to the mass depletion of the compounds in NAPL phase and the formation of the solid interfacial phase.

#### 4.5 References

1. Luthy, R.G., et al., Interfacial films in coal tar nonaqueous-phase liquid-water systems. *Environmental Science and Technology*, 1993. 27(13): p. 2914-18.
2. Nelson, E.C., et al., Chemical Characterization of Coal Tar-Water Interfacial Films. *Environmental Science and Technology*, 1996. 30(3): p. 1014-22.
3. Zheng, J., J. Shao, and S.E. Powers, Asphaltenes from Coal Tar and Creosote: Their Role in Reversing the Wettability of Aquifer Systems. *Journal of Colloid and Interface Science*, 2001. 244(2): p. 365-371.
4. Jeribi, M., et al., Adsorption kinetics of asphaltenes at liquid interfaces. *Journal of Colloid and Interface Science*, 2002. 256(2): p. 268-272.
5. Ghoshal, S., C. Pasion, and M. Alshafie, Reduction of benzene and naphthalene mass transfer from crude oils by aging-induced interfacial films. *Environmental Science & Technology*, 2004. 38(7): p. 2102-2110.
6. Eberhardt, C.G., P., Time scales of organic contaminant dissolution from complex source zones: coal tar pools vs. blobs. *Journal of Contaminant Hydrology*, 2002. 59(1-2): p. 45-66.
7. Mukherji, S., C.A. Peters, and W.J. Weber, Jr., Mass Transfer of Polynuclear Aromatic Hydrocarbons from Complex DNAPL Mixtures. *Environmental Science and Technology*, 1997. 31(2): p. 416-423.

8. Barranco, F.T. and H.E. Dawson, Influence of aqueous pH on the interfacial properties of coal tar. *Environmental Science & Technology*, 1999. 33(10): p. 1598-1603.
9. Liu, J., et al., Colloidal interactions between asphaltene surfaces in aqueous solutions. *Langmuir : the ACS journal of surfaces and colloids* FIELD Publication Date:2006, 2006. 22(4): p. 1485-92. FIELD Reference Number: FIELD Journal Code:9882736 FIELD Call Number:.
10. Mader, B.T., K. Uwe-Goss, and S.J. Eisenreich, Sorption of Nonionic, Hydrophobic Organic Chemicals to Mineral Surfaces. *Environmental Science and Technology*, 1997. 31(4): p. 1079-1086.
11. Andersen, S.I., et al., Interaction and solubilization of water by petroleum asphaltenes in organic solution. *Langmuir*, 2001. 17(2): p. 307-313.
12. Dong, J., B. Chowdhry, and S. Leharne, Investigation of the Wetting Behavior of Coal Tar in Three Phase Systems and its Modification by Poloxamine Block Copolymeric Surfactants. *Environmental Science and Technology*, 2004. 38(2): p. 594-602.
13. Endo, S. and T.C. Schmidt, Prediction of Partitioning between Complex Organic Mixtures and Water: Application of Polyparameter Linear Free Energy Relationships. *Environmental Science and Technology*, 2006. 40(2): p. 536-545.
14. Mahjoub, B., et al., Phase partition of organic pollutants between coal tar and water under variable experimental conditions. *Water Research*, 2000. 34(14): p. 3551-3560.

# **Chapter 5 Mass Transfer Process from NAPLs to water studied in a Continuously Stirring Flow Through Reactor**

## **5.1 Introduction**

Aquifers and soils are often contaminated by non-aqueous phase liquids (NAPLs), which are long term sources for groundwater plumes. As groundwater flows passes trapped ganglia or NAPL pools, a fraction of the NAPL dissolves in the aqueous phase creating a plume of dissolved hydrocarbons. This may cause the contamination of the groundwater, which is a worldwide major source of drinking water [1-3]. The mass transfer kinetics of solutes from NAPLs has been extensively studied. Several theoretically and experimentally derived mass transfer relationships are available in the literatures to describe the dissolution of NAPL pools and residual NAPL blobs [4-13].

Various empirical correlations for estimating the over all mass transfer coefficients  $k$  (cm/s), a measure of the resistance to mass transfer have been proposed and involving parameters such as water velocity, NAPL saturation, and grain-size of the porous medium [1, 14-16]. For the mathematical models of contaminant transport originating from NAPL pool dissolution, it is often assumed that mass transfer rates inside the NAPL are faster than the advective dispersive transport of the dissolved NAPLs away from the interface, i.e. the water boundary layer is limiting the dissolution process. However, in some situations, especially the presence of a solid or semi-solid interfacial film formed due to the aging phenomena, the resistance of this interfacial layer may not be neglectable [11, 17].

## **5.2 Research Objectives**

The main objectives of this work are, (i) to design an experimental set-up for the determination of mass transfer coefficients at different hydromechanical and physicochemical conditions, (ii) to test the applicability of Raoult's law for complex NAPL mixtures, and (iii) to establishment and/or modify a numerical model to describe the mass transfer process and to determine the related parameters.

## 5.3 Materials and methods

### 5.3.1 Materials - Model NAPL

In the single solute experiment, phenanthrene was used as the probe compound at a concentration of 3 g in 250 mL toluene. This concentration (12 g/L) is representative of most real NAPLs, e.g. coal tar or creosotes. This simple single solute model NAPL was used to check and improve the experimental set-up, sampling and analytical method as well as to validate the numerical model.

Subsequent experiments were carried out with a complex model NAPL. The compounds (with their associated purities) in a toluene solution were naphthalene (98%, Aldrich), phenanthrene (98%, Alfa Aesar), 2,3-benzofuran (99%, Aldrich), phenol (99.5%, Fluka), m-Cresol (99%, Aldrich), 1-Naphthol (99%, Aldrich) and phenoxathiin (98%, Alfa Aesar). These compounds are representatives of frequently detected contaminants including PAHs, phenols and heterocyclic aromatic compounds, and they are also major constituents of real NAPLs, except for phenoxathiin, which has never been reported in any contaminate sites. It was taken as a reference to validate the experimental and modeling process. The initial masses and concentrations ( $C_o$ ) of these compounds in the organic phase are listed in Table 5.1. The aqueous phase in contact with the model NAPL consisted of toluene pre-saturated water to avoid depletion of the solvent.

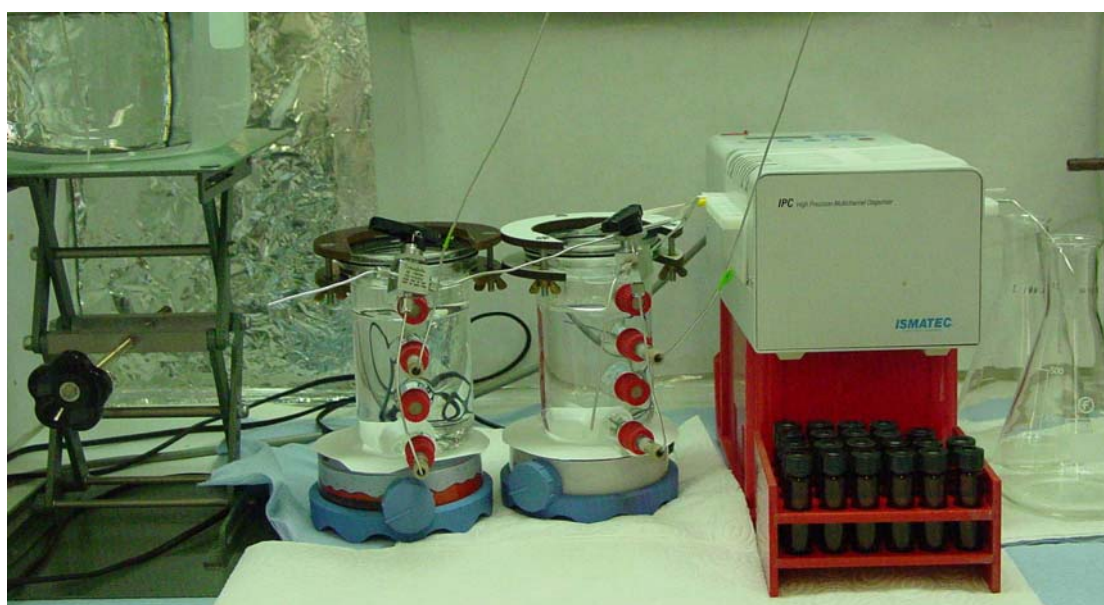
**Table 5.1 Composition of the complex model NAPL**

	<b>Mass (g)</b>	<b>MW (g/mol)</b>	<b><math>C_o</math> (g/L)</b>	<b>Mole</b>	<b>Mole fraction (%)</b>
Phenol	0.00088	94.1	0.0044	0.000009	0.0005
2,3-Benzofuran	0.0570	118.1	0.29	0.00048	0.026
m-Cresol	0.00094	108.1	0.0047	0.0000087	0.0005
Naphthalene	0.9081	128.2	4.54	0.0071	0.38
1-Naphthol	0.0019	144.2	0.0094	0.000013	0.0007
Phenoxathiin	2.003	200.2	10.0	0.010	0.54
Phenanthrene	1.993	178.2	9.96	0.011	0.60
Toluene (solvent)	200 mL	92.1	839.7	1.82	98.44



### 5.3.2 Continuously Stirred Flow Through Reaction System (CSFTRS)

An experimental system was set-up to measure mass transfer of contaminants from NAPL to water. The configuration of the set-up is shown in Figure 5.1. The self-designed cell (500 mL) is sealed by a Viton ring and a horse shoe to make it gas tight. Aqueous and NAPL phases were filled inside the cell with a constant or variable volume ratio. Figure 5.1 shows the LNAPL-water system, but the reactor can be operated also with DNAPL (e.g., TCE, coal tar) and even porous media with a certain NAPL saturation. Two magnetic stirring bars can be put at the top and bottom, respectively, to mix one or two phases without affecting the interfacial area. The cell was fed from the liquid reservoir by a peristaltic pump (ISMATEC, Switzerland) through stainless steel tubing (1/16", Klaus Ziemer GmbH, Mannheim), the flow rate of the aqueous phase can adjusted and controlled. A three way-valves connector (Swagelok 1/16") was used to connect the reactor with the pump and the sampling port. The CSFTRS can be operated at different hydromechanical (flow rate, volume ratio, with or without porous medium, variable NAPL saturation) and physicochemical conditions (pH, ionic strength, in the absence or presence of reactants such as oxidants, metals and organic compounds or microbe). The aqueous concentrations in the reactor effluent were sampled and measured by Gas Chromatography (GC) with a mass detector.



**Figure 5.1** Setting up of the continuous stirring flow through reaction system

The preliminary tests were run for 24 hours, and a steady state concentration was observed after 6 h at a flow rate of 0.5 mL/min, the average resident time of the water

in the reactor was 13 hr. Subsequently, the subsequent experiments were performed for 8 hours (0.5 mL/min), and 18 aqueous samples were collected. The first sample was taken in 5 min after the NAPL and aqueous having contacted. The sampling interval was 10 min within first 2 hours, later the interval extended to 20, 30 and 60 min.

### 5.3.3 Chemical analyses

Aqueous sample (5 mL) was spiked with 5-10  $\mu\text{L}$  of internal standard, acenaphthylene (2 g/L) dissolved in toluene solution, and extracted by 1 mL ethyl acetate. The extractants was analysed by GC-MS (HP 5890/II with HP 5972 MSD) together with four external standards (mixture of all organic compounds in cyclohexane at four different concentrations). The linear regression was used to determine the relationship between measured areas of signal and concentrations of standards. The concentrations of the aqueous sample were calculated according to the slop of this linear relationship.

Analytes were separated using a 30 m  $\times$  0.25 mm DB-5MS column (J&W Scientific) with 0.25  $\mu\text{m}$  film thickness. The injector temperature was maintained at 270  $^{\circ}\text{C}$ , and the injection volume was 1  $\mu\text{L}$ . Helium was used as the carrier gas at a constant flow of 0.6 mL/min. The oven temperature programme was 50  $^{\circ}\text{C}$  for 2 min then increased at a rate of 8  $^{\circ}\text{C}/\text{min}$  to 90  $^{\circ}\text{C}$ , increased to 270  $^{\circ}\text{C}$  at a rate of 18  $^{\circ}\text{C}$ , held for 10 min and finally raised to 310  $^{\circ}\text{C}$  (held for 6.5 min), the total time period is 48.5 min. The chromatogram of a sample is shown in Figure 5.2.

### 5.3.4 Modeling approach

In this system the mass transfer from NAPL to water is due to the diffusion and advective flow. Consequently, the change in the aqueous phase concentrations in the reactor with respect to time can be described by two terms (see eq. 5.1) [2, 10, 11].

$$\frac{dC_i}{dt} = \frac{A}{V_w} k_i (C_{i,eq} - C_i) - \frac{Q}{V_w} C_i \quad (5.1)$$

where,  $C_i$  ( $\mu\text{g}/\text{mL}$ , or  $\mu\text{g}/\text{L}$ ) is the time-dependent concentrations of solute  $i$  in water phase, and  $A$  ( $\text{cm}^2$ ),  $V_w$  ( $\text{cm}^3$ ),  $Q$  ( $\text{ml}/\text{min}$ ) are the interfacial area, water volume and flow rate, respectively.  $C_{i,eq}$  is the equilibrium aqueous phase concentration at time  $t$  of the compound  $i$ . The overall mass transfer coefficient for the solute  $i$  is  $k_i$  ( $\text{cm}/\text{min}$ ).

Note that both terms in equation 5.1 have the units of mass per volume per time ( $\mu\text{g}/\text{cm}^3/\text{min}$ ). The first term on the right hand side is referred to as the exchange term  $E$  between the organic and the aqueous phase. This term also represents the sink to the organic phase.

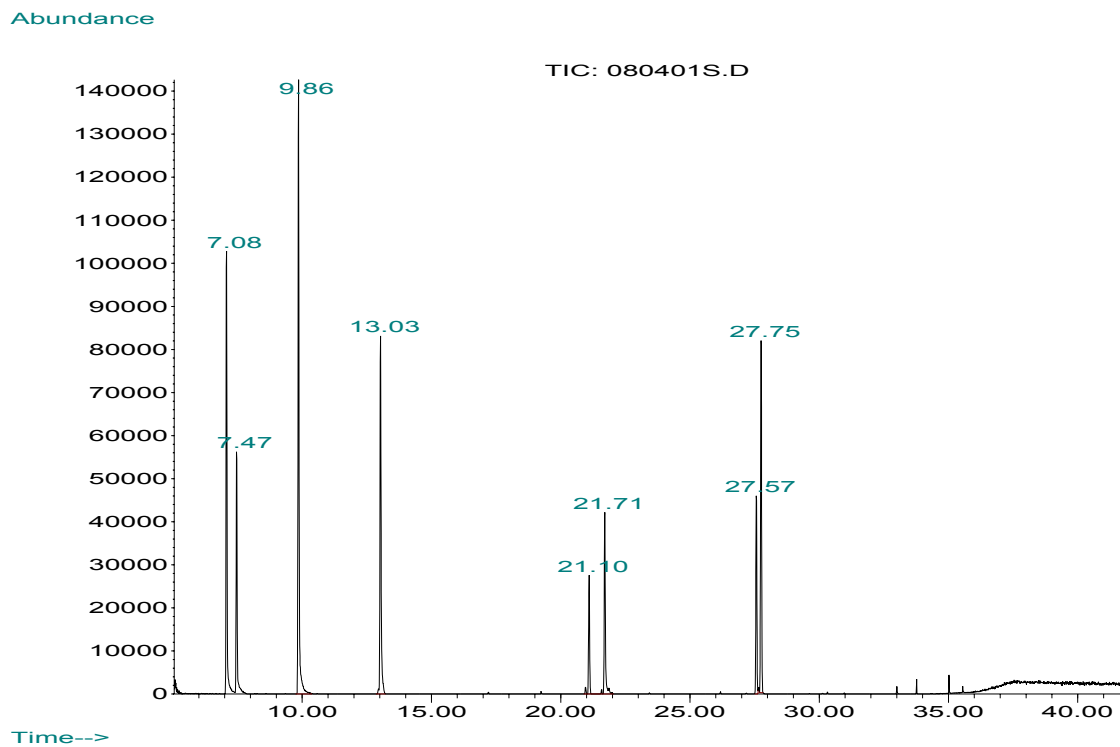


Figure 5.2 Chromatograph of a representative sample. The compounds are phenol, benzofuran, m-cresol, naphthalene, acenaphthylene, 1-naphthol, phenoxathiin and phenanthrene.

### Analytical model

In the single solute experiment, phenanthrene was used as the probe compound, and the mass leached of this solute from the NAPL phase was negligible compared to the total mass (or remaining mass) due to its low water solubility ( $<0.06\%$ ). The concentration of solute in the NAPL phase was constant, in particular,  $C_{i,eq}$  can be treated as a constant. During flushing period the change in NAPL volume and  $k_i$  was considered negligible. The eq. 5.1 can be integrated to yield:

$$C_i = \frac{A \cdot k_i \cdot C_{i,eq}}{A \cdot k_i + Q} - \left( \frac{A \cdot k_i \cdot C_{i,eq}}{A \cdot k_i + Q} - C_{i,0} \right) \cdot e^{-\left( \frac{A}{V_w} k_i + \frac{Q}{V_w} \right) (t - t_0)} \quad (5.2)$$

where  $t_0$  is the initial time,  $C_{i,0}$  is the initial concentration. The goodness of fit  $k_i$  for each set of aqueous concentration data was evaluated by the values of the relative residual sum of squares (RRSS) as eq 2.7.

### Numerical model

In the complex model NAPL, the well soluble compounds, e.g., phenols, 2,3-benzofuran were depleted significantly from the phase during the experimental period. Therefore,  $C_{i,eq}$  may decrease and it could not be taken as a constant. In this case, there is no analytical solution for eq 5.1 and a numerical solution is required. This problem can be solved by introducing *Raoult's law*.

$$C_{i,eq} = \chi_i \cdot \gamma_i \cdot S_{i,sub} \quad (5.3)$$

where preliminary,  $\chi_i$  are the activity coefficient and mole fraction of  $i$  in NAPL phase,  $S_{i,sub}$  is the subcooled liquid solubility. Previous research has demonstrated that Raoult's law with  $\gamma_i$  of unity or very close to unity holds for monocyclic and polycyclic aromatic hydrocarbons in model and real NAPLs [17-20]. However,  $\gamma_i$  is unity only for ideal solutions. Under more complex conditions,  $\gamma_i$  may become a function of individual compounds'  $\chi_i$  [21]. If a power law dependence of the activity coefficient on the component mole fraction is assumed using an exponent  $n$  ( $\gamma_i = \text{constant} \cdot \chi_i^n$ ), it may be useful to lump the mole fraction dependence to obtain:

$$C_{i,eq} = \gamma_i^* \cdot \chi_i^{n+1} \cdot S_{i,sub} \quad (5.4)$$

with  $n$  as an empirical exponent of  $\chi_i$ , it could be (i) negative ( $n < 0$ ) for the compounds which may involve strong polar interactions in the solute : water interaction, (ii) close to zero ( $\chi_i$  close to 1) for the solutes in which molecular interactions in the organic solutions are nearly the same as in the pure liquid compound, and (iii) positive ( $n > 0$ ) for the solute and solvent both acquire additional intermolecular interactions that were unavailable to them in their pure liquid phases.  $\gamma_i^*$  as a mole fraction independent activity coefficient, and  $\chi_i$  can be obtained from the iterative formulas:

$$C_{i,eq} = \gamma_i^* \cdot \left( M_i / \sum_{j=1}^m M_j \right)^{n+1} \cdot S_i \quad (5.5)$$

$$E_i = A \cdot k_i \cdot (C_{i,eq} - C_{i,w}) \quad (5.6)$$

$$M_{i,t} = M_{i,t-1} - \frac{\Delta t}{2} \cdot (E_{i,t} + E_{i,t-1}) \quad (5.7)$$

$$C_{w,i,t} = \frac{C_{w,i,t-1} + \frac{\Delta t}{2} \cdot \frac{A \cdot k_i \cdot C_{i,eq}}{V_w} + \frac{\Delta t}{2} \cdot \frac{E_{i,t-1} - Q \cdot C_{i,w,t-1}}{V_w}}{1 + \frac{\Delta t}{2} \cdot \frac{Q + A \cdot k_i}{V_w}} \quad (5.8)$$

where,  $\Delta t$  is the time step,  $m$  the number of compounds,  $M$  the component mass within the organic phase in (mol) and  $E$  the exchange term (first term on the right hand side

of eq 5.1).  $M$  and  $C_w$  are marked by subscripts ( $t$ ) to account for the current time level and ( $t-1$ ) for the previous time level.  $\Delta t$  should be small enough for the simulation, and it was 0.0001 min in this case. The total elapsed time of simulation is the experimental time period as 480 min.

The model is based on eq 5.1 and was programmed in FORTRAN 90. The non-linear system was solved numerically by Gauss-Seidel iterations with centered time-weighting over the set of eq 5.5 –5. 8 until convergence is achieved. The time step was automatically adjusted to split the time until depletion of the currently most soluble component into a sufficient number of steps (=100) until that particular compound is totally depleted.

## 5.4 Results and discussion

### 5.4.1 Simple model NAPL

Simulated results of the single solute NAPL depletion experiment are shown in Figure 5.3. The obtained best fitting  $k$  varied between 3 to 12E-4 cm/s for all of the tests. This range of fitted  $k$  of phenanthrene matched well with the published literature data listed in Appendix Table 2 but falls on the higher end [5, 8, 10, 11, 15, 21]. The reason for the relatively high value of  $k$  may be that the model NAPL is a low viscosity mixture with toluene as solvent and does not include high molecular weight hydrocarbons (i.e., asphaltene and resin) present in real world NAPLs such as coal tar and creosote.

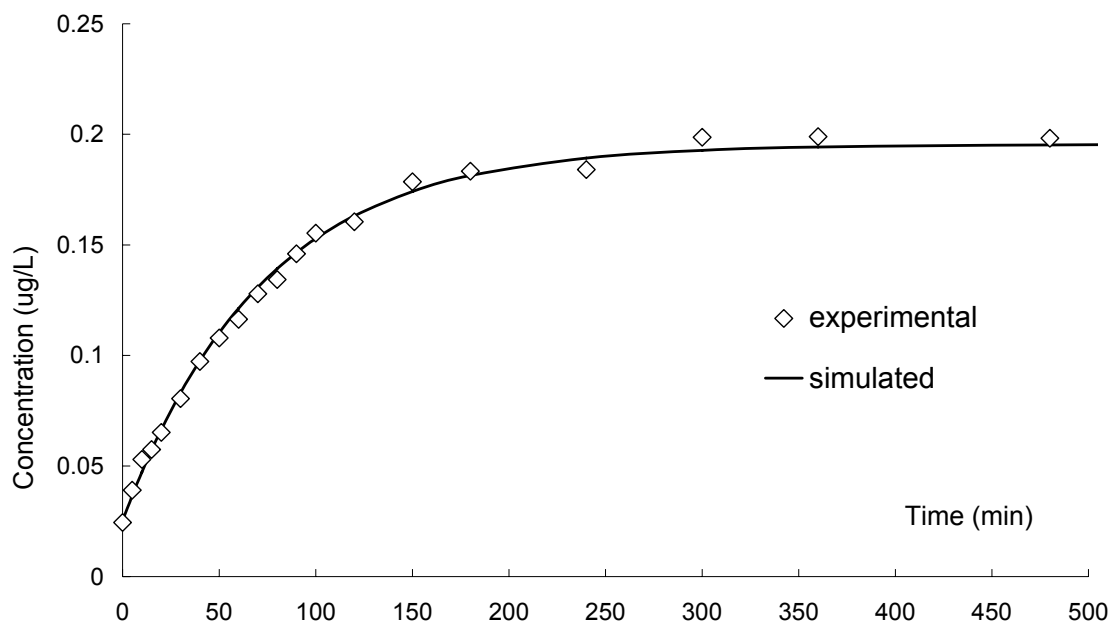


Figure 5.3. Fitting vs. measured concentration of simple model NAPL. RRSS was 0.026.

## 5.4 Results and discussion

### 5.4.1 Simple model NAPL

Simulated results of the single solute NAPL depletion experiment are shown in Figure 5.3. The obtained best fitting  $k$  varied between 3 to 12E-4 cm/s for all of the tests. This range of fitted  $k$  of phenanthrene matched well with the published literature data listed in Appendix Table 2 but falls on the higher end (Alshafie & Ghoshal, 2004; Ghoshal et al., 2004; Ghoshal et al., 1996; Mukherji et al., 1997; Ortiz et al., 1999; Schluep et al., 2001). The reason for the relatively high value of  $k$  may be that the model NAPL is a low viscosity mixture with toluene as solvent and does not include high molecular weight hydrocarbons (i.e., asphaltene and resin) present in real world NAPLs such as coal tar and creosote.

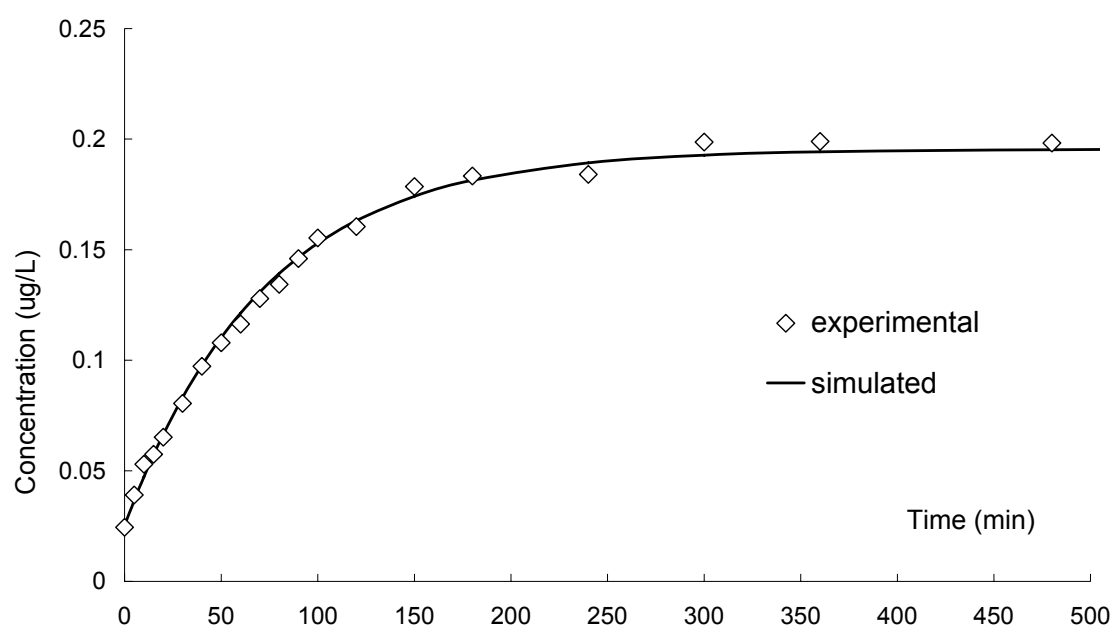


Figure 5.3. Fitting vs. measured concentration of simple model NAPL. RRSS was 0.026.

### 5.4.1 Complex model NAPL

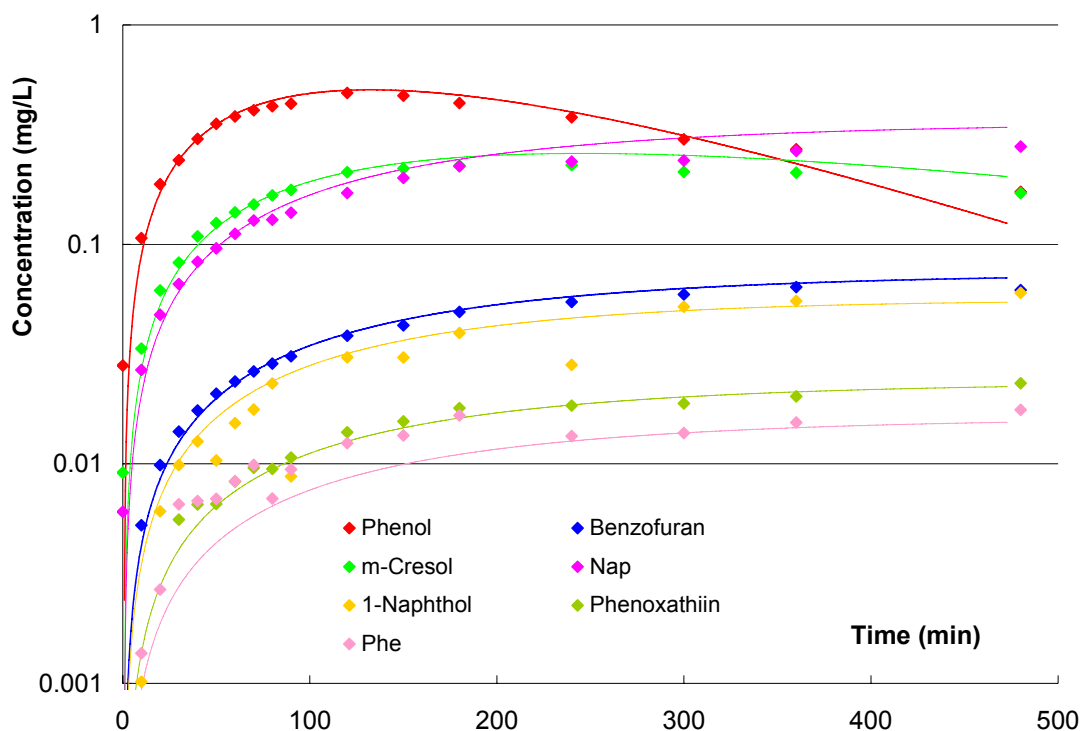
#### Eluents' profiles of the experiment

The eluent profiles of components of the complex model NAPL-water system are shown in Figure 5.4. The aqueous phase concentrations of phenol and m-Cresol increased to the maxima in 100 min and decreased slowly. The concentrations of PAHs and heterocyclic hydrocarbon increased to steady state concentrations at

different time periods and kept relatively constant similar to the elution profiles of phenanthrene in simple model NAPL system.

### Model results

If all of  $\gamma^i$  were assumed to be equal to or very close to 1 the simulated concentrations deviated dramatically from the measured data indicating that a non ideal chemical environment existed in the model NAPL for certain solutes. These findings is contrary earlier studies which applied Raoult's law under ideal conditions (Brown et al., 2005; Cline et al., 1991; Lee et al., 1992; Peters et al., 1997). Consequently, in this system,  $\gamma_i$  should be variable for some compounds during the experiment and was described as a function of the  $\chi_i$ . In this work a simplified power law function  $\gamma_i = \chi_i^n$  as suggested in chapter 2 was used. The exponent,  $n$ , of  $\gamma^i$  should be negative ( $n < 0$ ) for the polar compounds, close to zero for PAHs and 2,3-benzofuran because of their specific ability to be engaged in polar interactions in toluene and aqueous solutions.



**Figure 5.4. Experimental and simulated eluent profiles for the multi component model NAPL. Solid lines show the simulated concentrations, and the diamonds represent the experimental data.**

A numerical solution according to the above equations was utilized to simulate the experimental concentrations. The simulated results are shown in Figure 5.4. The figure shows clearly that all of the simulated profiles match with the experimental

concentrations except for a few points of phenoxathiin and phenanthrene at the beginning of the test. This maybe due to measurement errors associated with their very low aqueous phase concentrations at the beginning of the experiment. With this model, the fitting parameters of the mass transfer coefficient  $k$ , empirical parameter  $n$ , and the function describing the relationship of  $\gamma_i$  and  $\chi_i$  were also obtained and are listed in Table 5.2. The  $k$  of naphthalene and phenanthrene fall within the high end of the published data. As discussed before for the single solute NAPL, the relatively high values may be due to the high viscosity of the toluene based NAPL, which lacks any high molecular weight compounds and solid particles. The resistance to mass transfer was thus expected to be less than in real mixtures as diesel, petrolatum etc. with high molecular weight compounds of asphaltenes and resins. With regard to a PAH, data of  $k$  located in a small range in both model and real NAPLs, and that of 2 and 3 ring PHAs changed only a small amount in same matrix. The reason may be their physicochemical properties (e.g. molecular structure) being similar, and these properties are important to mass transfer under definite condition. In addition, there was no published data for phenol, 2,3-benzofuran, m-cresol and phenoxathiin. However, their  $k$  are higher than others except for phenol. For phenol, its low initial  $C_o$  combined with high water solubility could contribute to the low remained mass in NAPL phase after a short leaching time period. The concentration gradient should be small and diffusive process was therefore very slow.

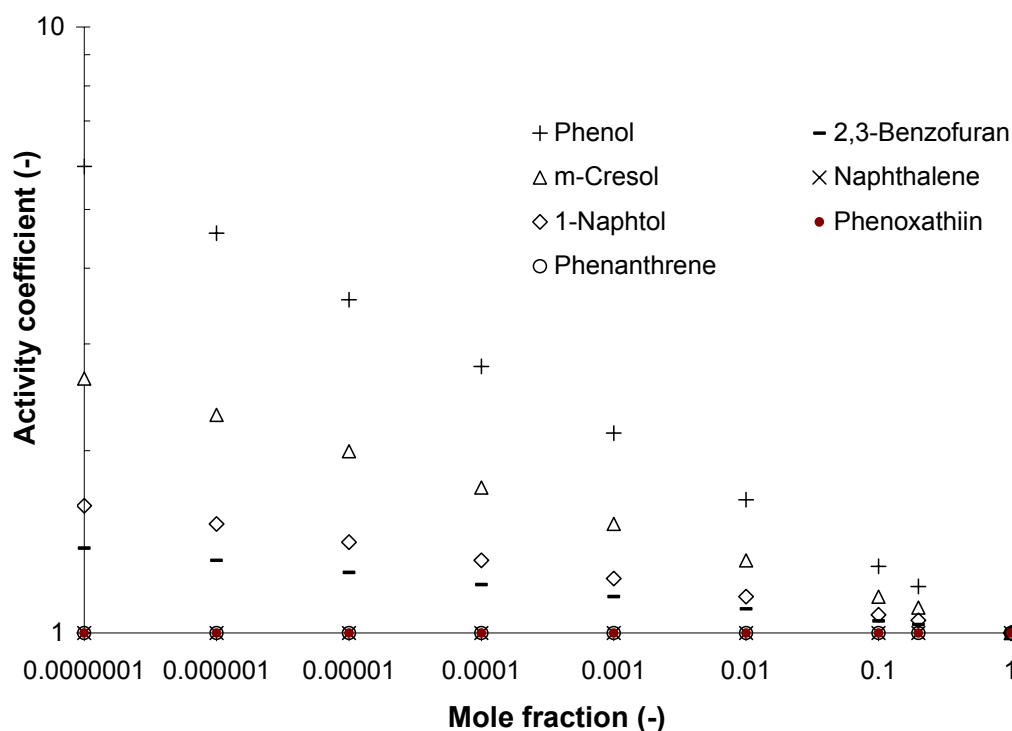
**Table 5.2. Simulated results of the complex model NAPL-water system**

	Phenol	2,3-Benzofuran	m-Cresol	Naphthalene	1-Naphtol	Phenoxathiin	Phenanthrene
$n$	-0.11	-0.02	-0.06	0	-0.03	0	0
$\gamma^i$	$X^{-0.11}$	$X^{-0.02}$	$X^{-0.06}$	1	$X^{-0.03}$	1	1
$k_i$ (cm/s) 10e-4	2.25	7.2	21.7	13.3	15.8	30	10

The  $\chi_i$  of the compounds changed with the depletion of the chemicals, especially for the well soluble compounds, and led to proportional enrichment of rarely soluble compounds. The  $\gamma_i$  of some compounds deviated subsequently away from unity in this dilute organic solution and the mass transfer resistance may also shift to NAPL phase. Regarding to the change of  $\gamma_i$  for some compounds, it could be simulated as a function



of  $\chi_i$  by numerical model according to the experimental concentrations. This numerical model provides a simple method to estimate the  $\gamma_i$  of the compound in the complex and real NAPLs, which is an important and always lacking parameter. Figure 5.5 shows clearly the trends of simulated  $\gamma_i$  of the compounds in the model NAPL-water system while extrapolating the relationship of  $\chi_i$  and  $\gamma_i$  to the boundary condition, which is the pure liquid compound. PAHs and Phenoxathiin behaved ideally in this system. For phenols, the  $\gamma_i$  increase with lower mole fractions in the NAPL consistent with the less polar nature of the solvent. Further, the  $\gamma_i$  values of phenols increase with their polarities in the dilute solutions, as a  $-\text{CH}_2-$  group and aromatic ring will lead to a decrease of polarities. 2,3-Benzofuran behaved similar to PAHs, which prefers to stay in aqueous phase rather than in NAPL phase in the dilution solution.



**Figure 5.5 Simulated activity coefficients vs. mole fractions according to the numerical simulation results. PAHs and phenoxathiin behaved ideally, the  $\gamma_i$  were unities.**

For the possible shift of the mass transfer resistance, it could not be simulated by this model, since  $k$  is an overall parameter describing the whole system and was assumed as an invariable during the simulating process. If another model and real NAPLs were used to conduct the experiment by CSFTRS in next step study, the effect of the diffusion in aqueous, NAPL and interfacial phases maybe understood and simulated

by numerical model. Further study is needed to foster our understanding of mass transfer process.

## 5.5 Conclusions

The self-designed continuously stirring flow through reaction system can be used to perform the mass transfer experiment for different NAPLs under different hydromechanical and physicochemical conditions. *Raoult's law* with an ideal assumption ( $\gamma_i=1$ ) does not hold for all of the determined compounds in a complex model NAPL-water system. For the tested multi components model NAPL, a numerical model was established according to the mass balance equation and a *general form* of Raoult's law, where the activity coefficient varied with system composition and was described as a power function of mole fraction. The simulated concentrations' profiles with this model system matched with the experimental profiles. The mass transfer coefficients for the determined compounds were also obtained and all of the values were admittedly acceptable compared to the data in the published literatures. Furthermore, the numerical model method derived a tool for prediction of the activity coefficients in organic mixtures. The activity coefficients were simulated as a variant for phenol, m-cresol and 2,3-benzofuran, and were unity for naphthalene, phenanthrene and phenoxathiin. The activity coefficients of phenols were positive and decreased with an additional  $-\text{CH}_2-$  group and aromatic ring as expected. The value of PAHs and phenoxathiin being 1 was due to their similar molecular structure to the solvent. Further, the activity coefficients of 2,3-benzofuran were near unity in dilute toluene solution, and no further experimental data was available being a reference. Next step should perform experiments with more solutes and modify further this numerical model with experimental data.

## 5.6 References

1. Powers, S.E., et al., Theoretical study of the significance of nonequilibrium dissolution of nonaqueous phase liquids in subsurface systems. *Water Resources Research*, 1991. 27(4): p. 463-77.
2. Luthy, R.G., et al., Remediating Tar-Contaminated Soils at Manufactured Gas Plant Sites. *Environmental Science & Technology*, 1994. 28: p. 266a-276a.
3. Heyse, E., et al., Nonaqueous phase liquid dissolution and soil organic matter sorption in porous media: review of system similarities. *Critical Reviews in Environmental Science and Technology*, 2002. 32(4): p. 337-397.

4. Ahn, B.S. and W.K. Lee, Simulation and experimental analysis of mass transfer in a liquid-liquid stirred tank extractor. *Industrial & Engineering Chemistry Research*, 1990. 29(9): p. 1927-35.
5. Mukherji, S., C.A. Peters, and W.J. Weber, Jr., Mass Transfer of Polynuclear Aromatic Hydrocarbons from Complex DNAPL Mixtures. *Environmental Science and Technology*, 1997. 31(2): p. 416-423.
6. Ramaswami, A. and R.G. Luthy, Mass Transfer and Bioavailability of PAH Compounds in Coal Tar NAPL-Slurry Systems. 1. Model Development. *Environmental Science and Technology*, 1997. 31(8): p. 2260-2267.
7. Ramaswami, A., S. Ghoshal, and R.G. Luthy, Mass Transfer and Bioavailability of PAH Compounds in Coal Tar NAPL-Slurry Systems. 2. Experimental Evaluations. *Environmental Science and Technology*, 1997. 31(8): p. 2268-2276.
8. Schluep, M., et al., Mechanisms affecting the dissolution of nonaqueous phase liquids into the aqueous phase in slow-stirring batch systems. *Environmental Toxicology and Chemistry*, 2001. 20(3): p. 459-466.
9. Chrysikopoulos, C.V., et al., Mass transfer coefficient and concentration boundary layer thickness for a dissolving NAPL pool in porous media. *Journal of Hazardous Materials*, 2003. 97(1-3): p. 245-255.
10. Alshafie, M. and S. Ghoshal, The role of interfacial films in the mass transfer of naphthalene from creosotes to water. *Journal of Contaminant Hydrology*, 2004. 74(1-4): p. 283-298.
11. Ghoshal, S., C. Pasion, and M. Alshafie, Reduction of benzene and naphthalene mass transfer from crude oils by aging-induced interfacial films. *Environmental Science & Technology*, 2004. 38(7): p. 2102-2110.
12. Cho, J., M.D. Annable, and P.S.C. Rao, Measured Mass Transfer Coefficients in Porous Media Using Specific Interfacial Area. *Environmental Science and Technology*, 2005. 39(20): p. 7883-7888.
13. Benhabib, K., M.-O. Simonnot, and M. Sardin, PAHs and Organic Matter Partitioning and Mass Transfer from Coal Tar Particles to Water. *Environmental Science & Technology*, 2006. 40(19): p. 6038-6043.
14. Powers, S.E., L.M. Abriola, and W.J. Weber, Jr., An experimental investigation of nonaqueous phase liquid dissolution in saturated subsurface systems: steady state mass transfer rates. *Water Resources Research*, 1992. 28(10): p. 2691-705.
15. Ortiz, E., M. Kraatz, and R.G. Luthy, Organic phase resistance to dissolution of polycyclic aromatic hydrocarbon compounds. *Environmental Science & Technology*, 1999. 33(2): p. 235-242.
16. Brusseau, M.L., Q. Hu, and R. Srivastava, Using flow interruption to identify factors causing nonideal contaminant transport. *Journal of Contaminant Hydrology*, 1997. 24(3-4): p. 205-219.
17. Luthy, R.G., et al., Interfacial films in coal tar nonaqueous-phase liquid-water systems. *Environmental Science and Technology*, 1993. 27(13): p. 2914-18.

18. Cline, P.V., J.J. Delfino, and P.S.C. Rao, Partitioning of aromatic constituents into water from gasoline and other complex solvent mixtures. *Environmental Science and Technology*, 1991. 25(5): p. 914-20.
19. Lane, W.F. and R.C. Loehr, Estimating the equilibrium aqueous concentrations of polynuclear aromatic hydrocarbons in complex mixtures. *Environmental Science and Technology*, 1992. 26(5): p. 983-90.
20. Eberhardt, C.G., P., Time scales of organic contaminant dissolution from complex source zones: coal tar pools vs. blobs. *Journal of Contaminant Hydrology*, 2002. 59(1-2): p. 45-66.
21. Ghoshal, S., A. Ramaswami, and R.G. Luthy, Biodegradation of Naphthalene from Coal Tar and Heptamethylnonane in Mixed Batch Systems. *Environmental Science and Technology*, 1996. 30(4): p. 1282-91.
22. Lee, L.S., P.S.C. Rao, and I. Okuda, Equilibrium partitioning of polycyclic aromatic hydrocarbons from coal tar into water. *Environmental Science and Technology*, 1992. 26(11): p. 2110-15.
23. Peters, C.A., et al., Phase Stability of Multicomponent NAPLs Containing PAHs. *Environmental Science and Technology*, 1997. 31(9): p. 2540-2546.
24. Brown, D.G., et al., Raoult's law-based method for determination of coal tar average molecular weight. *Environmental Toxicology and Chemistry*, 2005. 24(8): p. 1886-1892.

## **Chapter 6 Conclusions and Outlook**

### **6.1 Research of aging phenomena**

All of the NAPLs (five kinds of coal tars and six kinds of crude oils) tested in this study showed visible aging phenomena. Different NAPLs experienced different aging processes under the same environmental conditions. Depletion of well water soluble compounds is important to the aging of crude oil, and evaporation/volatilisation contribute more to the aging of coal tar. The compositional and environmental

conditions decide the aging process and affect the properties of NAPLs. The existence of oxidant, which was hydrogen peroxide in continuously flow through experiment accelerated the aging process, and pH of the solution contacting with NAPLs is decisive to the leaching properties of the compounds from NAPLs phase. The compositions of the aged coal tars changed dramatically comparing to the fresh coal tar, especially for BTEX, phenols, 2,3-benzofuran and light molecular weight PAHs. However, there is little compositional information about the heterocycles compounds (except for 2,3-benzofuran) and organic acid of NAPLs. Therefore, next step should further estimate the composition of fresh and aged NAPLs, especially for the heterocyclic hydrocarbons (e.g., pyrroles, pyridines, imidazols pyrimidins and furans), quinoline, organic acids, organometallic compounds, metal and metal oxide. Then the study can focus on the investigation of the oxides of phenol, styrene and olefin, which include dihydroxylated rings such as ortho- and para- hydroquinone, benzaldehyde and styrene oxide, because this study have checked only the possible effect of oxidation with the present of oxygen and hydrogen peroxide solution. Styrene and phenol present commonly in various fresh NAPLs and can be oxidized in the presence of oxygen, fenton reagent and/or tiny amount of metal or metal oxide (Mn, Co, Ti, Fe, V and TiO<sub>2</sub>) being catalyst. Later, the research can address to the possible peroxidative product of alkenes, the mesophases and polymers of phenol and styrene and the surface active high molecular weigh compounds such as asphaltene and resin, if analytical instruments (e.g., state of the art liquid and solid phase NMR, high field FT ion cyclotron resonance MS etc.) are available. This work would lead possibly to the confirmation of the compounds contributing to the formation of aged interfacial films and could, also gain insight into the underlying reactions.

In addition to the knowledge gap of the composition of NAPLs, there is little information referring to the structure of the NAPLs interfacial phase. An improved understanding of the structure of this phase may reach only with the combined information from the various techniques such as rheological, novel spectroscopic and electrochemical manipulation and measurement, which depends highly on the level of apparatus and needs to cooperating closely in interdisciplinary fields.

## 6.2 Study of mass transfer process

The mass transfer process was investigated by the batch experiments for the simple model NAPLs and aged coal tar, and by CSFTRS for simple and complex model NAPLs. The mass transfer coefficients ( $k$ ) were obtained as best fitting parameters for the analyzed compounds. The estimated  $k$  were about two orders of magnitude lower in aged coal tars than those in model and fresh NAPLs, which indicates that the mass transfer resistance increased with the aging process of NAPLs. However, there are limited data for the dynamic mass transfer process of real NAPLs system. Therefore, column, tank experiments and CSFTRS could be performed with real NAPLs-water system during the next step work.

The experiment could be performed under different hydrological conditions, e.g., flow rate, volume ratio, with variable NAPLs saturated porous medium. The results of these experiments could possibly answer the question that which processes/phases/conditions is/are the rate limit for the mass transfer process. The physicochemical parameters related to mass transfer process (mass transfer coefficients, partitioning coefficients etc.) could also be obtained, which combining with NAPLs and aqueous phase concentrations will be useful to the modification and validation of the mass transfer model.

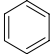
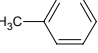
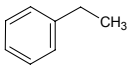

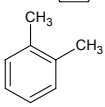
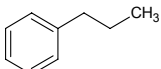
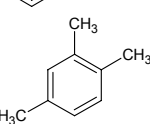
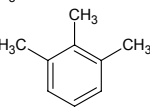
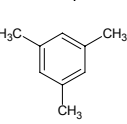
## 6.3 Model research

The batch model was used to simulate the simple model NAPL and aged coal tar-water systems, and mass transfer coefficients were obtained as the best fitting parameters for the detected compounds. The continuous flow model coupling mass transfer through the interface and advective flow, which exists commonly in the real subsurface was used to describe simple and complex model NAPLs-water systems. The analytical solution for this model only exists and can only simulate the mass transfer process for simple model NAPLs-water system. A numerical model considering activity coefficients and Raoult's law can simulate the eluent profiles of complex NAPLs-water system. The mass transfer coefficients and functions of activity coefficient to mole fraction were also simulated from this numerical model. However, the experimental data of real NAPLs-water system is limited and some experiments are scheduled to perform in next step work (see above section). Therefore, the numerical model could be further validated with the data obtained from real

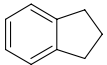
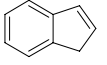
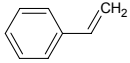
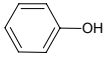
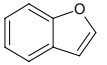
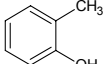
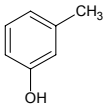
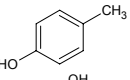
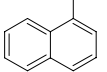
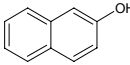
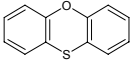
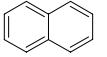
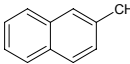
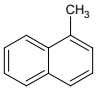
NAPL-water system. The numerical model may finally describe the dynamic mass transfer process while the NAPLs undergo aging process. The simulated parameters such as mass transfer resistances and the activity coefficients for fresh and aged NAPLs are the important input data to the risk assessment and remediation effectiveness to the contaminated sites with NAPLs.

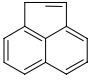
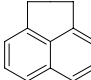
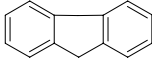
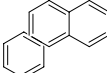
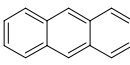
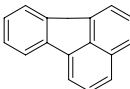
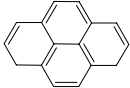
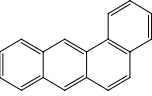
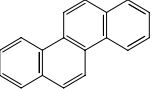
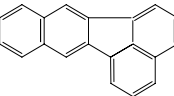
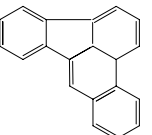
## Appendixes

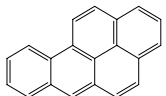
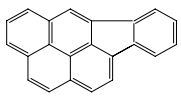
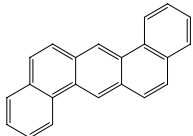
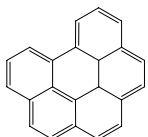
Table 1 Physical chemical properties of the major compounds tested in this study

	Abbreviation	Structure	Mol. Wt g/mol	Aqueous Solubility at 25°C Si [mg/l]	Melting Point (°C)	Boiling Point (°C)	Fugacity Ratio at 25°C ( $f^s/f^l$ )	Vapor pressure at 25°C (mmHg)
Benzene			78.1	1790	5.5	80.1	1	94.8
Toluene			92.1	526	-93	110.6	1	28.4
Ethylbenzene			106.2	161.2	-94.9	136.1	1	9.6
p-Xylene			106.2	198	13.3	138.3	1	8.84
o-Xylene			106.2	175	-25.2	144	1	6.61
Propylbenzene			120.2	55	-101.6	159		3.42
1,2,4-Trimethylbenzene	1,2,4-TMB		120.2	59	-43.8	169		2.1
1,2,3-Trimethylbenzene	1,2,3-TMB		120.2	75.2	-25	175		1.69
1,3,5-Trimethylbenzene	1,3,5-TMB		120.2	48.2	-44.7	165		2.48



Indane			118.2	109.1	-51	176.5	1	1.47
Indene			116.16	332.4	-1.8	181.6		1.1
Styrene			104.1	310	-30.6	145.2		6.4
Phenol			94.1	82800	40.5	181.7		0.35
Benzofuran	BF		118.1	678	< -18	173		0.44
o-Cresol			108.1	25900	30.9	191		0.11
m-Cresol			108.1	22700	11.5	202.2		0.17
p-Cresol			108.1	21500	35.5	201.6		0.299
1-Naphthol			144.2	866	95	288		2.74e-4
2-Naphthol			144.2	755	123	285		3.2e-4
Phenoxathiin			200.3	0.449	59-60	311		1.44e-4
Naphthalene	Nap		128	31.7*	80.6	218	0.3	0.085
2-Methylnaphthalene	2-MNap		142	25.4*	34.58	241	0.86	0.055
1-Methylnaphthalene	1-MNap		142	28	-22	240-243	1	0.067

Acenaphthylene	Any		152	9.804*	93.5-94.5	265	0.22	0.00668
Acenaphthene	Ace		154.2	3.93*	95	279	0.2	0.00215
Fluorene	Fln		166	1.98*	116	295	0.16	0.0006
Phenanthrene	Phe		178	1.18*	99.5	340	0.28	1.12e-4
Anthracene	Ant		178	0.05	217.5	340	0.01	6.53e-6
Fluoranthene	Fth		202	0.26	110.8	375	0.21	9.22e-6
Pyrene	Py		202	0.13	156	404	0.11	4.5e-6
Benz(a)anthracene	BaA		228	0.014*	159.8	437.6	0.04	5.49e-9
Chrysene	Chr		228	0.002	255.8	448	0.0097	6.23e-9
Benzo(b)fluoranthene	BbF		252	0.00323*	167	357	0.039	5e-7
Benzo(k)fluoranthene	BkF		252	0.00055*	215.7	480	0.013	9.65e-10

Benzo(a)pyrene	BaP		252	0.0038*	176.5	495	0.03	5.49e-9
Indeno(1,2,3-cd)pyrene	Indeno		276	0.062	162.5	536	0.0451	1.25e-10
Dibenzo(a,h)anthracene	DahA		278	0.0005	266	524	0.004	9.55e-10
Benzo(g,h,i)perylene	BghiP		276	0.00026	278.3	500	0.003	1e-10

**Table 2. Published data for mass transfer coefficients (10E-4 cm/s)**

NAPL	Authors	Phe	Nap	Py	Benzene	m/p-Xylene
Diesel	Schluep 2001	3.2	3.4		3.9	3.2
Creosote	Alshafie 2004		4			
Crude oil	Ghoshal 2004		7		6-11	
Gasoline	Ghoshal 2004		11.7		6.7	
Coal tar	Ghoshal 1996		2.44-3.05			
Coal tar	Benhabib 2006	0.4-1.3*				
Model NAPL	Mukherji 1997		8.5-14.2			
Petrolatum	Ortiz 1999	7	6	9		

\* for all PAHs

**Table 3 Composition of fresh coal tar ( $\mu\text{g/g}$ )**

	<b>Abbreviation</b>	<b>This work <math>\pm</math>SD</b>	<b>C. E (2002)<sup>a</sup></b>
Benzene		1338 $\pm$ 99	950
Toluene		1230 $\pm$ 38	1074
Ethylbenzene		7.9 <sup>b</sup>	44
p-Xylene		595.8 $\pm$ 9.2	692.2
o-Xylene		191.3 $\pm$ .8	251
Pyopylbenzene		<40	6
1,2,4-Trimethylbenzene	1,2,4-TMB	175.1 $\pm$ 7.2	235
1,2,3-Trimethylbenzene	1,2,3-TMB	37.7 $\pm$ 7.0	61
1,3,5-Trimethylbenzene	1,3,5-TMB	98.2 $\pm$ 11	125
Indane		50.1 $\pm$ 3.9	90
Indene		9104 $\pm$ 115	10648
Styrene		1013 $\pm$ 10	
Phenol		131.4 $\pm$ 7.7	
Benzofuran	BF	1094 $\pm$ 14	913
o-Cresol		22.8 $\pm$ 1.1	
m+p-Cresol		73.8 $\pm$ 4.3	
Naphthalene	Nap	149885 $\pm$ 1263	140900
2-Methylnaphthalene	2-MNAP	16869 $\pm$ 423	16100
1-Methylnaphthalene	1-MNAP	7162 $\pm$ 240	6900
Acenaphthylene	Any	19453 $\pm$ 558	19900
Acenaphthene	Ace	3117 $\pm$ 116	3100
1-Naphthol		69.1 $\pm$ 4.2	
2-Naphthol		66.5 $\pm$ 4.1	
Fluorine	Fln	14091 $\pm$ 160	16900
Phenanthrene	Phe	40325 $\pm$ 1100	55100
Anthracene	Ant	8504 $\pm$ 224	13500
Fluoranthene	Fth	27011 $\pm$ 1623	29500
Pyrene	Py	18223 $\pm$ 1161	21300
Benz(a)anthracene	BaA	7112 $\pm$ 449	10800
Chrysene	Chr	3739 $\pm$ 327	7600
Benzo(b)fluoranthene	BbF	12700 $\pm$ 1013	11700
Benzo(k)fluoranthene	BkF		
Benzo(a)pyrene	BaP	6461 $\pm$ 704	7400
Indeno(1,2,3-cd)pyrene	Indeno	1500 $\pm$ 264	4000
Dibenzo(a,h)anthracene	DahA	182.3 $\pm$ 28	700
Benzo(g,h,i)perylene	BghiP	899.7 $\pm$ 115	2700
$\Sigma$ identified compounds %		33.1	38.32
Cyclohexane soluble, not identified %		14.8	22.58
Cyclohexane insoluble %		52.1	39.1

**a. from (Eberhardt, 2002) b. only one sample can be detected for this compound**

**Table 4 Composition of coal tars aged at different environmental conditions ( $\mu\text{g/g}$ )**

	<b>16 months aged in water BE</b>	<b>16 months aged in open air BE</b>	<b>16 months CFTE 2% H<sub>2</sub>O<sub>2</sub></b>	<b>16 months CFTE millipore water</b>	<b>16 months CFTE degassed millipore water</b>	<b>SC 7 day in air</b>	<b>SC 7 day in N<sub>2</sub></b>	<b>SC 2 day in air</b>	<b>SC 2 day in N<sub>2</sub></b>
Styrene	74.84±2.4	10.7±0.19	30.41±0.80	23.30±0.19	22.46±0.16	9.21±0.24	8.05±0.14	7.56±0.20	8.90±0.32
Phenol	31.53±0.53	24.9±0.52	0.14±0.01	0.11±0.00048	0.11±0.0027	0.53±0.0053	0.68±0.018	1.75±0.058	1.31±0.17
BF	54.52±4.3	0.43±0.035	12.1±0.22	9.48±0.33	10.66±0.36	0.36±0.054	0.22±0.017	0.31±0.073	0.25±0.036
o-Cresol	11.82±0.14	6.74±0.15	0.03±0.0033	0.02±0.0012	0.01±0.0036	0.19±0.012	0.14±0.0036	0.68±0.0050	0.39±0.011
m+p-Cresol	34.99±0.50	25.2±0.50	0.08±0.0079	0.06±0.00033	0.06±0.0072	0.75±0.046	0.62±0.02	2.83±0.10	2.00±0.050
Nap	110061±3723	21564±434	42975±1057	37997±264	39854±305	77.9±0.77	71.6±1.76	256±3.8	87.4±1.1
2-Mnap	15852±571	8493±139	10381±249	10233±22.1	10659±104	65.9±1.25	46.8±1.15	279±4.6	109.89±1.9
1-Mnap	6825±258	3891±68.9	4391±108	4294±13.5	4415±40.8	78.1±7.51	32.6±2.39	276±4.7	97.2±0.72
Any	15506±502	12595±283	9768±249	9598±33.9	9781±102	1718±49.6	897±22.0	3799±41.3	3019±41.1
Ace	3001±99.3	2448±38.3	2097±49.4	2117±7.31	2134±18.6	344±6.34	153±3.65	790±9.1	646±6.9
1-Naphthol	41.17±1.6	3.35±41.2	1.81±0.027	1.88±0.16	1.80±0.094	1.69±0.40	2.16±0.30	18.5±1.9	29.9±1.9
2-Naphthol	72.34±0.82	27.5±72.3	3.83±0.35	3.06±0.16	3.15±0.088	26.0±2.48	32.5±1.2	36.5±1.2	51.7±1.9
Fln	12727±399	13489±282	11130±263	11354±60.1	11673±51.5	4282±20.7	4049±84.7	6523±99.6	8494±130

Phe	33680±1098	34439±566	29292±646	30260±123	30678±151	26840±237	28985±748	28367±440	35555±583
Ant	7474±233	7512±155	6454±155	6767±51.9	6819±53.0	6031±56.6	6534±169	6348±104	7829±113
Fth	29596±927	27379±512	24096±496	24954±194	24468±72.4	26716±323	26481±662	25934±555	31272±514
Py	41487±426	41342±1227	16269±365	16918±151	24263±1347	17319±259	17145±410	16867±287	20622±357
BaA	8694±121	10009±170	8306±322	9353±502	9031±137	9719±128	9791±267	9733±167	11812±209
Chr	3976±129	4154±90.2	3628±94.2	3794±26.1	3652±23.1	4305±27.0	4167±114	4168±69.9	5080±88.4
BbF+ BkF	14044±336	15445±214	13825±409	14379±160	13480±92.5	15302±101	14977±438	15505±263	19616±388
BaP	7304±168	7775±239	6712±184	6989±101	6590±128	7973±128	7747±226	7872±45.1	9951±174
Indeno	2940±36.3	3886±63.7	3331±122	3559±37.0	3300±16.5	4032±54.0	3930±104	4156±73.1	5365±184
DahA	328.6±9.6	556.0±8.9	438.1±24.2	494.0±9.8	458.4±2.05	462.7±32.6	502.4±13.9	524.5±10.6	711.1±33.0
BghiP	1515±31.1	1904±35.2	1703±49.2	1787±10.7	1608±11.2	2183±17.7	2043±52.9	2233±37.7	2825±85.5
Σidentified compounds %	31.5	21.7	18.7	20.3	20.3	12.7	12.8	13.4	16.3
Cyclohexane insoluble %	45.9	78.0	77.5	77.7	88.8	81.9	84.7	82.1	77.0

Data are mean value ± S.D

**Table 5 Equilibrium and steady state aqueous phase concentrations of analyzed compounds in fresh and aged coal tar-water systems (µg/L)**

	Equilibrium concentrations								Steady state concentrations			
	Fresh coal tar		Aged coal tar						16 months CFTE 2% H <sub>2</sub> O <sub>2</sub>	16 months CFTE millipore water	16 months CFTE degassed millipore water	
	16 months aged in water batch	C. E (2002) dialysis membrane	2 year Batch acid (pH=5)	2 year Batch neutral (pH=5.5)	2 year Batch basic (pH=8)	7 day Aged in Air	7 day Aged in N <sub>2</sub>	2 day Aged in Air				2 day Aged in N <sub>2</sub>
Styrene	635±8.4		209±8.8	358±35	413±28	3.37	3.35	4.78	5.71	0.65±0.42	0.57±0.38	0.54±0.37
Phenol	278±7.2		589±17	593±31	624±12	0.085	0.090	0.25	0.19	0.0001±0.000007	0.0001±0.000005	0.00011±0.000004
BF	1558±23	1132	838±19	1146±56	1325±67					0.12±0.042	0.21±0.18	0.19±0.14
o-Cresol	150±3.8		190±3.7	190±8.4	194±4.2	0.13	0.080	0.42	0.29	0.0004±0.00007	0.00001±0.0000007	0.00002±0.000001
m+p-Cresol	356±8.2		478±12	476±23	496±10	0.34	0.22	1.11	1.11	0.00018±0.00003	0.00004±0.000002	0.00005±0.000003
Nap	29102±559	26520	22163±927	23599±1142	35124±4014	84.89	25.22	187.70	29.93	348±190	403±228	400±217
2-Mnap	946±19	842	762±43	787±53	2111±522	13.22	4.20	42.17	14.91	37.5±21	50.1±30	53.7±34
1-Mnap	395±23	393	316±12	328±21	955±248	23.89	8.80	68.80	42.29	14.9±9.3	20.8±13	21.7±15
Any	898±17	1048	809±40	804±40	2082±476	182.46	60.54	378.86	426.99	34.0±23.8	44.3±28	43.1±32
Ace	106±5.6	96	80.0±4.6	78.7±5.2	319±94	24.35	9.60	48.06	55.94	4.27±3.1	5.46±3.4	5.56±3.8
1-Naphthol	45.0±9.5		4.32±0.25	3.08±0.31	4.46±0.46	3.58	4.21	0.26	0.28	0.025±0.001	0.0036±0.0009	0.0030±0.002
2-Naphthol	240±4.1		138±2.6	151±7.9	68.8±3.7	29.06	36.11	46.49	58.43	0.011±0.0032	0.0090±0.0038	0.0100±0.0065



Flu	264±5.3	263	245±15	240±14	1456±494	169.33	174.46	190.59	327.71	15.0±8.3	19.5±11	20.37±13
Phe	278±3.7	253	239±15	224±13	3602±1330	389.83	458.70	324.58	477.44	16.0±8.0	20.2±11	21.46±12
Ant	64.8±1.4	49	57.5±2.6	53.4±2.9	765±290	95.60	98.74	72.40	148.05	2.8±1.4	3.5±2.0	3.78±2.2
Fth	71.1±4.2	35	48.1±4.0	39.7±3.1	3064±1202	107.73	132.77	90.28	123.11	3.0±1.5	3.7±2.0	3.99±2.3
Py	47.0±2.9	24	31.2±2.4	25.2±2.0	2113±808	75.68	88.68	58.34	82.20	1.9±1.0	2.4±1.3	2.52±1.4
BaA	13.6±1.4	2.1	3.20±0.66	2.09±0.22	1078±487	23.42	23.10	11.53	30.38	0.23±0.14	0.20±0.11	0.20±0.13
Chr	7.03±0.89	1.6	2.14±0.52	1.40±0.13	530±232	21.59	15.38	7.11	28.43	0.07±0.036	0.08±0.044	0.09±0.051
BbF+ BkF	13.2±1.9	1.3	2.49±1.4	0.82±0.08	2083±954	19.17	26.36	8.93	20.60	0.04±0.017	0.05±0.012	0.04±0.012
BaP	4.3±0.47	0.69	0.78±0.39	0.25±0.08	1016±417	7.98	11.17	4.03	7.66	0.01293±0.006	0.01218±0.004	0.01048±0.004
Indeno	1.8±0.51	0.19	0.31±0.3		605±294	2.00	3.12	0.74	1.07	0.00186±0.001	0.00099±0.0003	0.00073±0.0002
DahA	0.31±0.065	0.036			63.4±28	0.29	0.47	0.13	0.19	0.00040±0.0005	0.00015±0.00003	
BghiP	1.51±0.29	0.15	0.36±0.14		376±185	1.21	1.93	1.31	1.55	0.00135±0.001	0.00097±0.0003	0.00074±0.0004

The data are mean value ± S.D. for most of the samples, except for the 2 and 7 day aged samples.

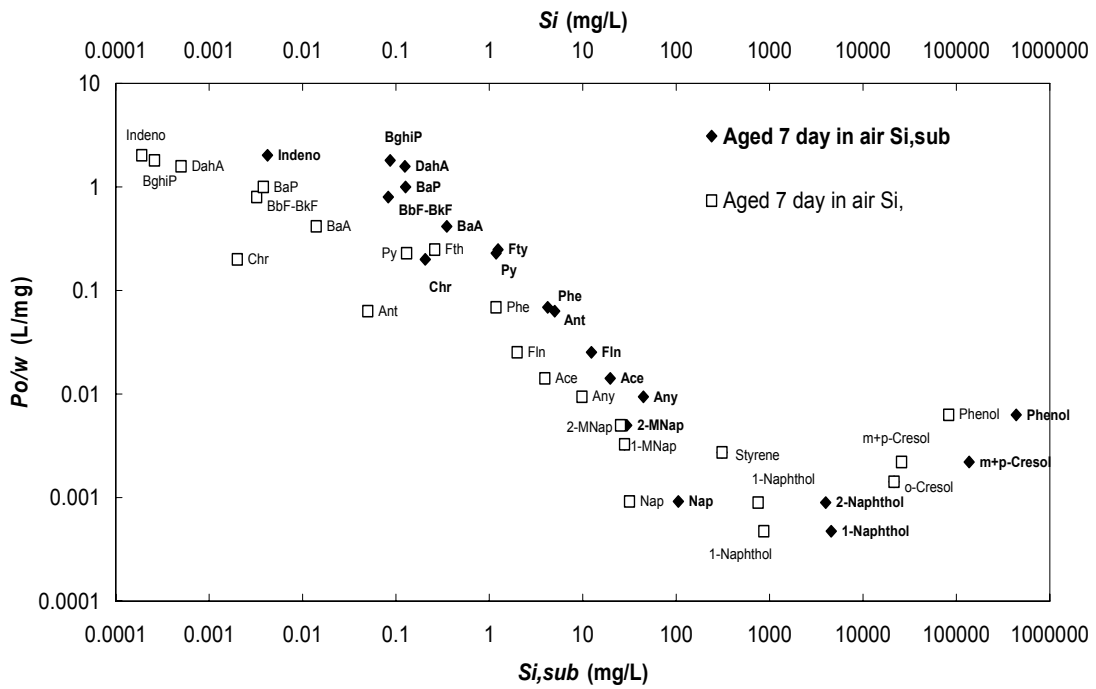
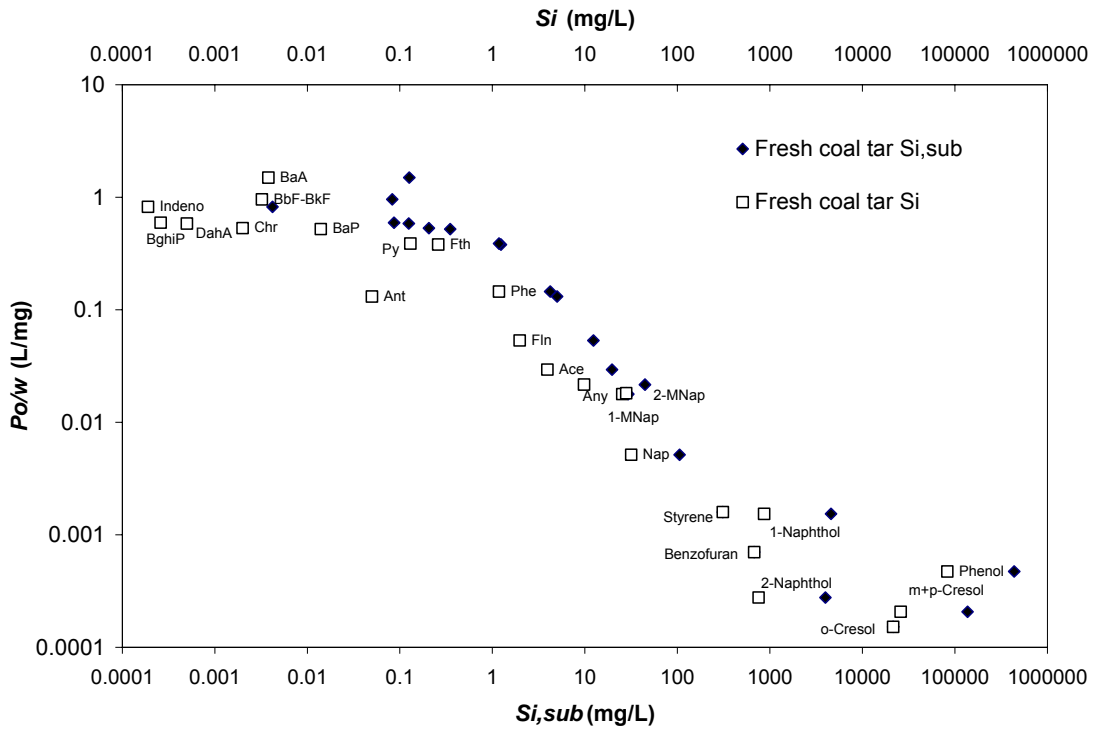
**Table 6 Aqueous phase concentrations of analyzed compounds at different time period in coal tar (aged 7 day, 2 day in air and nitrogen atmosphere)-water system (µg/L)**

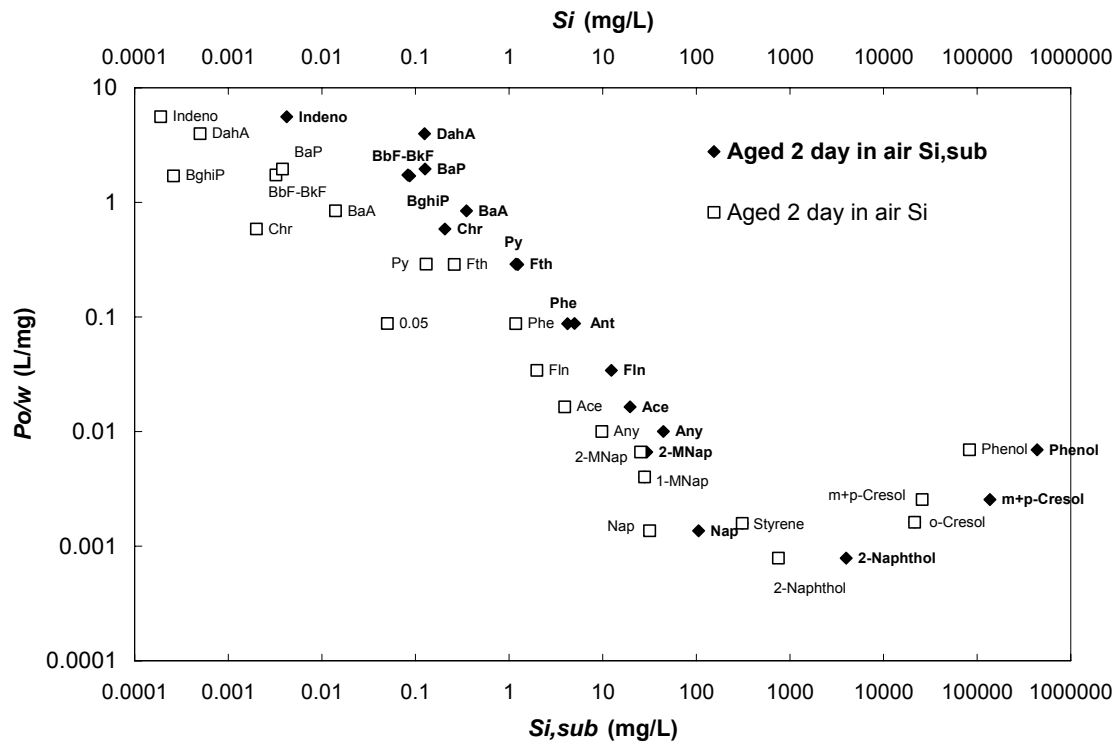
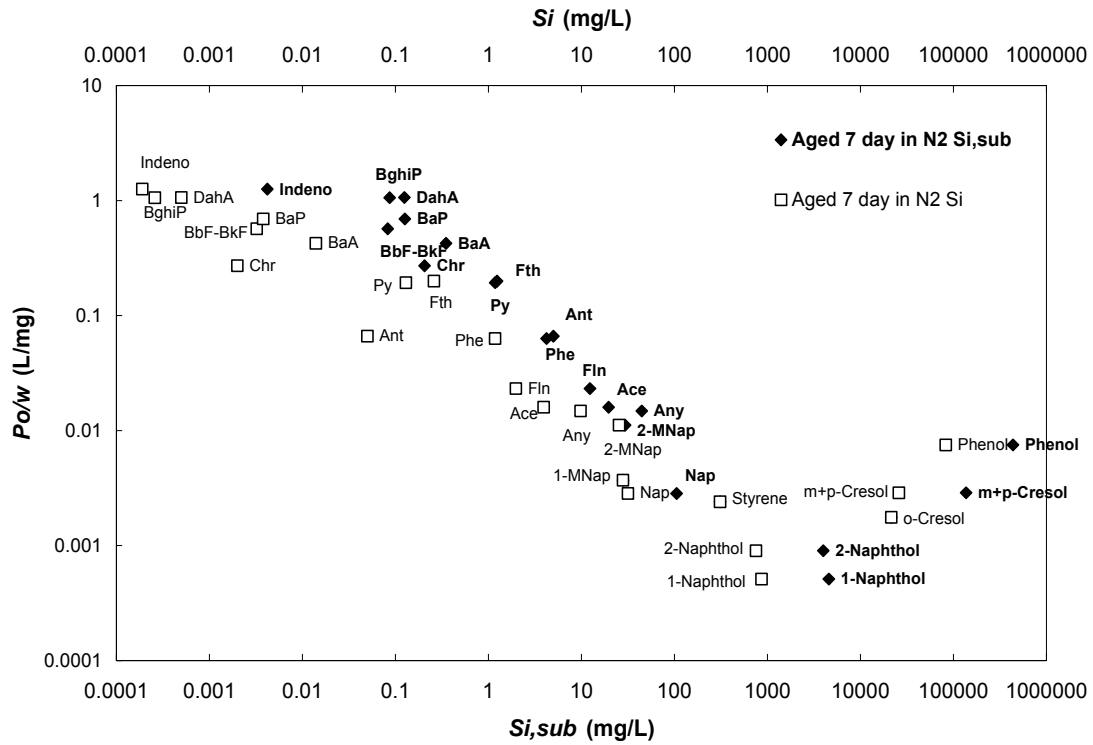
Day	7 day Aged in Air								7 day Aged in N2							
	1	2	5	9	13	17	30	45	1	2	5	9	13	17	30	45
Styrene	0.89	1.24	1.83	2.58	3.02	3.37	5.38	5.62	0.93	1.14	2.01	2.72	2.99	3.35	5.06	6.27
Phenol	0.03	0.03	0.04	0.08	0.08	0.08	0.09	0.11	0.029	0.038	0.048	0.088	0.076	0.090	0.090	0.12
Benzofuran								0.094								0.20
o-Cresol	0.05	0.06	0.07	0.12	0.13	0.13	0.13	0.14	0.029	0.037	0.043	0.074	0.074	0.080	0.077	0.10
m+p-Cresol	0.11	0.13	0.18	0.31	0.32	0.34	0.35	0.41	0.072	0.092	0.11	0.20	0.20	0.22	0.23	0.29
Naphthalene	73.8	74.5	83.1	83.8	84.7	84.9	81.5	70.3	24.1	23.5	24.9	24.8	23.9	25.2	24.4	25.3
2-Methylnaphthalene	10.1	10.3	12.4	13.1	13.1	13.2	13.2	11.4	3.64	3.62	3.98	4.11	4.07	4.20	4.22	4.35
1-Methylnaphthalene	15.3	17.9	20.0	22.3	23.6	23.9	20.4	20.4	7.63	7.55	6.34	10.40	8.80	11.37	6.00	7.21
Acenaphthylene	138	141	170	177	180	182	178	166	45.1	45.1	54.5	56.3	56.0	60.5	62.4	67.1
Acenaphthene	18.6	18.7	22.5	23.8	24.0	24.3	25.1	22.7	7.35	7.40	8.74	9.08	8.89	9.60	9.71	9.98
1-Naphthol	0.09	0.30	3.58	2.06	0.28	0.09	0.19	0.00	0.12	0.58	4.21	6.78	0.65	0.11	0.28	
2-Naphthol	10.4	14.5	21.4	32.5	32.1	29.1	31.6	30.1	15.1	21.3	27.8	42.8	37.2	36.1	45.3	37.9
Fluorine	136	139	163	166	165	169	141	130	147	143	167	169	164	174	142	149
Phenanthrene	307	308	357	373	372	390	369	339	364	347	405	429	417	459	404	436
Anthracene	72.6	76.1	97.0	106	102	95.6	79.5	75.9	85.1	82.5	99.0	110	99.0	98.7	81.1	78.7
Fluoranthene	62.5	70.0	90.4	93.1	99.6	108	160	148	70.3	67.2	91.9	106	113	133	147	179
Pyrene	39.2	44.5	57.7	58.0	64.2	75.7	147	97.4	46.5	43.5	42.9	87.0	77.1	88.7	98.9	123

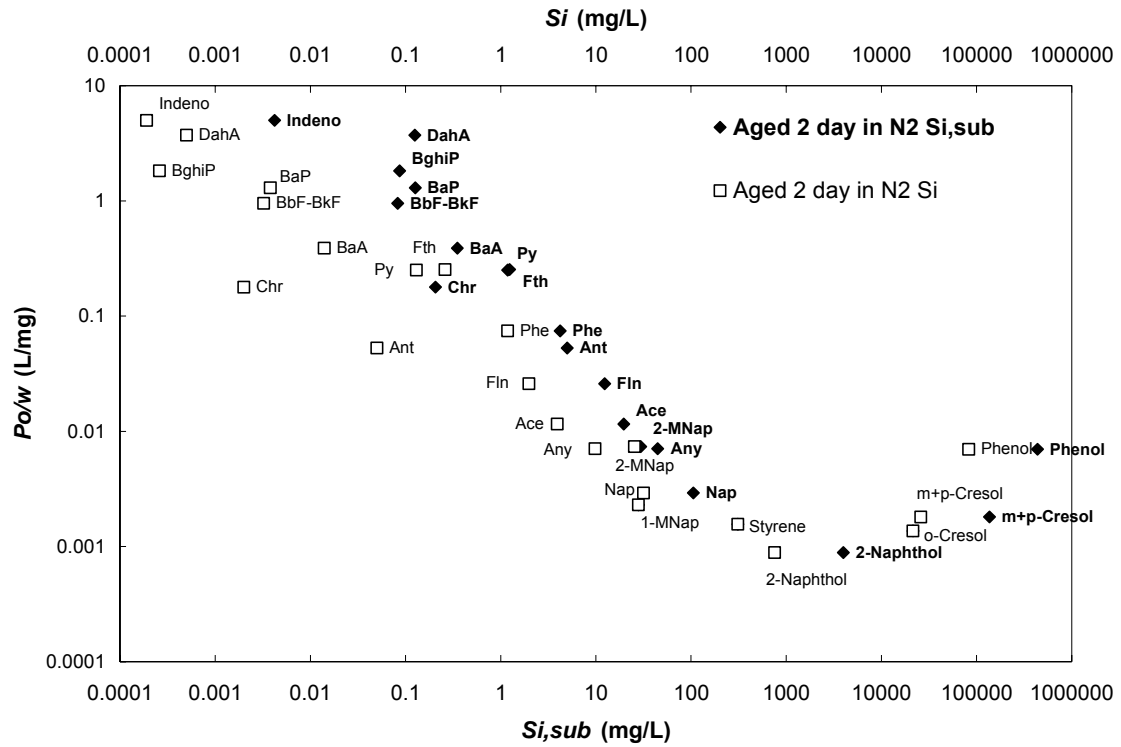


1-Naphthol	0.16	0.19	0.22	0.20	0.21	0.28	<i>0.26</i>	0.00	0.00	0.20	0.17	0.23	0.24	0.20	<i>0.18</i>		
2-Naphthol	31.2	34.9	37.9	35.6	37.0	48.9	<i>46.5</i>	38.9	35.8	49.8	52.3	73.0	47.6	55.0	<i>58.4</i>	45.3	45.7
Fluorine	203	199	216	197	207	215	<i>191</i>	217	216	284	290	313	216	306	<i>328</i>	315	305
Phenanthrene	329	321	350	319	342	361	<i>325</i>	387	396	370	382	428	310	430	<i>477</i>	507	453
Anthracene	76.7	76.3	88.0	77.0	80.8	115	<i>72.4</i>	75.1	78.0	85.3	106	194	135	152	<i>148</i>	137	117
Fluoranthene	68.4	66.2	78.9	65.3	83.1	90.1	<i>90.3</i>	127.9	138.1	70.0	72.0	87.3	70.7	104	<i>123</i>	191	123
Pyrene	42.9	60.3	75.6	40.8	52.2	73.0	<i>58.3</i>	84.4	90.2	44.4	45.8	53.3	44.3	76.2	<i>82.2</i>	121.3	76.3
Benz(a)anthracene	6.56	6.48	10.6	6.72	9.12	14.2	<i>11.5</i>	14.9	17.4	6.09	9.72	14.01	15.99	19.76	<i>30.38</i>	46.19	32.10
Chrysene	4.02	4.00	6.61	4.15	5.63	13.1	<i>7.11</i>	7.88	9.20	3.75	5.95	15.13	19.43	20.89	<i>28.43</i>	36.74	32.65
Benzo(b)fluoranthene	2.11	2.42	3.40	1.05	5.21	7.99	<i>8.93</i>	17.3	15.06	2.14	2.81	5.62	9.61	17.29	<i>20.60</i>	43.78	15.71
Benzo(a)pyrene	0.54	0.66	0.95	0.69	2.08	3.19	<i>4.03</i>	6.79	5.73	0.60	0.82	2.07	3.56	6.64	<i>7.66</i>	15.73	5.36
Indeno(1,2,3-cd)pyrene	0.11	0.14	0.16	0.11	0.36	0.52	<i>0.74</i>	1.42	0.47	0.082	0.11	0.21	0.44	1.14	<i>1.07</i>	2.92	0.56
Dibenzo(a,h)anthracence	0.027	0.027	0.028	0.016	0.075	0.064	<i>0.13</i>	0.18	0.06	0.014	0.017	0.046	0.11	0.12	<i>0.19</i>	0.41	0.10
Benzo(g,h,i)perylene	0.48	0.58	0.44	0.21	0.81	1.15	<i>1.31</i>	3.07	0.94	0.21	0.33	0.49	1.12	1.75	<i>1.55</i>	7.14	1.31

**Italic marked the data of equilibrium aqueous phase concentrations.**







**Appendix Figure Partitioning coefficient ( $P_{o/w}$ ) vs.  $S_i$  and  $S_{i,sub}$  for compounds in fresh and treated coal tars**

Styrene, 2,3-Benzofuran, o-Cresol and 1-MNap are liquid in the ambient temperature, therefore, the diamond and square points were overlapped.

**In der Reihe C Hydro-, Ingenieur- und Umweltgeologie  
der Tübinger Geowissenschaftlichen Arbeiten (TGA) sind bisher erschienen:**

- Nr. 1: Grathwohl, Peter (1989): Verteilung unpolarer organischer Verbindungen in der wasserun-gesättigten Bodenzone am Beispiel der leichtflüchtigen aliphatischen Chlorkohlenwasser-stoffe. 102 S.
- Nr. 2: Eisele, Gerhard (1989): Labor- und Felduntersuchungen zur Ausbreitung und Verteilung leichtflüchtiger chlorierter Kohlenwasserstoffe (LCKW) im Übergangsbereich wasserunge-sättigte/wassergesättigte Zone. 84 S.
- Nr. 3: Ehmann, Michael (1989): Auswirkungen atmogener Stoffeinträge auf Boden- und Grund-wässer sowie Stoffbilanzierungen in drei bewaldeten Einzugsgebieten im Oberen Buntsand-stein (Nordschwarzwald). 134 S.
- Nr. 4: Irouschek, Thomas (1990): Hydrogeologie und Stoffumsatz im Buntsandstein des Nord-schwarzwaldes. 144 S.
- Nr. 5: Sanns, Matthias (1990): Experimentelle Untersuchungen zum Ausbreitungsverhalten von leichtflüchtigen Chlorkohlenwasserstoffen (LCKW) in der wassergesättigten Zone. 122 S. **(Vergriffen!)**
- Nr. 6: Seeger, Thomas (1990): Abfluß- und Stofffrachtseparation im Buntsandstein des Nord-schwarzwaldes. 154 S.
- Nr. 7: Einsele, Gerhard & Pfeffer, Karl-Heinz (Hrsg.) (1990): Untersuchungen über die Auswir-kungen des Reaktorunfalls von Tschernobyl auf Böden, Klärschlamm und Sickerwasser im Raum von Oberschwaben und Tübingen. 151 S.
- Nr. 8: Douveas, Nikon G. (1990): Verwitterungstiefe und Untergrundabdichtung beim Talsper-renbau in dem verkarsteten Nord-Pindos-Flysch (Projekt Pigai-Aoos, NW-Griechenland). 165 S.
- Nr. 9: Schlöser, Heike (1991): Quantifizierung der Silikatverwitterung in karbonatfreien Deck-schichten des Mittleren Buntsandsteins im Nordschwarzwald. 93 S.
- Nr.10: Köhler, Wulf-Rainer (1992): Beschaffenheit ausgewählter, nicht direkt anthropogen beein-flußter oberflächennaher und tiefer Grundwasservorkommen in Baden-Württemberg. 144 S.
- Nr.11: Bundschuh, Jochen (1991): Der Aquifer als thermodynamisch offenes System. – Untersu-chungen zum Wärmetransport in oberflächennahen Grundwasserleitern unter besonderer Berücksichtigung von Quellwassertemperaturen (Modellversuche und Geländebeispiele). 100 S. **(Vergriffen!)**



- Nr.12: Herbert, Mike (1992): Sorptions- und Desorptionsverhalten von ausgewählten polyzyklischen aromatischen Kohlenwasserstoffen (PAK) im Grundwasserbereich. 111 S.
- Nr.13: Sauter, Martin (1993): Quantification and forecasting of regional groundwater flow and transport in a karst aquifer (Gallusquelle, Malm, SW-Germany). 150 S.
- Nr.14: Bauer, Michael (1993): Wasserhaushalt, aktueller und holozäner Lösungsabtrag im Wutachgebiet (Südschwarzwald). 130 S.
- Nr.15: Einsele, Gerhard & Ricken, Werner (Hrsg.) (1993): Eintiefungsgeschichte und Stoffaustrag im Wutachgebiet (SW-Deutschland). 215 S.
- Nr.16: Jordan, Ulrich (1993): Die holozänen Massenverlagerungen des Wutachgebietes (Süd-schwarzwald). 132 S. **(Vergriffen!)**
- Nr.17: Krejci, Dieter (1994): Grundwasserchemismus im Umfeld der Sonderabfalldeponie Billigheim und Strategie zur Erkennung eines Deponiesickerwassereinflusses. 121 S.
- Nr.18: Hekel, Uwe (1994): Hydrogeologische Erkundung toniger Festgesteine am Beispiel des Opalinustons (Unteres Aalenium). 170 S. **(Vergriffen!)**
- Nr.19: Schüth, Christoph (1994): Sorptionskinetik und Transportverhalten von polyzyklischen aromatischen Kohlenwasserstoffen (PAK) im Grundwasser - Laborversuche. 80 S.
- Nr.20: Schlöser, Helmut (1994): Lösungsgleichgewichte im Mineralwasser des überdeckten Muschelkalks in Mittel-Württemberg. 76 S.
- Nr.21: Pyka, Wilhelm (1994): Freisetzung von Teerinhaltstoffen aus residualer Teerphase in das Grundwasser: Laboruntersuchungen zur Lösungsrate und Lösungsvermittlung. 76 S.
- Nr.22: Biehler, Daniel (1995): Kluftgrundwasser im kristallinen Grundgebirge des Schwarzwaldes – Ergebnisse von Untersuchungen in Stollen. 103 S.
- Nr.23: Schmid, Thomas (1995): Wasserhaushalt und Stoffumsatz in Grünlandgebieten im württem-bergischen Allgäu. 145+ 92 S.
- Nr.24: Kretschmar, Thomas (1995): Hydrochemische, petrographische und thermodynamische Untersuchungen zur Genese tiefer Buntsandsteinwässer in Baden-Württemberg. 142 S. **(Vergriffen!)**
- Nr.25: Hebestreit, Christoph (1995): Zur jungpleistozänen und holozänen Entwicklung der Wutach (SW-Deutschland). 88 S.
- Nr.26: Hinderer, Matthias (1995): Simulation langfristiger Trends der Boden- und Grundwasser-versauerung im Buntsandstein-Schwarzwald auf der Grundlage langjähriger Stoffbilanzen. 175 S.

- Nr.27: Körner, Johannes (1996): Abflußbildung, Interflow und Stoffbilanz im Schönbuch Waldgebiet. 206 S.
- Nr.28: Gewalt, Thomas (1996): Der Einfluß der Desorptionskinetik bei der Freisetzung von Tri-chlorethen (TCE) aus verschiedenen Aquifersanden. 67 S.
- Nr.29: Schanz, Ulrich (1996): Geophysikalische Untersuchungen im Nahbereich eines Karst-systems (westliche Schwäbische Alb). 114 S.
- Nr.30: Renner, Sven (1996): Wärmetransport in Einzelklüften und Kluftaquiferen – Untersuchungen und Modellrechnungen am Beispiel eines Karstaquifers. 89 S.
- Nr.31: Mohrlök, Ulf (1996): Parameter-Identifikation in Doppel-Kontinuum-Modellen am Beispiel von Karstaquiferen. 125 S.
- Nr.32: Merkel, Peter (1996): Desorption and Release of Polycyclic Aromatic Hydrocarbons (PAHs) from Contaminated Aquifer Materials. 76 S.
- Nr.33: Schiedek, Thomas (1996): Auftreten und Verhalten von ausgewählten Phthalaten in Wasser und Boden. 112 S.
- Nr.34: Herbert, Mike & Teutsch, Georg (Hrsg.) (1997): Aquifersysteme Südwestdeutschlands - Eine Vorlesungsreihe an der Eberhard-Karls-Universität Tübingen. 162 S.
- Nr.35: Schad, Hermann (1997): Variability of Hydraulic Parameters in Non-Uniform Porous Media: Experiments and Stochastic Modelling at Different Scales. 233 S.
- Nr.36: Herbert, Mike & Kovar, Karel (Eds.) (1998): GROUNDWATER QUALITY 1998: Remediation and Protection - Posters -.- Proceedings of the GQ'98 conference, Tübingen, Sept. 21-25, 1998, Poster Papers. 146 S.
- Nr.37: Klein, Rainer (1998): Mechanische Bodenbearbeitungsverfahren zur Verbesserung der Sanierungseffizienz bei In-situ-Maßnahmen. 106 S.
- Nr.38: Schollenberger, Uli (1998): Beschaffenheit und Dynamik des Kiesgrundwassers im Neckartal bei Tübingen. 74 S.
- Nr.39: Rügner, Hermann (1998): Einfluß der Aquiferlithologie des Neckartals auf die Sorption und Sorptionskinetik organischer Schadstoffe. 78 S.
- Nr.40: Fechner, Thomas (1998): Seismische Tomographie zur Beschreibung heterogener Grund-wasserleiter. 113 S.
- Nr.41: Kleineidam, Sybille (1998): Der Einfluß von Sedimentologie und Sedimentpetrographie auf den Transport gelöster organischer Schadstoffe im Grundwasser. 82 S.
- Nr.42: Hückinghaus, Dirk (1998): Simulation der Aquifergenese und des Wärmetransports in Karstaquiferen. 124 S.

- Nr.43: Klingbeil, Ralf (1998): Outcrop Analogue Studies – Implications for Groundwater Flow and Contaminant Transport in Heterogeneous Glaciofluvial Quaternary Deposits. 111 S.
- Nr.44: Loyek, Diana (1998): Die Löslichkeit und Lösungskinetik von polyzyklischen aromatischen Kohlenwasserstoffen (PAK) aus der Teerphase. 81 S.
- Nr.45: Weiß, Hansjörg (1998): Säulenversuche zur Gefahrenbeurteilung für das Grundwasser an PAK-kontaminierten Standorten. 111 S.
- Nr.46: Jianping Yan (1998): Numerical Modeling of Topographically-closed Lakes: Impact of Climate on Lake Level, Hydrochemistry and Chemical Sedimentation. 144 S.
- Nr.47: Finkel, Michael (1999): Quantitative Beschreibung des Transports von polyzyklischen aro-matischen Kohlenwasserstoffen (PAK) und Tensiden in porösen Medien. 98 S.
- Nr.48: Jaritz, Renate (1999): Quantifizierung der Heterogenität einer Sandsteinmatrix (Mittlerer Keuper, Württemberg). 106 S.
- Nr.49: Danzer, Jörg (1999): Surfactant Transport and Coupled Transport of Polycyclic Aromatic Hydrocarbons (PAHs) and Surfactants in Natural Aquifer Material - Laboratory Experiments. 75 S.
- Nr.50: Dietrich, Peter (1999): Konzeption und Auswertung gleichstromgeoelektrischer Tracer-versuche unter Verwendung von Sensitivitätskoeffizienten. 130 S.
- Nr.51: Baraka-Lokmane, Salima (1999): Determination of Hydraulic Conductivities from Discrete Geometrical Characterisation of Fractured Sandstone Cores. 119 S.
- Nr.52: M<sup>c</sup>Dermott, Christopher I. (1999): New Experimental and Modelling Techniques to Investigate the Fractured System. 170 S.
- Nr.53: Zamfirescu, Daniela (2000): Release and Fate of Specific Organic Contaminants at a Former Gasworks Site. 96 S.
- Nr.54: Herfort, Martin (2000): Reactive Transport of Organic Compounds Within a Heterogeneous Porous Aquifer. 76 S.
- Nr.55: Klenk, Ingo (2000): Transport of Volatile Organic Compounds (VOC's) From Soilgas to Groundwater. 70 S.
- Nr.56: Martin, Holger (2000): Entwicklung von Passivsammlern zum zeitlich integrierenden Depositions- und Grundwassermonitoring: Adsorberkartuschen und Keramikdosimeter. 84 S.

- Nr. 57: Diallo, Mamadou Sanou (2000): Acoustic Waves Attenuation and Velocity Dispersion in Fluid-Filled Porous Media: Theoretical and Experimental Investigations. 101 S.
- Nr. 58: Lörcher, Gerhard (2000): Verarbeitung und Auswertung hyperspektraler Fernerkundungsdaten für die Charakterisierung hydrothermalen Systeme (Goldfield/Cuprite, Yellowstone National Park). 158 S.
- Nr. 59: Heinz, Jürgen (2001): Sedimentary Geology of Glacial and Periglacial Gravel Bodies (SW-Germany): Dynamic Stratigraphy and Aquifer Sedimentology. 102 S.
- Nr. 60: Birk, Steffen (2002): Characterisation of Karst Systems by Simulating Aquifer Genesis and Spring Responses: Model Development and Application to Gypsum Karst. 122 S.
- Nr. 61: Halm, Dietrich & Grathwohl, Peter (Eds.) (2002): Proceedings of the 1st International Workshop on Groundwater Risk Assessment at Contaminated Sites (GRACOS). 280 S.
- Nr. 62: Bauer, Sebastian (2002): Simulation of the genesis of karst aquifers in carbonate rocks. 143 S.
- Nr. 63: Rahman, Mokhlesur (2002): Sorption and Transport Behaviour of Hydrophobic Organic Compounds in Soils and Sediments of Bangladesh and their Impact on Groundwater Pollution – Laboratory Investigations and Model Simulations. 73 S.
- Nr. 64: Peter, Anita (2002): Assessing natural attenuation at field scale by stochastic reactive transport modelling. 101 S.
- Nr. 65: Leven-Pfister, Carsten (2002): Effects of Heterogeneous Parameter Distributions on Hydraulic Tests - Analysis and Assessment. 94 S.
- Nr. 66: Schwarz, Rainer (2002): Grundwasser-Gefährdungsabschätzungen durch Emissions- und Immissionsmessungen an Deponien und Altlasten. 100 S.
- Nr. 67: Abel, Thekla (2003): Untersuchungen zur Genese des Malmkarsts der Mittleren Schwäbi-schen Alb im Quartär und jüngeren Tertiär. 187 S.
- Nr. 68: Prokop, Gundula & Bittens, Martin & Cofalka, Piotr & Roehl, Karl Ernst & Schamann, Martin & Younger, Paul (Eds.) (2003): Summary Report on the 1<sup>st</sup> IMAGE-TRAIN Advanced Study Course “Innovative Groundwater Management Technologies”. 119 S.
- Nr. 69: Halm, Dietrich & Grathwohl, Peter (Eds.) (2003): Proceedings of the 2<sup>nd</sup> International Workshop on Groundwater Risk Assessment at Contaminated Sites (GRACOS) and Integrated Soil and Water Protection (SOWA). 260 S.

- Nr. 70: Bayer, Peter (2004): Modelling, economic assessment and optimisation of in-situ groundwater remediation systems. 78 S.
- Nr. 71: Kraft, Siegfried (2004): Untersuchungen zum Langzeiteinsatz der in-situ Aktivkohlefiltration zur Entfernung von organischen Schadstoffen aus Grundwasser. 64 S.
- Nr. 72: Bold, Steffen (2004): Process-based prediction of the long-term risk of groundwater pollution by organic non-volatile contaminants. 76 S.
- Nr. 73: Maier, Ulrich (2004): Modelling of Natural Attenuation in Soil and Groundwater. 81 S.
- Nr. 74: Susset, Bernd (2004): Materialuntersuchungen und Modellierungen zur Unterscheidung Gleichgewicht / Ungleichgewicht in Säulenversuchen für die Sickerwasserprognose organischer Schadstoffe. 100 S.
- Nr. 75: Madlener, Iris (2004): Quantifizierung und Modellierung des PAK-Desorptionsverhaltens aus feinkörnigem Material mittels Säulenversuchen (DIN V 19736) und Hochdruck-Temperatur-Elution (ASE). 86 S.
- Nr. 76: Henzler, Rainer (2004): Quantifizierung und Modellierung der PAK-Elution aus verfestigten und unverfestigten Abfallmaterialien. 98 S.
- Nr. 77: Valley, Stephan (2004): Natural Attenuation of Volatile Organic Compounds (VOC) in Groundwater: A Method for the Determination of Compound-Specific Stable Carbon Isotope Ratios at Low Concentration Levels. 67 S.
- Nr. 78: Röttgen, Klaus Peter (2004): Kritische Analyse des Aufwandes zur Erkundung von Kontaminationen in niedersächsischen Grundwassergeringleitern. 84 S.
- Nr. 79: Gocht, Tilman (2005): Die vier Griechischen Elemente: Massenbilanzierung von polyzyklischen aromatischen Kohlenwasserstoffen (PAK) in Kleinzugsgebieten des ländlichen Raumes. VI, 140, 42.
- Nr. 80: Halm, Dietrich & Grathwohl, Peter (Eds.) (2004): Proceedings of the 2<sup>nd</sup> International Work-shop on Integrated Soil and Water Protection (SOWA). 161 S.
- Nr. 81: Prokop, Gundula, Bittens, Martin, Moraczewska-Maikut, Katarzyna, Roehl, Karl Ernst, Schamann, Martin & Younger, Paul (Eds.) (2004): Summary Report on the 3<sup>rd</sup> IMAGE-TRAIN Advanced Study Course "Quantitative Risk Assessment". 66 S.
- Nr. 82: Hoffmann, Ruth (2004): Optimierungsansätze zur Datenerfassung und Interpretation von Multielektrodenmessungen. 91 S.

- Nr. 83: Kostic, Boris (2004): 3D sedimentary architecture of Quaternary gravel bodies (SW-Germany): implications for hydrogeology and raw materials geology. 103 S.
- Nr. 84: Bayer-Raich, Marti (2004): Integral pumping tests for the characterization of groundwater contamination. 112 S.
- Nr. 85: Piepenbrink, Matthias (2006): – **Im Druck.**
- Nr. 86: Becht, Andreas (2004): Geophysical methods for the characterization of gravel aquifers: case studies and evaluation experiments. 75 S.
- Nr. 87: Brauchler, Ralf (2005): Characterization of Fractured Porous Media Using Multivariate Statistics and Hydraulic Travel Time Tomography. 74 S.
- Nr. 88: Stefan Gödeke (2004): Evaluierung und Modellierung des Natural Attenuation Potentials am Industriestandort Zeitz. 139 S.
- Nr. 89: Nicolai-Alexeji Kummer (2005): Entwicklung eines kommerziell einsetzbaren Katalysators zur Grundwassersanierung: Katalytische Hydrodehalogenierung und Hydrierung umwelt-relevanter (Chlor-) Kohlenwasserstoffverbindungen an trägergestützten Edelmetallkatalysatoren. 122 S.
- Nr. 90: Beinhorn, Martin (2005): Contributions to computational hydrology: Non-linear flow processes in subsurface and surface hydrosystems. 87 S.
- Nr. 91: Olsson, Asa (2005): Investigation and Modelling of Dispersion-Reaction Processes in Natural Attenuation Groundwater. 68 S.
- Nr. 92: Safinowski, Michael (2005): Anaerobic biodegradation of polycyclic aromatic hydrocarbons. 65 S.
- Nr.93: Bürger, Claudius (2005): Technical-economic optimization of in-situ reactive barrier systems under uncertainty. 94 S.
- Nr. 94: Jahn, Michael (2006): Microbial dissimilatory iron(III) reduction: Studies on the mechanism and on processes of environmental relevance. 63 S.
- Nr. 95: Bi, Erping (2006): Sorption and transport of heterocyclic aromatic compounds in soils. 63 S.
- Nr. 96: Kübert, Markus (2006): Modelling and Technical-Economic Evaluation of Point Scale and Integral Approaches for Investigating Contaminant Plumes in Groundwater. 124 S.
- Nr. 97: Chen, Cui (2006): Integrating GIS Methods for the Analysis of Geosystems. 157 S.

- Nr. 98: Regierungspräsidium Freiburg, Abt. Landesamt für Geologie, Rohstoffe und Bergbau (Hrsg.) (2006): Untersuchungen zur Aquiferdynamik im Einzugsgebiet des Blautopfs (Oberjura, Süddeutschland). 77 S.
- Nr. 99: Jochmann, Maik (2006): Solventless Extraction and Enrichment for Compound Specific Isotope Analysis. ... S. – **Im Druck.**
- Nr. 100: Kouznetsova, Irina (2006): Development and application of a phenomenological modelling concept for simulating the long-term performance of zero-valent iron. 99 S.
- Nr. 101: Gronewold, Jan (2006): Entwicklung eines Internet Informationssystems zur Modellierung natürlicher Rückhalte- und Abbauprozesse im Grundwasser. 72 S.
- Nr. 102: Rein, Arno (2006): Remediation of PCB-contaminated soils – Risk analysis of biological in situ processes. 181 S.
- Nr. 103: Dietze, Michael (2007): Evaluierung von Feldmethoden zur Quantifizierung von Schad-stoffminderungen im Fahnenbereich am Beispiel eines BTEX-Schadens. 156 S.
- Nr. 104: Kunapuli, Umakanth (2007): Anaerobic degradation of monoaromatic hydrocarbons by dissimilatory iron(III)-reducing pure and enrichment cultures. 73 S.
- Nr. 105: Miles, Benedict (2007): Practical Approaches to Modelling Natural Attenuation Processes at LNAPL Contaminated Sites. 127 S.
- Nr. 106: Walsh, Robert (2007): Numerical Modeling of THM Coupled Processes in Fractured Porous Media. 98 S.
- Nr. 107: Wang, Guohui (2008): Sorption / Desorption Reversibility of Polycyclic Aromatic Hydrocarbons (PAHs) in Soils and Carbonaceous Materials. 100 S.
- Nr. 108: Liu, Lihua (2008): Aging of NAPLs interfaces in porous media and their effects on mass transfer of organic contaminants. 80 S.